Role of SORLA in neuronal insulin signaling

Inaugural-Dissertation

to obtain the academic degree

Doctor rerum naturalium (Dr. rer. nat.)

submitted to the Department of Biology, Chemistry, Pharmacy

of Freie Universität Berlin

by

Rishabhdev Sinha

2021

The work was carried out from 01/2018 to 11/2021 under the supervision of Prof. Dr. Thomas E. Willnow at the Max Delbrück Center for Molecular Medicine in Berlin.

1st Reviewer: Prof. Dr. Thomas E. Willnow

Max Delbrück Center for Molecular Medicine

2nd Reviewer: Prof. Dr. Petra Knaus

Freie Universität Berlin

Date of defense: 05.07.2022

Selbstständigkeitserklärung

Hiermit erklare ich, dass ich die vorliegende Arbeit mit dem Titel “Role of SORLA in neuronal insulin signaling” selbststandig und ohne Hilfe Dritter angefertigt habe. Sämtliche Hilfsmittel, Hilfen sowie Literaturquellen sind als solche kenntlich gemacht. Außerdem erklare ich hiermit, dass ich mich nicht anderweitig um einen entsprechenden Doktorgrad beworben habe. Die Promotionsordnung des Fachbereichs Biologie, Chemie und Pharmazie der Freien Universitat Berlin habe ich gelesen und akzeptiert.

Berlin, November 2021
Rishabhdev Sinha

Table of Contents

Summary

Alzheimer's disease (AD) is the most common cause of age-related dementia, characterized by cortical shrinkage and brain deposition of amyloid plaques and neurofibrillary tangles. Metabolic complications, such as type 2 diabetes (T2D), are a major risk factor for developing AD. In fact, defects in neuronal insulin signaling are central to both AD and T2D, although the causal mechanisms linking both disease entities are not well understood. Recently, a sorting receptor termed sorting related receptor with A-type repeats (SORLA) has been shown to increase the cell surface expression of the insulin receptor (IR) in adipocytes, thereby enhancing the cellular response to insulin signals. Interestingly, SORLA has also been recognized as a major genetic risk factor for AD. However, a possible role for SORLA in brain insulin signaling and the relevance of this activity in context of AD has not been explored so far.

As SORLA facilitates insulin signaling in adipocytes, I hypothesized that SORLA may also control IR activity in neurons, thereby impacting both neuronal glucose metabolism and amyloidogenic processes. To test my hypothesis, initially I evaluated insulin signaling in primary neurons cultured from wildtype (WT) and SORLA deficient (KO) mice. In line with my hypothesis, SORLA deficiency in primary neurons resulted in a decrease in total IR levels and insulin signaling strength, although neuronal glucose uptake was not impacted. To query the role of SORLA in neuronal insulin signaling *in vivo,* I next generated a mouse line carrying a neuron-specific knockout of SORLA (cKO) mice. Unlike in primary neurons where SORLA facilitated insulin signaling, neuronal loss of SORLA in cKO mice brain did not impact brain insulin signaling and glucose uptake globally. Still, neuronal SORLA deficiency led to a decrease in body weight due to reduced muscle mass. Also, cKO mice showed a higher insulin sensitivity in stress tests, indicating a function for neuronal SORLA in central control of peripheral insulin sensitivity. To understand the relevance of SORLA-dependent stimulation of neuronal insulin signaling in the context of AD, I tested the expression of amyloid degrading enzymes in primary neuronal cultures and in the murine brains. Interestingly, transcript and protein levels of insulin degrading enzyme (IDE), a major amyloid degrading enzyme, were significantly lower in SORLA-deficient neurons, possibly

impacting amyloid levels in these cultures. Acute and chronic pharmacological inhibition of key insulin signaling molecules did not affect IDE levels in neurons, implicating hormone-independent pathways in SORLA-mediated control of IDE expression.

Taken together, my results indicated that SORLA function controls neuronal insulin signaling, a mechanism possibly involved in central control of the peripheral metabolism. Additionally, I uncovered IDE as a target of SORLA-dependent expression control, a process linking receptor action in metabolism and neurodegeneration. Further studies in cell and mouse models should aim at elucidating the mode of SORLA action in functional expression of IDE, and its impact on amyloid burden in the AD brain.

Zusammenfassung

Die Alzheimer Erkrankung ist die häufigste Ursache für altersbedingte Demenz. Die Krankheit ist durch eine Schrumpfung der Hirnrinde und durch Ablagerungen (Plaques) von Amyloid-beta Peptiden und neurofibrillären Tangles im Gehirn gekennzeichnet. Stoffwechselkomplikationen wie zum Beispiel Typ-2-Diabetes (T2D) sind wichtige Risikofaktoren für die Entwicklung der Alzheimer Erkrankung. Tatsächlich sind Defekte in der neuronalen Insulinsignalübertragung sowohl bei der Alzheimer Erkrankung als auch bei T2D von zentraler Bedeutung, auch wenn die kausalen Mechanismen, die beide Krankheiten miteinander verbinden, nicht gut verstanden sind. Kürzlich wurde gezeigt, dass ein Sortierrezeptor, der als Sorting Related Receptor with A-type Repeats (SORLA) bezeichnet wird, die Zelloberflächenexpression des Insulinrezeptors (IR) in Adipozyten erhöht und dadurch die zelluläre Reaktion auf Insulinsignale verstärkt. Interessanterweise stellt SORLA auch ein wichtiger genetischer Risikofaktor für Alzheimer dar. Eine mögliche Rolle von SORLA bei der Insulinsignalübertragung im Gehirn und die Bedeutung dieser Aktivität im Zusammenhang mit Alzheimer ist jedoch bisher nicht untersucht worden.

Da SORLA die Insulinsignalübertragung in Adipozyten erleichtert, stellte ich die Hypothese auf, dass SORLA auch die IR-Aktivität in Neuronen kontrolliert und dadurch sowohl den neuronalen Glukosestoffwechsel als auch amyloidogene Prozesse beeinflussen könnte. Um meine Hypothese zu testen, untersuchte ich zunächst die Insulinsignalkaskade in primären Neuronen, die von Wildtyp- (WT) und SORLA-defizienten (KO) Mäusen generiert wurden. In Übereinstimmung mit meiner Hypothese führte der SORLA-Mangel in primären Neuronen zu einem Rückgang der gesamten IR-Spiegel und zu einer Abschwächung der Insulinsignale, obwohl die neuronale Glukoseaufnahme nicht beeinträchtigt wurde. Um die Rolle von SORLA bei dem neuronalen Insulinsignalweg *in vivo* zu untersuchen, habe ich als nächstes eine Mauslinie erzeugt, die einen neuronenspezifischen Knockout von SORLA (cKO) aufweist. Im Gegensatz zu primären Neuronen, in denen SORLA den Insulinsignalweg erleichtert, hatte der neuronale Verlust von SORLA im Gehirn von cKO-Mäusen keine Auswirkungen auf die Insulinübertragung in die Zelle und die Glukoseaufnahme im Gehirn. Dennoch führte der neuronale SORLA-Mangel zu

einer Abnahme des Körpergewichts aufgrund einer geringeren Muskelmasse. Außerdem zeigten cKO-Mäuse eine höhere Insulinsensitivität in peripheren Stresstests, was auf eine Regulation mittels neuronalem SORLA auf die periphere Insulinsensitivität hinweist. Um die Bedeutung der SORLA-abhängigen Stimulierung des neuroarfnalen Insulinsignalwegs im Zusammenhang mit Alzheimer zu verstehen, habe ich die Expression von Amyloid-abbauenden Enzymen in primären neuronalen Kulturen und im Gehirn von Mäusen untersucht. Interessanterweise waren die Transkript- und Proteinkonzentrationen des Insulin-abbauenden Enzyms (IDE), welches auch ein wichtiges Amyloid-abbauendes Enzyms ist, in SORLA-defizienten Neuronen deutlich niedriger. Dies könnte sich möglicherweise auf die Amyloidkonzentrationen in diesen Kulturen auswirken. Die akute und chronische pharmakologische Hemmung wichtiger Insulin-Signalmoleküle hatte keinen Einfluss auf die IDE-Spiegel in den Neuronen, was auf hormonunabhängige Wege bei der SORLA-vermittelten Kontrolle der IDE-Expression hindeutet.

Insgesamt zeigen meine Ergebnisse, dass die SORLA-Funktion den neuronalen Insulinsignalweg kontrolliert, ein Mechanismus, der möglicherweise auch den peripheren Stoffwechsel kontrolliert. Darüber hinaus habe ich IDE als Ziel der SORLA-abhängigen Expressionskontrolle aufgedeckt, ein Prozess, der möglicherweise eine Verbindung zwischen der Rezeptorwirkung im Stoffwechsel und der Neurodegeneration herstellt. Weitere Studien in Zell- und Mausmodellen sollten darauf abzielen, die Wirkungsweise von SORLA bei der funktionellen Expression von IDE und seine Auswirkungen auf die Amyloidbelastung im Gehirn von Alzheimer Patienten zu klären.

List of figures

List of tables

List of abbreviations

AD	Alzheimer's disease
ADE	Amyloid degrading enzyme
AGE	Advanced glycation end products
AICD	APP intracellular domain
AKT	Protein kinase B
ANOVA	Analysis of variance
APOE	Apolipoprotein E
APP	Amyloid precursor protein
ARF	ADP ribosylation factor
ATP	Adenosine triphosphate
AUC	Area under the curve
BAF	Brg-1 associated factor
BBB	Blood-brain barrier
BCA	Bicinchoninic acid
BDNF	Brain-derived neurotrophic factor
BIN1	Bridge-integrator 1
BMI	Body mass index
BMPR	Bone morphogenetic protein receptor
BSA	Bovine serum albumin
CA2	Cornu ammonis 2
CD	Cluster of differentiation
CHO	Chinese hamster ovary
CNS	Central nervous system
CR	Complement-type repeat
CTF	Carboxy terminal fragment
DAPI	4′,6-diamidino-2-phenylindole
DHA	Docosahexaenoic acid
DMEM	Dulbecco's Modified Eagle Medium
EAAT3	Excitatory amino acid transporter 3
ECE	Endothelin converting enzyme
EGF	Epidermal growth factor

ELISA	Enzyme linked immunosorbent assay
EOAD	Early-onset Alzheimer's disease
ERK	Extracellular regulated kinase
F1	Filial 1 hybrid
FACS	Fluorescent activated cell sorting
FBS	Fetal bovine serum
FDG	Fluorodeoxyglucose
FPG	Fasting plasma glucose
FRET	Fluorescence resonance energy transfer
GAPDH	Glyceraldehyde 3-phosphate dehydrogenase
GDNF	Glial cell line-derived neurotrophic factor
GFAP	Glial fibrillary acidic protein
GGA	Golgi-localizing γ-adaptin ear homology domain ARF-interacting proteins
GLUT	Glucose transporter
GSK	Glycogen synthase kinase
GTT	Glucose tolerance test
GWAS	Genome-wide association studies
HBK	HEPES-buffered Krebs-like buffer
HBSS	Hank's balanced salt solution
HEPES	N-2-Hydroxyethylpiperazine-N'-2-Ethanesulfonic Acid
HFD	High-fat diet
HOMA-IR	Homeostatic model of insulin resistance
IBA1	Ionized calcium binding adaptor molecule 1
i.c.v	intracerebroventricular
IDE	Insulin degrading enzyme
IF	Immunofluorescence
IGF	Insulin-like growth factor
IGFR	Insulin-like growth factor receptor
IHC	Immunohistochemistry
IL-6R	Interleukin-6 receptor
IN	Intranasal
i.p.	intraperitoneal

IR	Insulin receptor
IRS	Insulin receptor substrate
ITT	Insulin tolerance test
i.v.	intravenous
JNK	Jun N-terminal Kinase
KO	Knockout
LOAD	Late-onset Alzheimer's disease
LRP1	LDL receptor related protein 1
LTP	Long-term potentiation
MACS	Magnetic activated cell sorting
MAPK	Mitogen activated protein kinase
NBDG	[N-(7-nitrobenz-2-oxa-1,3-diazol-4-yl) amino]-2-deoxy-D-glucose
NFT	Neurofibrillary tangles
NMR	Nuclear magnetic resonance
NPY	Neuropeptide Y
OPS	Observational prospective study
PACS1	Phosphofurin acidic cluster sorting protein 1
PAGE	Polyacrylamide gel electrophoresis
PBS	Phosphate buffered saline
PCR	Polymerase chain reaction
PDK1	Phosphoinositide-dependent kinase 1
PET	Positron emission tomography
PFA	Paraformaldehyde
PI3K	Phosphoinsotide-3-kinase
PICALM	Phosphatidylinositol-binding clathrin assembly protein
PIP2	Phosphatidylinositol 4,5-bisphosphate
PLEKHA1	Pleckstrin homology containing domain A1
POMC	Pro-opiomelanocortin
PPAR	Peroxisome proliferator activated receptor γ
PPRE	PPARγ response binding element
PSEN	Presinilin
PUFA	Polyunsaturated fatty acid
RCT	Randomised controlled trial

RNA	Ribonucleic acid
RT	Room temperature
SDS	Sodium dodecyl sulphate
SEM	Standard error of mean
SNP	Single nucleotide polymorphism
SNS	Sympathetic nervous system
SORCS	Sortilin-related receptors CNS expressed
SORLA	Sorting-related receptor with A type repeats
T2D	Type 2 diabetes
TGN	*trans*-Golgi network
tM	Mander's coefficient
TOMM40	Translocase of outer mitochondrial membrane 40
mTOR	mammalian target of rapamycin
US	United States
VPS10P	Vacuolar protein sorting 10 protein
WAT	White adipose tissue
WHO	World Health Organisation
WB	Western blotting
WT	Wildtype

1 Introduction

1.1 Alzheimer's disease

1.1.1 Occurance and clinical features of Alzheimer's disease

Alzheimer's disease (AD) is the leading cause of age-related dementia and contributes to around 60-70% of the 50 million cases worldwide (World Health Organisation, 2021). While deaths caused by cardiovascular diseases and infections have decreased substantially in the last 20 years, deaths resulting from AD have increased a staggering 145%. Based on a recent report, AD is the sixth-leading cause of death in the US and the expected number of AD patients will double in the next 30 years ("2021 Alzheimer's Disease Facts and Figures," 2021). On an average, people aged 65 and above survive between four to eight years after diagnosis of AD increasing the costs of care and dependence on public health support. Additionally, the lack of disease modifying therapies for AD creates a huge socioeconomic burden worldwide (Gustavsson et al., 2020; Mehta et al., 2017; Yiannopoulou et al., 2019).

AD is characterised by a progressive decline of memory and cognitive functions impacting daily life functions (Fan et al., 2020). The two major pathological features of AD are brain deposition of extracellular amyloid plaques and intracellular neurofibrillary tangles (NFTs). These pathologies cause neuronal dysfunction and severe brain atrophy eventually leading to death (Long & Holtzman, 2019) (Figure 1.1).

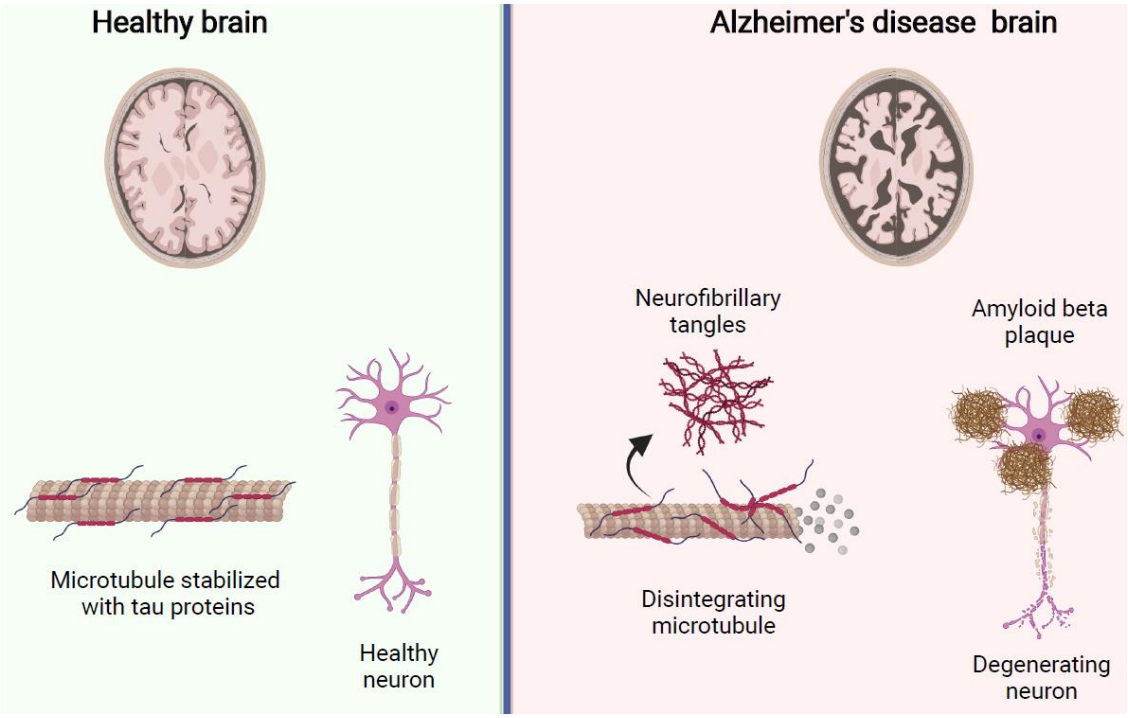

Figure 1.1: Pathological hallmarks of the Alzheimer's disease brains. In a healthy brain (left), few neurotoxic Aβ peptides are formed and the microtubules in the neurons are stabilized by tau proteins. In AD brain (right), excessive extracellular deposition of Aβ into senile plaque as well as hyperphosphorylation of tau, leading to disintegration of microtubules and formation of neurofibrillary tangles are responsible for neuronal degeneration and brain atrophy. Created with BioRender.com.

Amyloid beta (Aβ), the major constituent of amyloid plaques, is produced upon proteolytic cleavage of amyloid precursor protein (APP), a single pass transmembrane protein which has important functions in neurite outgrowth, synaptogenesis, synaptic transmission and homeostasis (Kamenetz et al., 2003; Southam et al., 2019). APP can either undergo processing via the the non-amyloidogenic pathway or the amyloidogenic pathway to produce protein fragments of different lengths and cellular functions (Ricciarelli & Fedele, 2017). In the non-amyloidogenic pathway, APP is cleaved by α secretase at the cell surface to produce a membrane-tethered carboxy terminal fragment α (CTFα) and a soluble sAPPα fragment. The latter promotes adult neurogenesis, important for learning and memory formation (Habib et al., 2018). CTFα is further cleaved by γ secretase to produce a fragment P3 and APP intracellular domain (AICD) protein which acts a modulator for gene expression, upregulating genes involved in cytoskeletal dynamics (Müller et al., 2008). Alternatively, APP processing by amyloidogenic pathway involves its internalisation into the intracellular endocytic compartments. There, internalised APP undergoes cleavage by β secretase to produce a soluble

sAPPβ fragment and CTFβ which is further processed by γ secretase to release AICD and neurotoxic Aβ peptides (Figure 1.2). The imprecise cleavage of CTFβ by γ secretase results in generation of Aβ peptides of varying lengths. Out of the several Aβ forms, the two forms which are extensively studied are Aβ40 and Aβ42 (Chen et al., 2017). Monomeric Aβ peptides can take different conformations and form assemblies with different physical and chemical properties. Aβ monomer can form fibrils which are large and insoluble and are the main constituent of senile plaques (Brown et al., 2020). In contrast it can also form soluble oligomers and spread across the brain causing neurodegeneration. Aβ42 monomer has a greater propensity to aggregate into amyloid plaques and is more neurotoxic than the Aβ40 form (Festa et al., 2019). However, recent studies have shown no correlation of plaque burden with loss of synapse in AD patients. Instead, the levels of soluble Aβ42 oligomers were shown to correlate with synapse failure and memory impairments (Brito-Moreira et al., 2017; Darocha-Souto et al., 2011; Ferreira et al., 2015; He et al., 2019).

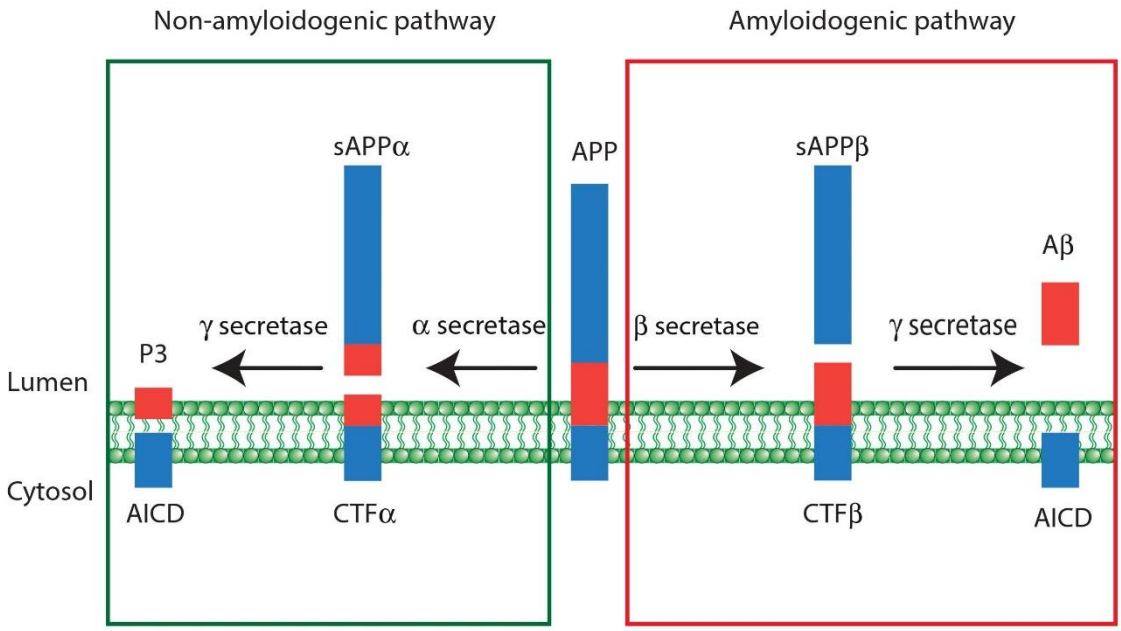

Figure 1.2: Amyloidogenic and non-amyloidogenic processing of amyloid precursor protein (APP). In the amyloidogenic pathway (right, red box), APP is cleaved by β secretase to release a soluble sAPPβ fragment and membrane-bound carboxy terminal fragment β (CTFβ) which is further processed by γ secretase to release the APP intracellular domain (AICD) and neurotoxic Aβ peptide. In the non-amyloidogenic pathway (left, green box), APP is cleaved by α secretase to produce soluble sAPPα and a membrane bound carboxy terminal fragment α (CTFα) which, when further cleaved by γ secretase, produces AICD and a non-neurotoxic P3 fragment. Adapted from Bergström et al., 2016.

The pathophysiological changes in AD arise typically 15-20 years before the onset of clinical symptoms of memory loss and cognitive impairment (Scheltens et al., 2016). Biomarker and imaging studies have shown that during this preclinical phase of AD, there is a gradual increase in amyloid deposits over time which brings about neuroinflammatory changes marked by activation of microglia (Márquez & Yassa, 2019; Young et al., 2020). This phase is followed by the accumulation and spread of NFTs leading to neurodegeneration which correlates well with cognitive decline.

Based on age of onset, AD can be classified into early-onset Alzheimer's disease (EOAD) or late-onset Alzheimer's disease (LOAD). EOAD occurs in individuals younger than 65 years and carry mutations in genes encoding APP, presenilin 1 (PSEN1) and presenilin 2 (PSEN2) (Naj & Schellenberg, 2017). These mutations promote accelerated amyloidogenic processing of APP into Aβ. LOAD typically occurs in individuals older than 65 years and is caused by different environmental and genetic risk factors (Tellechea et al., 2018). AD can further be classified based on the heritability of the disease genes into familial and sporadic AD. Familial AD is characterised by inherited dominant mutations in APP, PSEN1 and PSEN2 and accounts for less than 1% of the total AD cases (Fan et al., 2020). Contrarily, the factors affecting sporadic AD are unclear and remain to be elucidated (Braak & del Tredici, 2012, 2015).

1.1.2 Risk factors for late-onset Alzheimer's disease

Risk factors for LOAD can be grouped into two categories, (i) non-modifiable risk factors such as age, family history, and genetics and (ii) modifiable risk factors including obesity, type 2 diabetes (T2D), smoking, and hypertension (Edwards et al., 2019; Xu et al., 2015). Age is is the greatest risk factors for AD. In US, it has been reported that 5.3% of the population in the age group between 65-74 years have AD. This number increases to 34.6% for individuals aged 85 years and above ("2021 Alzheimer's Disease Facts and Figures," 2021).

Genome-wide association studies (GWAS) have identified several genes implicated in LOAD (Jansen et al., 2019; Marioni et al., 2018; Shen & Jia, 2016). The prevalence of these genes in the population, indicative of the gene penetrance shows the relative impact that they have on the disease. Among the genes that

have relatively high prevalence and risk for AD is *APOE*, the gene which encodes apolipoprotein E (APOE). APOE is a glycoprotein responsible for delivering lipids to the neurons in the brain (Holtzman et al., 2012). It is primarily secreted by astrocytes and microglia into the brain interstitial fluid where it binds with the lipids. These lipid-glycoprotein complexes are endocytosed by endocytic receptors on the neuronal cell surface (Flowers & Rebeck, 2020; Michaelson, 2014). Three gene variants of *APOE* exist differing in two single-nucleotide polymorphisms (SNPs) encoding the three isoforms apoE2, apoE3, and apoE4 (Corder et al. 1993). Individuals homozygous for apoE4 have eight-fold higher risk of developing LOAD than non-carriers. The risk also depends on the copy number of the alleles inherited. Individuals carrying two copies of apoE4 have twelve fold higher risk of developing AD than individuals having two copies of apoE3. Individuals carrying the apoE2 isoform have reduced risk of developing AD when compared with the apoE3 isoform ("2021 Alzheimer's Disease Facts and Figures," 2021; Long & Holtzman, 2019).

A recent meta-analysis has substantiated the involvement of bridge integrator-1 (*BIN1*) gene variants as an important risk factor for LOAD (Schwartzentruber et al., 2021). BIN1 regulates several aspects of AD like APP trafficking, tau stabilisation and immune function in the brain. Several SNPs in *BIN1* gene locus have been associated with an increased risk of AD in different population cohorts validating its relevance as an important risk gene in AD (Tan et al., 2013).

Another GWAS has identified variants in genes encoding phosphatidylinositol binding clathrin assembly protein (PICALM) and clusterin to be associated with AD (Kunkle et al., 2019). PICALM is enriched at the synapses and mediates the endocytosis of nutrients, growth factors and neurotransmitters essential for sustaining neuronal function. Clusterin is a protein which binds to the soluble form of Aβ and is proposed to mediate its clearance from the brain via the blood brain barrier (BBB). Variants affecting clusterin expression in the brain are linked to AD (Harold et al., 2009).

Another meta-analysis has identified genes which are implicated in T2D and AD (J. Zhang et al., 2017). Among the several genes that were identified, a SNP in Pleckstrin homology containing domain A1 (PLEKHA1) is associated with both T2D and AD. PLEKHA1 binds to phosphatidylinositol 4,5 bisphosphate (PIP2) and

regulates the phosphorylation of protein kinase B (AKT), a substrate central to insulin signaling. SNPs in Translocase of outer mitochondrial membrane 40 (TOMM40) and tumor protein 53-induced nuclear protein 1 (TP53INP1) are linked to defects in mitochondrial oxidative stress response, a common pathological feature in both T2D and AD.

Several large scale meta-analysis studies have been conducted using different assessment criterias to understand the modifiable risk factors for AD. A recent study based on several observational prospective studies (OPS) and randomized controlled trials (RCT) have categorized such risk factors of AD into two groups, based on the strength of evidence (Yu et al., 2020). Weak evidence exists for association of AD with lifestyle factors such as smoking, lack of physical exercise, or sleep depriviation. Strong evidence, however exists for metabolic complications, like increased body mass index (BMI), hypertension, and T2D as important risk factors of AD. Another study characterised the risk factors of AD based on the association of gene variants with the AD phenotype. In this study, SNPs in genes regulating blood pressure, cholesterol and blood glucose levels in T2D were strongly associated with AD implicating the involvement of metabolic disorders in the increased risk of AD (Andrews et al., 2020).

1.2 Type 2 diabetes and AD

1.2.1 Link between type 2 diabetes and AD

T2D is characterised by failure of insulin-sensitive cells in peripheral tissues, such as skeletal muscle, adipose tissue, or liver, to respond to insulin. It affects around 420 million people globally and significantly increases the risk of AD by 2 folds (Luchsinger et al., 2004; Reusch & Manson, 2017). Mitochondrial dysfunction, oxidative stress, hyperglycemia and brain insulin resistance are common to both AD and T2D and hence AD is sometimes referred to as type 3 diabetes (Monte, 2015).

Compiling data from longitudinal research it has been established that T2D increases risk for AD. In a clinical trial, it was shown that around 80% of AD patients

had either T2D or impaired fasting glucose (Janson et al., 2004). AD mouse models have been extensively used to understand whether changes in glucose or insulin sensitivity observed in T2D precede AD pathology or are a consequence of it (Götz et al., 2018). In 3x-Tg AD mouse model (transgenic mice carrying mutations in human *APP*, *PSEN* and *MAPT* genes) dysregulation in brain insulin signaling was observed before peripheral insulin resistance set in. Cognitive deficits and AD pathology coincided with impaired insulin signaling in the murine brain (Velazquez et al., 2017). In another study using a leptin-receptor deficient (db/db) mouse model, a model used for studying T2D related pathologies, it was shown that, when compared with the control mice, these mice had an age-dependent increased phosphorylation of tau as well as increased levels of tau cleavage products which acted as nucleation sites for formation of NFT (B. Kim et al., 2009). In yet another study using the db/db mouse model, it was shown that the mutant mice had increased BBB permeability, cognitive deficits and increased microglia activation compared to wildtype (WT) mice (Ramos-Rodriguez et al., 2015). The data from clinical trials and studies in mouse models suggest changes in T2D can lead to impaired brain insulin signaling as well structural changes in BBB possibly triggering cascade of pathophysiological changes in AD brain.

1.2.2 Glucose homeostasis and insulin signaling

The blood glucose levels in humans are tightly regulated within a normal range of 4-6 mM by an interplay of two hormones secreted by pancreas, namely insulin and glucagon (Donovan & Watts, 2014). Post-meal increase in blood glucose levels triggers the pancreas to release insulin into the bloodstream which is taken up by adipose tissue, muscle, liver and brain. Insulin action in these tissues increases glucose uptake hence normalising the blood glucose levels. In addition, insulin facilitates the conversion of glucose into glycogen (glycogenesis) in the liver and muscle, which is stored and made readily available in times of energy deficit. Between meals, when the blood glucose levels fall below the normal range, the pancreas secrete glucagon which initiates the breakdown of glycogen to glucose (glycogenolysis), which is released into the bloodstream to restore blood glucose levels. Glucagon also stimulates glucose production from non-carbohydrate carbon

sources (gluconeogenesis), such as lactate, glycerol and amino acids, to increase blood glucose levels during fasting (Saltiel & Kahn, 2011).

At the cellular level, insulin binds to either the insulin receptor (IR) or the insulin-like growth factor receptor (IGFR) at the cell surface. Insulin binding to these receptors leads to their autophosphorylation, initiating a cascade of downstream reactions regulating metabolic processes, like glucose, lipid and protein synthesis as well as promoting cell proliferation and differentiation (Figure 1.3). These are the two distinct functions of insulin and henceforth referred to as the metabolic and mitogenic arms of insulin signaling pathway, respectively (Haeusler et al., 2017; Tokarz et al., 2018).

Metabolic actions of the insulin signaling pathway involve phosphorylation of insulin receptor substrates (IRS) by the activated IR (Figure 1.3). This reaction leads to further activation of downstream signaling molecules, like phosphoinositide-3-kinase (PI3K) and phosphoinositide-dependent kinase 1 (PDK1). The main effector functions of this metabolic arm of the insulin signaling pathway are mediated by the phosphorylation of AKT which mediates the translocation of glucose transporter 4 (GLUT4) containing vesicles from the cytosol to the cell surface (B. D. Manning & Toker, 2017a). The fusion of these vesicles with the plasma membrane leads to an increased uptake of glucose in the cells (Klip et al., 2019; Stöckli et al., 2012). Once inside the cell, glucose is converted into glycogen for storage, a process mediated by glycogen synthase kinase β (GSK3β), the phosphorylation of which is dependent on AKT. Apart from having a role in glycogen synthesis, GSK3β is known to phosphorylate proteins implicated in AD (Stoothoff & Johnson, 2005). Specifically, it phosphorylates tau leading to the formation of NFTs (Avila et al., 2012; C. W. C. Lee et al., 2003). GSK3β also phosphorylates APP, although the consequences of this relation for APP function and AD processes are unclear so far (Ploia et al., 2010).

The cell growth and differentiation action of insulin is mediated by mitogen-activated protein kinase (MAPK) pathway (Pirola et al., 2004) (Figure 1.3) Insulin induces phosphorylation of Src homology 2 and collagen homology domains (Shc) which interacts with the adaptor protein growth factor receptor-bound protein 2 (Grb2). This interaction leads to the recruitment of Son-of-Sevenless (SOS) protein

essential for the activation of Ras. Ras then leads to the sequential phosphorylation of Raf, mitogen protein kinase kinase (MEK) and extracellular regulated kinase (ERK). ERK translocates to the nucleus and phosphorylates transcription factors essential for synthesis of genes for maintaining cell growth, differentiation and survival (Taniguchi et al., 2006). Interestingly, c-Jun N-terminal kinase (JNK), a member of the MAPK family is known to negatively regulate insulin signaling pathway by phosphorylating and inhibiting IRS (A. M. Manning & Davis, 2003). Increased activation of JNK has been reported in T2D as well as AD (Burillo et al., 2021).

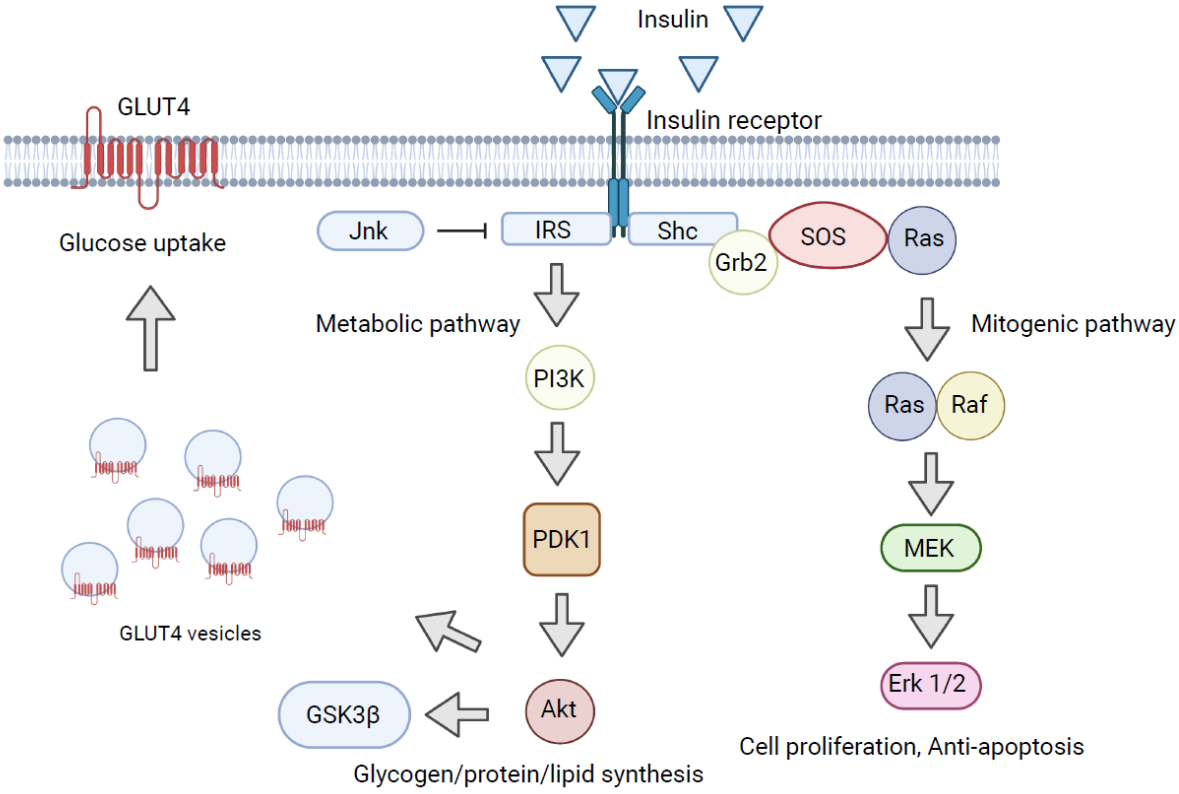

Figure 1.3: Insulin action at the cellular level. Insulin binds to the insulin receptor (IR) and activates downstream signaling cascade mediated mainly by phosphoinsotide-3-kinase (PI3K) and extracellular signal-regulated kinases (ERK). PI3K regulates insulin-mediated metabolic functions, such as glucose uptake and synthesis of glycogen, proteins and lipids. ERK, in turn, regulates the mitogenic functions of the hormone by promoting cell proliferation and preventing apoptosis. Adapted from Saltiel & Kahn, 2011; created with BioRender.com.

1.2.3 Insulin signaling in the brain

For years, the brain was considered an insulin-insensitive organ because glucose utilisation in this tissue is majorly insulin-independent. However, lately this notion has been corrected by numerous studies (Heni et al., 2015; Ketterer et al., 2011; Kullmann et al., 2015). For example, ubiquitous expression of IR in the brain challenges the theory of the brain being unresponsive to insulin (Pomytkin et al., 2018; Spencer et al., 2018). Moreover, the expression of IR is not just limited to neurons, but to other brain cell types, like astrocytes, microglia, and endothelial cells (Kleinridders & Ferris, 2014).

Insulin produced in the pancreas enters the blood and has to cross the blood-brain barrier (BBB) to have an effect in the brain. At the BBB, insulin undergoes transcytosis mediated by the IR to reach the brain interstitial fluid from where it is distributed to the different brain regions (Gray et al., 2017). Recent studies have shown that insulin stimulates glucose uptake in the brain which is dependent on different glucose transporters (GLUTs) (Bingham et al., 2002; Dienel, 2019; Gabbouj, Natunen, et al., 2019; Mergenthaler et al., 2013). Glucose from the peripheral circulation crosses the BBB and reaches the brain interstitial fluid and this process is facilitated by GLUT1. The glucose transport by GLUT1 is insulin-independent and mediates glucose uptake in astrocytes and microglia (Camandola, 2017). Neurons are dependent on glucose for rapid generation of ATP required for synaptic vesicle recycling to maintain synaptic activity (Ashrafi & Ryan, 2017). GLUT3 is the major neuronal glucose transporter which regulates the basal glucose uptake (in absence of insulin) in the different brain regions. In addition to GLUT3, neurons express GLUT4 which is insulin inducible and increases glucose uptake rapidly to meet the neuronal energy demand (Ashrafi et al., 2017). Loss of function studies in mice with neuron-specific GLUT4 deletion have shown that these mice have reduced brain glucose uptake. In addition to GLUT3 and GLUT4, certain hypothalamic neuronal populations also express GLUT2 which sense glucose concentrations in the brain and regulate the peripheral glucose levels (Reno et al., 2017).

Insulin effector functions in the brain are diverse and region specific. In the cortex and hippocampus, it improves memory and cognition by promoting AKT-dependent

long-term potentiation (LTP) (Biessels & Reagan, 2015; Gabbouj, Ryhänen, et al., 2019; S. H. Lee et al., 2016). In the arcuate nucleus of the hypothalamus, insulin has opposing effects on two different neuronal populations regulating feeding behaviour and energy homeostasis (Roh et al., 2016). Agouti-related peptide (AgRP) neurons colocalise with neuropeptide Y (NPY) neurons and are orexiegic, i.e., they promote feeding behaviour and decrease energy expenditure. Pro-opiomelanocortin (POMC) neurons are anorectic inducing satiety and increasing energy expenditure. Insulin stimulates POMC neurons but attenuates signaling in AgRP/NPY neurons, thereby leading to an overall decrease in food intake and an increase in energy expenditure (Loh et al., 2017; Shin et al., 2017). Hypothalamic insulin signaling affects peripheral metabolism, the actions of which are mediated by the innervations of the sympathetic nervous system (SNS) to the respective organs. For example, hypothalamic insulin signaling via the SNS improves hepatic insulin sensitivity and decreases hepatic glucose output (Ruud et al., 2017). Insulin signaling in hypothalamus also promotes browning of white adipose tissue (WAT), a process wherein WAT is converted into beige adipocytes thereby promoting energy expenditure (Beddows & Dodd, 2021). In essence, brain insulin signaling not only has local metabolic effects, but has an extensive role in whole body glucose and energy homeostasis (Figure 1.4).

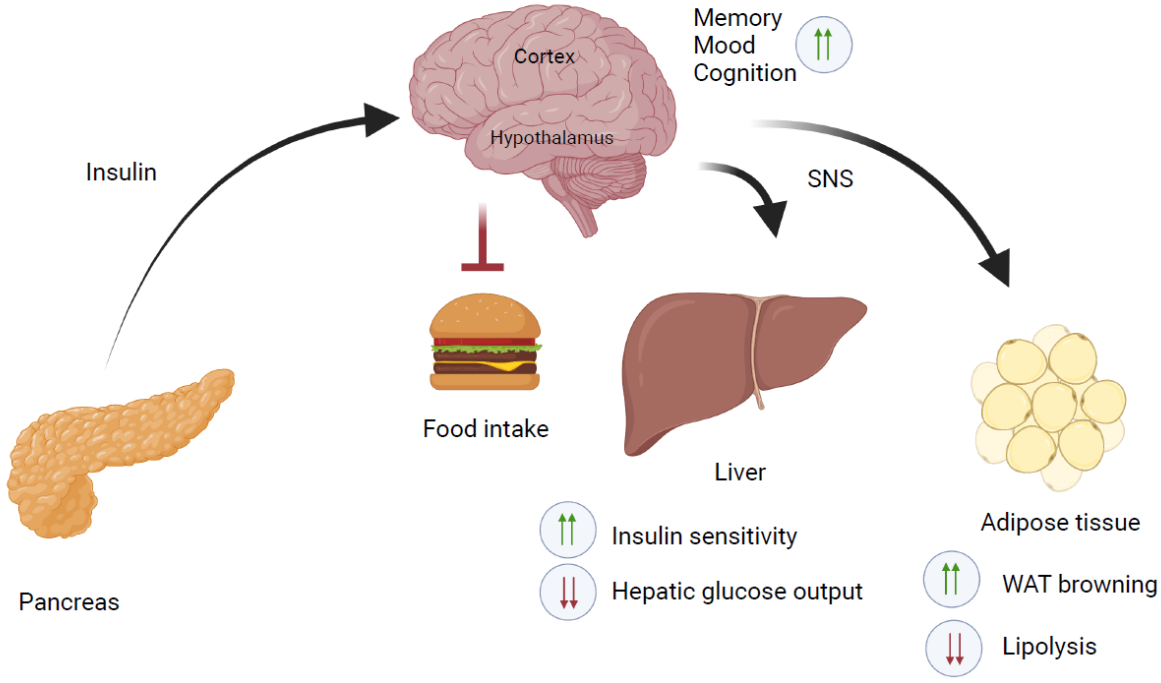

Figure 1.4: Insulin actions in the brain and its implications for central control of metabolism. Insulin secreted from the pancreas crosses the blood-brain barrier and has different physiological implications in different brain regions. It acts in the cortex and hippocampus improving cognition, memory and mood. In the hypothalamus, insulin action leads to a negative energy balance as it suppresses food intake and increases energy expenditure. Hypothalamic insulin action also leads to decreased hepatic glucose output and increased browning of white adipose tissue. Adapted from Dodd & Tiganis, 2017 ; created with BioRender.com.

1.2.4 Insulin signaling and neurodegeneration

T2D is characterised by hyperglycemia and hyperinsulinemia and is linked to neurodegenerative disorders like AD and Parkinson's disease (PD) (Fiory et al., 2019; Hassan et al., 2020; Kellar & Craft, 2020). Hyperinsulinemia leads to downregulation of IR at the BBB decreasing brain delivery of insulin thereby impacting brain insulin signaling (Schwartz et al., 1990). In the neurons, impaired insulin signaling leads to a decrease in the phosphorylation of AKT. This decrease in pAKT levels prevents the mobilisation of GLUT4 vesicles to the plasma membrane further leading to decreased glucose uptake in neurons. A lower glycolytic drive in these neurons decreases ATP production essential for neurotransmitter release and maintenance of synaptic activity (Mergenthaler et al., 2013). Efficient and sustained synaptic activity is important for long-term memory formation. Therefore, defects in insulin signaling have a significant impact on long-

term memory which is often seen in T2D patients (Martins, 2019). In addition, impaired insulin signaling in neurons is also directly related to the pathophysiological changes in AD. Decreased insulin signaling leads to activation of GSK3β, which hyperphosphorylates tau, destabilises microtubules structure and forms NFT (Avila et al., 2012). Interestingly, tau hyperphosphorylation has been shown to also induce oligomeric insulin accumulation, which causes neuronal insulin resistance, forming a vicious cycle of sustained insulin resistance further triggering NFT formation (Winblad et al., 2017).

Prolonged hyperglycemia leads to aberrant glycation of proteins forming so called advanced glycation end products (AGE) (Pugazhenthi et al., 2017). AGE enhance production of reactive oxygen species which increases APP production and amyloid aggregation in the brain (Ko et al., 2015). Moreover, elevated glucose concentrations, typically in the range found in diabetic individuals, facilitates formation of Aβ42 oligomers (Kedia et al., 2017). Aβ prevents binding of insulin to the IR in neurons and therefore diminishes the insulin response by inhibiting the activation of IR as well as the downstream targets of the insulin signaling pathway (W. Zhao et al., 2008).

Finally, insulin has anti-amyloidogenic effects in human neuronal cells. It favours non-amyloidogenic processing of APP and reduces intracellular Aβ accumulation by trafficking APP from the *trans*-Golgi network (TGN) to the cell surface (Gasparini et al., 2001). It also stimulates the release of sAPPα via the PI3K-AKT pathway (Solano et al., 2000). Additionally, insulin decreases the transcription of pro-amyloidogenic genes, such as those encoding GSK3β and APP and upregulates the gene transcription of *insulin degrading enzyme* (*IDE*), encoding a major amyloid degrading enzyme (Pandini et al., 2013).

1.2.5 Amyloid degrading enzymes

Amyloid degrading enzymes (ADEs) are responsible for degradation of Aβ in the brain (Nalivaeva & Turner, 2019; Yoon & Jo, 2012). They have different cellular localisation and hence are responsible for the degradation of Aβ either within the cell or outside the cell. Neprilysin, a major ADE in the brain, is a cell surface

localized enzyme which mediates the extracellular degradation of Aβ (Zhou et al., 2013). Low neprilysin expression and enzyme activity have been observed in elderly AD patients (Yasojima et al., 2001). The intracellular degradation of Aβ takes place in endolysosomal compartments and is mediated by endothelin converting enzymes (ECEs) (Eckman et al., 2001). Among the different ADEs that have been discovered so far, one that implicated in both metabolic diseases and neurodegeneration is insulin degrading enzyme (IDE) (Figure 1.5).

IDE is a zinc metallopeptidase that mainly cleaves insulin but also other substrates like Aβ, glucagon, somatostatin, and amylin (Hulse et al., 2009; Tundo et al., 2017). It is expressed in several tissues with its expression being highest in the kidney and liver (Pivovarova et al., 2016). Expression of IDE in the human brain was confirmed by immunostainings showing a distinct localisation in neurons of the cortex (Bernstein et al., 1999). Another study confirmed its expression in brain microvessels. IDE immunoprecipitated from the vasculature was capable of degrading both insulin and Aβ *in vitro* (Morelli et al., 2004). The cellular localisation of IDE is mainly cytosolic, although it can be found at relatively low levels in endosomes, peroxisomes, mitochondria, and at the cell surface (Tundo et al., 2013). A few studies have reported that IDE is secreted in the extracellular space, although a recent work has shown that this is observed only when cell membrane integrity is lost (Song et al., 2018). There are several metabolic modulators which regulate IDE expression. Insulin has been shown to upregulate IDE expression in primary hippocampal neurons. This increase in IDE expression was abolished when neurons were treated with PI3K inhibitors, suggesting the involvement of the metabolic arm of the insulin signaling pathway in this process (L. Zhao et al., 2004). Glucose has been shown to regulate IDE activity in human hepatoma cell line. Insulin treatment in these cells under normal glucose concentration increased IDE activity, whereas insulin treatment under high glucose concentrations abrogated IDE activity (Pivovarova et al., 2009). Metformin, a drug prescribed to T2D patients to normalise glucose levels, upregulates IDE expression in a mouse model of AD, along with significantly improving learning and memory in these animals (Lu et al., 2020). In another study involving rat primary hippocampal neurons culture, agonists of the peroxisome proliferator activated receptor γ (PPARγ) increased IDE

expression by binding to the PPARγ response binding element (PPRE) in the *Ide* promotor region (Du et al., 2009).

APP levels also modulate IDE activity in different tissues. In an interesting study, APP KO mice had significantly higher levels of IDE transcript, protein, and enzyme activity compared to WT controls (Southam et al., 2019). Interestingly, compared to WT mice, APP KO mice had reduced insulin signaling in synaptosomal preparations from frozen brain indicated by a decreased phosphorylation of IR.

Jointly, these findings indicate a role for IDE in metabolism-driven neurodegenerative processes. This assumption is further supported by genetic association studies that identified single nucleotide polymorphisms (SNPs) in *IDE* with increased risk of AD (Bertram et al., 2007; Y. Zhang et al., 2013). The functional relevance of IDE for T2D and AD have been extensively studied in mouse models with global and tissue specific knockout of *Ide*. IDE KO mice exhibit symptoms of both T2D and AD. They have a significant decrease in Aβ degradation in the brain as well as in primary neuronal cultures leading to increased Aβ accumulation. Moreover, these mice have hyperinsulinemia and glucose intolerance, hallmarks of T2D (Abdul-Hay et al., 2011; Farris et al., 2003). Tissue-specific deletion of *Ide* may be used to further elucidate its specific roles in different tissues. Liver is a major site for insulin clearance in the body. To understand whether liver IDE is the major enzyme responsible for this action, mouse with *Ide* deletion in hepatocytes were generated. Liver-specific ablation of IDE activity led to a 20% increase in fasting plasma glucose levels, although plasma insulin levels were identical to the WT mice suggesting that liver IDE regulates plasma glucose levels by mechanisms other than hepatic insulin degradation. Interestingly, a significant reduction in liver IR and AKT levels were observed in these mice which led to a substantial decrease in insulin signaling further supporting a link between IDE and insulin signaling (Villa-Pérez et al., 2018).

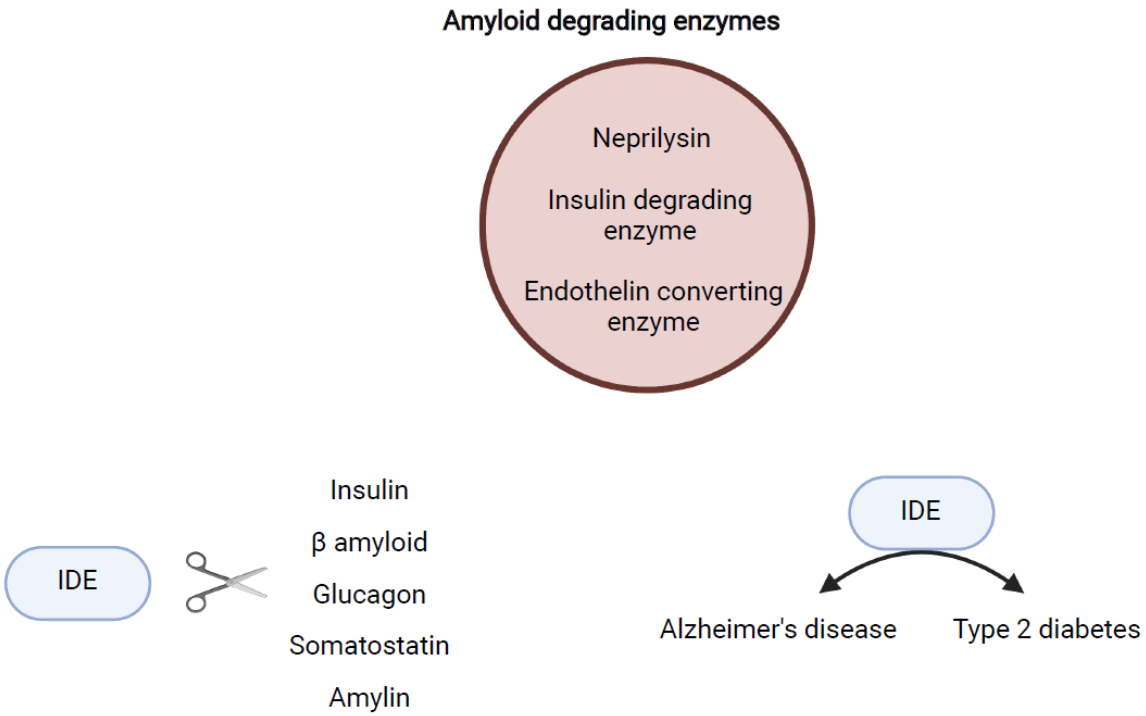

Figure 1.5: Amyloid degrading enzymes in Alzheimer's disease (AD) and type 2 diabetes (T2D). Amyloid degrading enzymes neprilysin, insulin degrading enzyme (IDE), and endothelin converting enzyme (ECE) reduce the amyloid load by clearing neurotoxic Aβ from the cells into the brain interstitial fluid as well as degrading Aβ within the cells. Of these, IDE, which cleaves a variety of substrates, has been implicated in both type 2 diabetes and AD. Created with BioRender.com.

1.3 VPS10P domain receptor family

1.3.1 Structural organisation, trafficking and functions of VPS10P domain receptors

The family of vacuolar protein sorting 10 protein (VPS10P) domain receptors consists of six intracellular sorting receptors which share a common 700 amino acids VPS10P domain (Willnow et al., 2008). This domain was initially identified as VPS10P, a sorting receptor in *Saccharomyces cerevisiae* trafficking newly synthesized enzymes from Golgi to the vacuole, the yeast lysosome (Marcusson et al., 1994). In addition to VSP10P, this gene family includes five mammalian receptors, termed sorting-related receptor with A type repeats (SORLA), sortilin, as well as sortilin-related receptors CNS expressed (SORCS) 1, -2 and -3 (Hermey, 2009). Apart from the VPS10P domain, all receptors share a single transmembrane domain and a cytoplasmic tail for interaction with adaptor proteins required for internalisation and intracellular sorting of the receptors. Among all the VPS10P

domain receptors, sortilin has the simplest structure with a single VPS10P domain and a segment of 10 conserved cysteine residue (10CC) domain. The SORCS receptors have a leucine rich domain sequestered between the VPS10P domain and the plasma membrane in addition to the 10CC domain. SORLA has the most diverse structure with different domains like epidermal growth factor (EGF) type repeat domain, fibronectin type III domain and complement-type repeat (CR) domain for protein-protein interactions (Schmidt et al., 2017) (Figure 1.6).The VPS10P domain in SORLA binds to a variety of ligands having diverse physiological roles in growth, immune response and neuronal health. It binds to growth factors such as glia-derived neurotrophic factor (GDNF) facilitating neurotrophic activity (Glerup et al., 2013). It also binds to cytokines and their receptors like interleukin-6 (IL-6) and interleukin-6 receptor (IL-6R) enabling cytokine signaling in astrocytes for acute phase immune response (Larsen & Petersen, 2017). Additionaly, the VPS10P domain in SORLA binds to Aβ and targets it to lysosomes for its degradation thereby reducing the amyloid load (Caglayan et al., 2014). The CR domain in SORLA binds to APP and regulates its intracellular trafficking promoting non-amyloidogenic APP processing (Spoelgen et al., 2006). SORLA binds to apoE and promotes the cellular uptake of Aβ wherein it can be degraded by different ADEs and this interaction is facilitated by the CR domain (Monti & Andersen, 2018; Yajima et al., 2015).

Trafficking of proteins to distinct sub-cellular compartments is essential for maintaining cell function and homeostasis. VPS10P domain receptors, which are predominantly expressed in the nervous system modulate the trafficking and availability of trophic factors and ligands important for neuronal survival, plasticity and metabolism. For example, SORCS2 prevents oxidative stress and epilepsy pathology by enhancing cell surface expression of cysteine transporter excitatory amino acid transporter 3 (EAAT3). Cysteine uptake is essential for generation of glutathione which protects from oxidative stress damage during epilepsy (Malik et al., 2019). Sortilin, another receptor in the VPS10P domain family, promotes the uptake and conversion of polyunsaturated fatty acid into endocannabinoids that facilitate neuroprotective gene expression in the brain. ApoE4, a major risk factor for AD, disrupts sortilin function by impairing its cell surface recycling and thereby impacting the uptake of polyunsaturated fatty acids (PUFAs) essential for

maintaining brain health (Asaro et al., 2020). Trafficking aberrations of ligands in the brain can have an impact on whole body energy homeostasis as well. It was shown that SORCS1 and SORCS3 share receptor homology and control energy expenditure in mice by regulating the levels of orexigenic peptide AgRP. Mice lacking both the receptors produce an excess of AgRP leading to chronic energy excess caused by increased food intake and decreased locomotor activity (Subkhangulova et al., 2018).

Newly synthesized VPS10P domain receptors contain an N-terminal propeptide which is cleaved in the biosynthetic pathway of the TGN, thereby enabling ligand binding. Mature receptors mediate the endocytosis and intracellular trafficking of ligands, a process facilitated by their tail interactions with cytosolic adaptors (Malik & Willnow, 2020a). Adaptor proteins (AP-1 and 2) and Golgi-localizing γ-adaptin ear homology domain ARF-interacting proteins (GGA-1, -2 and 3) mediate the anterograde trafficking of SORLA from the TGN to the endosomes. Retromer and phosphofurin acidic cluster sorting protein 1 (PACS1) are involved in the retrograde sorting of SORLA from the endosomes to the TGN (Dumanis et al., 2015).

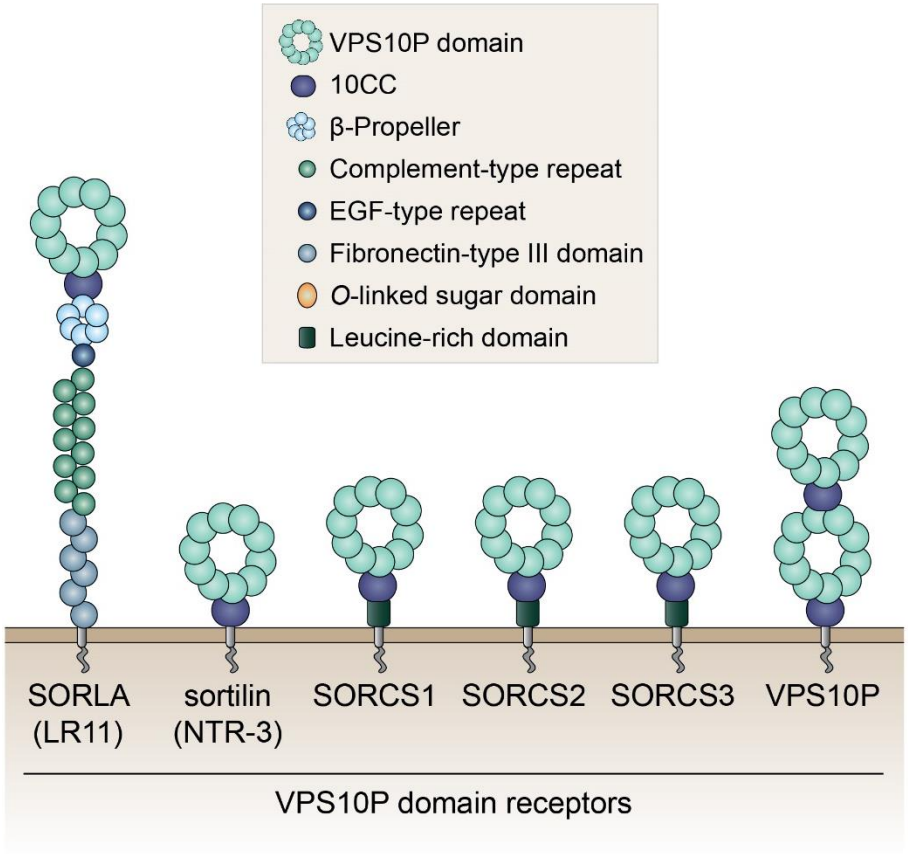

Figure 1.6: Structural organisation of vacuolar protein sorting 10 protein (VPS10P) domain receptors. The structural organisation of the members of the VPS10P domain receptor gene family is shown. Family members are type-1 transmembrane proteins sharing a common VPS10P domain. These receptors shuttle ligands to different intracellular compartments regulating important cellular processes such as regulated protein release, signal reception, or protein turnover. (SORLA: Sorting protein-related receptor with A-type repeats; SORCS: Sortilin-related receptors CNS expressed). Adapted from Malik & Willnow, 2020a.

1.3.2 SORLA and its role in neurodegeneration and metabolism

The VPS10P domain receptor which I have studied in my PhD thesis with relevance to AD is SORLA. SORLA was initially identified as a receptor for apolipoprotein E and was classified as a member of low-density lipoprotein receptor gene family (Motoi et al., 1999). Using immunohistochemical stainings and quantitative Western blots, it was shown that SORLA levels in the AD brains were significantly lower when compared with control individuals (Scherzer et al., 2004). Subsequently, its role in APP processing and Aβ generation were elucidated using cell culture and mouse models (Andersen et al., 2005; Rogaeva et al., 2007; Rohe et al., 2008; Spoelgen et al., 2006). Two models for SORLA-dependent APP processing and trafficking have been proposed. In the first model, SORLA promotes non-amyloidogenic processing of APP by retrieving it from the early endosome and bringing it to the TGN thus preventing its proteolytic cleavage into Aβ by β and γ secretase (Andersen et al., 2005; Offe et al., 2006). In the second model, it is proposed that SORLA prevents the homodimerization of APP in the TGN, which is the preferred substrate for secretase activity, thereby decreasing its amyloidogenic processing. Additionally, SORLA prevents the exit of APP to the cell surface further reducing its processing via the amyloidogenic and non-amyloidogenic pathways (Schmidt et al., 2012). These results were validated in a SORLA KO mouse model which had significantly higher levels of Aβ compared to the WT controls. Moreover, it was shown that SORLA directs nascent Aβ peptide for lysosomal catabolism (Figure 1.7) and this activity was lost in SORLA receptor carrying a familial mutation in *Sorl1* gene indicating a direct interaction of the receptor with Aβ (Caglayan et al., 2014).

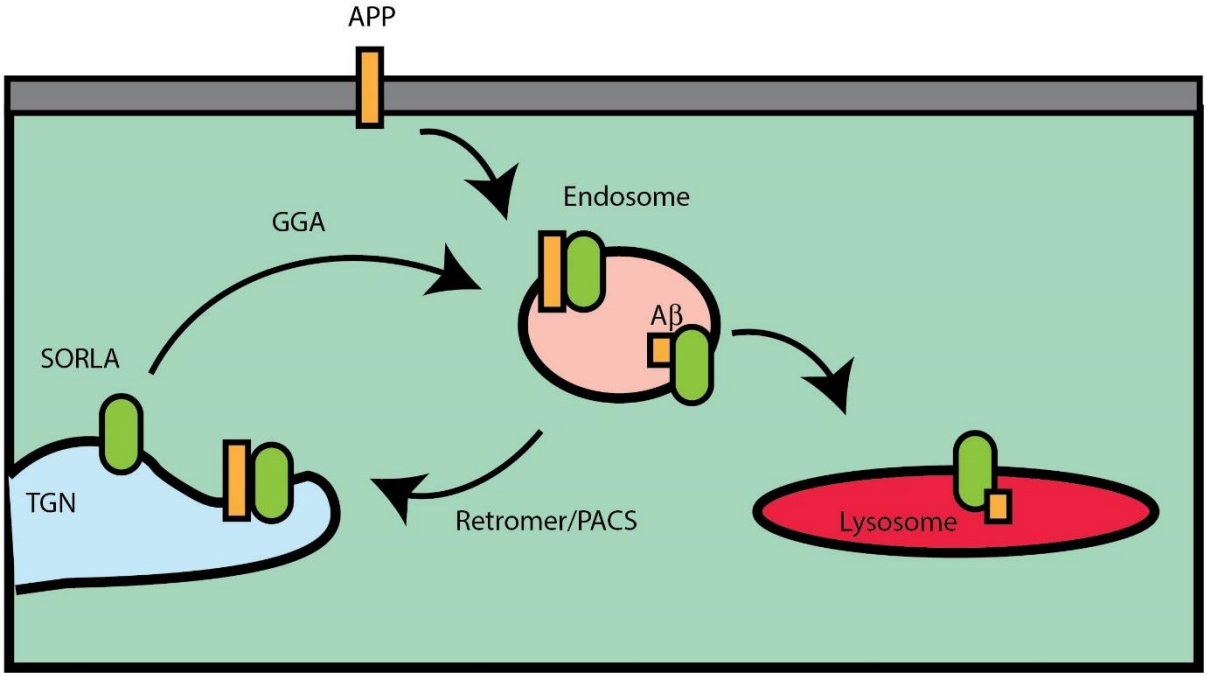

Figure 1.7: SORLA mediated trafficking of APP and Aβ in neurons. SORLA prevents amyloidogenic processing of APP by retrieving it from endosome and bringing it to TGN thus preventing its proteolytic cleavage into Aβ by β and γ secretase. In addition, SORLA aids degradation of intracellular Aβ by trafficking it to lysosomes. The anterograde trafficking of SORLA from the TGN to the endosome is mediated by GGA adaptor protein. Alternatively, the retrograde trafficking of SORLA from the endosome to the TGN is mediated by retromer and PACS. Adapted from Schmidt et al., 2017; Willnow et al., 2008.

Several studies since then have confirmed the association of SNPs in *Sorl1* with increased risk of both early onset and late onset AD (J. H. Lee et al., 2008; Pottier et al., 2012; Reitz, 2011). Two SNPs in the 3' region of *Sorl1* have been associated with poor SORLA expression in AD brains. These SNPs alter the nucleotide sequence leading to less efficient translation of transcripts into protein (Caglayan et al., 2012). Moreover, non-genetic factors like brain-derived neurotrophic factor (BDNF) and PUFAs like docosahexanoic acid (DHA) have been shown to affect *Sorl1* transcript levels. BDNF enhances *Sorl1* transcription which is mediated by the ERK signaling pathway although the downstream transcriptional regulators are yet to be defined (Rohe et al., 2009). Low DHA levels in the blood is associated with an increased risk of neurodegeneration (de Wilde et al., 2017). DHA was shown to induce SORLA expression in primary neuronal cultures, human neuroblastoma cell lines and mouse models validating its relevance as an important dietary factor relevant for AD (Ma et al., 2007). Apart from playing a vital role in preventing AD, SORLA also promotes neuronal growth and regeneration. It enhances cell surface

expression of tropomysin receptor kinase B (TrkB) potentiating BDNF signaling in neurons essential for synaptic transmission and axonal growth (Rohe et al., 2013). Soluble fraction of SORLA formed by ectodomain shedding has been shown to enhance neurite outgrowth and regeneration mediated by the activation of the ERK signaling pathway (Stupack et al., 2020).

The metabolic aspects of SORLA function has been studied in detail over the last few years. Large scale GWAS studies have identified SNPs in SORLA associated with waist circumference in humans and body fat percentage in mouse (Parks et al., 2013; Smith et al., 2010). In line with these findings, soluble SORLA levels positively correlate with BMI and adiposity in humans (Schmidt et al., 2016). Soluble SORLA inhibits thermogenesis in adipose tissue by binding to the bone morphogenetic protein receptor (BMPR) and inhibiting Smad phosphorylation. Mice lacking SORLA are protected from diet-induced obesity with an increased browning of white adipose tissue (Whittle et al., 2015). In another study, *Sorl1* transcript and protein levels in white adipose tissue were shown to positively correlate with BMI in humans. In the same study, it was shown that SORLA facilitated cell surface expression of IR in adipocytes (Figure 1.8). This enhanced IR activity mediated the insulin-induced suppression of lipolysis leading to increased accumulation of fat in these cells (Schmidt et al., 2016).

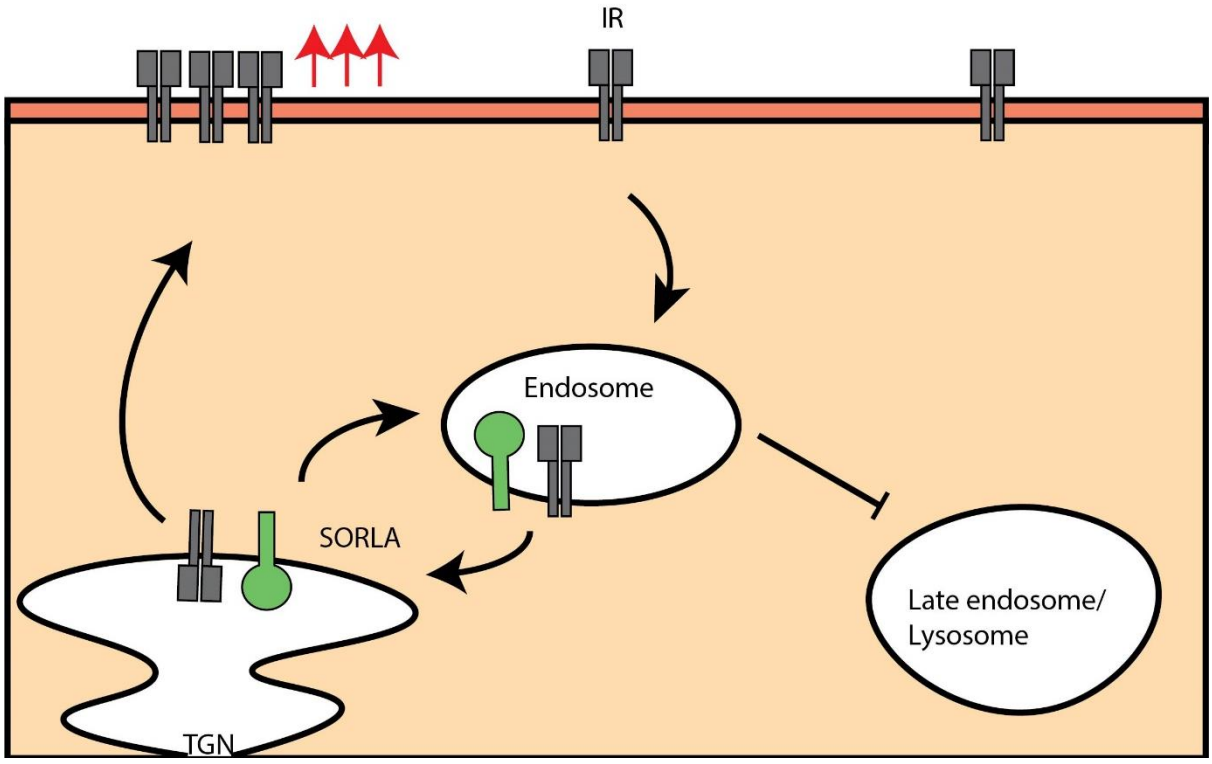

Figure 1.8: SORLA increases cell surface expression of IR potentiating insulin signaling in adipocytes. The internalised IR binds to SORLA in endosome which brings it to the TGN preventing its degradation in late endosomes/lysosomes. IR is then trafficked to the plasma membrane thus increasing its cell surface expression for enhanced insulin binding. Red arrows indicate cell surface levels of IR that are increased in presence of SORLA. Adapted from Schmidt et al., 2016.

These studies confirm that SORLA plays an essential role in whole body energy homeostasis by increased browning of white adipose tissue and enhanced adipocyte insulin signaling. Additionally, the role of SORLA in APP processing and its relevance for AD has been well established. However, whether SORLA also affects insulin signaling in the brain, and whether such activity may be relevant for SORLA's role in AD has not been explored yet. Addressing this question is the major goal of my thesis project.

2 Aim of the study

SORLA is a member of the VPS10P domain receptor family that reduces the amyloid burden in the brain. Additionally, it facilitates insulin signaling in adipocytes. However, whether this receptor plays a role in neuronal insulin signaling and, consequently, in brain or systemic metabolism remains unexplored. Therefore, the overall goal of my thesis project was to understand the role of SORLA in brain insulin signaling and how this activity may be relevant for processes in AD. To do so, I intended to perform e*x vivo* application of insulin and fluorescent-labelled glucose analogues in primary neurons from wildtype (WT) and SORLA-deficient (KO) mice to study the implication of SORLA deficiency for neuronal insulin action and cellular glucose homeostasis. To study the role of SORLA in brain insulin signaling and its effect on central and systemic glucose metabolism *in vivo*, I planned to generate a novel conditional knockout mouse (cKO) model with *Sorl1* deletion specifically in neurons. In this model, I wished to examine the consequences of neuronal receptor deficiency for metabolic processes in brain and peripheral tissues. Finally, I planned to query whether a presumed role for SORLA in neuronal insulin signaling may also impact AD-related cellular pathways, providing new insights into common mechanisms on which defects in metabolism and AD may converge.

3 Materials and methods

3.1 Materials

3.1.1 Oligonucleotides and TaqMan probes

Table 3.1: List of DNA primers used for genotyping PCR.

Gene	Primer orientation	Primer sequence
Sorl1	cKO forward primer	AGATCTGTCCTTCCTTCTGC
	cKO reverse primer	ATCATTAATTGCGTTGCGCC
	WT forward primer	GGGGAGTCTGTGGCAGTG
	WT reverse primer	AGAAAATGCCTTACAGCTGG
Cre	Forward primer	GCGGTCTGGCAGTAAAAACTATC
	Reverse primer	GTGAAACAGCATTGCTGTCACTT

Quantitative real-time PCR (qRT-PCR) was performed using TaqMan probes ordered from Thermo Fisher Scientific.

Table 3.2: List of TaqMan probes used for qRT-PCR.

Gene	Assay ID
Gapdh	Mm99999915_g1
B2m	Mm00437762_m1
Insr	Mm01211785_m1
Ide	Mm00473077_m1

3.1.2 Antibodies

All peroxidase labeled secondary antibodies for Western blotting were purchased from Sigma-Aldrich and used at the dilution 1:5000. Fluorophore-conjugated secondary antibodies for immunofluorescence were purchased from Thermo Fischer Scientific and used at the dilution 1:1000.

Table 3.3: List of primary antibodies used in this study.

Target protein	Commercial provider	Catalogue number	Dilution	Application
SORLA	BD Biosciences	611860	1:1000	WB
IR	Cell Signaling Technology	3025S	1:1000	WB
GLUT4	Cell Signaling Technology	2213S	1:500	WB
GLUT3	Abcam	ab15311	1:1000	WB
pIR	Cell Signaling Technology	3918S	1:1000	WB
AKT	Cell Signaling Technology	9272S	1:1000	WB
pAKT	Cell Signaling Technology	2965S	1:1000	WB
GSK3β	Cell Signaling Technology	12456S	1:1000	WB
pGSK3β	Cell Signaling Technology	9323S	1:1000	WB
GAPDH	GeneTex	GTX627408-01	1:1000	WB
IDE	Abcam	ab32216	1:500	WB

ERK	Cell Signaling Technology	9102S	1:1000	WB
pERK	Cell Signaling Technology	4370S	1:1000	WB
JNK	Cell Signaling Technology	9258S	1:1000	WB
pJNK	Cell Signaling Technology	9251S	1:1000	WB
EEA1	BD Biosciences	610457	1:200	IF
VTI1B	BD Biosciences	611405	1:200	IF
RAB11	BD Biosciences	610657	1:200	IF
RAB9	Thermo Scientific	MA3-067	1:200	IF
RAB4	BD Biosciences	610889	1:200	IF
SORLA	Home-made	-	1:500	IF/IHC
IBA1	Abcam	ab5076	1:500	IHC
CD31	BD Biosciences	550274	1:100	IHC
NEUN	Abcam	ab104224	1:250	IHC
GFAP	Abcam	ab53554	1:500	IHC

* WB-Western blotting; IF-immunofluorescence; IHC-Immunohistochemistry

3.1.3 Buffer solutions and cell culture media

Table 3.4: List of buffer solutions and cell culture media.

Buffer Solution	**Composition**
Enzyme solution	2 mg Cystein
	1 mM $CaCl_2$

	0.5 mM EDTA, pH 8
	in DMEM
Stop solution	5% FBS (Gibco, 10270106),
	1% penicillin/streptomycin (Gibco, 15150122)
	2.5 mg/ml albumin (Sigma-Aldrich, A9418)
	2.5 mg/ml trypsin inhibitor (Sigma-Aldrich, T9253)
	in DMEM (Gibco 41966029)
Neuronal Plating Media	2% B-27 (Gibco, 17504044)
	1% GlutaMAX (Gibco, 35050061)
	1% penicillin/streptomycin (Gibco, 15150122)
	in Neurobasal (Gibco, 21103049)
RIPA buffer	50 mM Tris-HCl, pH 7.4
	150 mM NaCl
	0.1% SDS
	0.5% sodium deoxycholate
	1% NP-40
	in water
Lysis buffer	50 mM Tris HCL, pH 7.4
	140 mM NaCl
	1% Triton X-100
	in water

Base solution	25 mM NaOH
	0.2 mM EDTA
	in water
Neutralization solution	40 mM Tris-HCl
	In water
Cryoprotectant solution	30% glycerol
	30% ethylene glycol
	0.02 M phosphate buffer pH 7.4
HEPES-buffered Krebs-like buffer (HBK)	143 mM NaCl
	4.7 mM KCl
	1.3 mM $MgSO_4$
	1.2 mM $CaCl_2$
	20 mM HEPES
	0.1 mM NaH_2PO_4
	10 mM D-glucose
	In water pH adjusted to 7.4
Astrocytes culture media	10% FBS
	1% P/S
	In DMEM
Trypsin/DNase solution	2 g trypsin
	100 mg DNase
	In 200 ml HBSS

3.2 Methods for *ex vivo* experiments

3.2.1 Primary neuron-enriched cultures

Primary mixed cortical and hippocampal neurons were isolated from newborn mice (postnatal day 0-1). Animals were sacrificed by decapitation. Cortex and hippocampus were rapidly dissected in cold HBSS containing Ca^{2+} and Mg^{2+} and subjected to the digestion with papain (Sigma P3125-100mg) in enzyme solution for 1 hour at 37°C by shaking at 900 rpm. 20-25 units of papain in 1 ml of enzyme solution were used for the digestion of the dissected tissues. The digestion was stopped by replacing the enzyme solution with stop solution for 5 minutes at 37°C by shaking at 900 rpm. Afterwards, the tissue was washed (2x) in Neurobasal plating medium. Finally, the tissue was gently resuspended in the same medium using a pipette, and plated in 6-well plates precoated with poly-D-lysine (Corning Biocoat- 356413) (800,000 cells/well). Neurons were cultured for 10-12 days *in vitro* before being used for Western blotting or qRT-PCR. The medium was not changed during the culture period.

For insulin treatment experiments, the Neurobasal medium was removed from the culture and fresh Neurobasal without B27 supplemented with 1% P/S and 1% glutamax was added to the plates for 3 hours. Thereafter, Neurobasal medium was removed and 250 nM of insulin (Sigma-I9278) prepared in Neurobasal without B27 supplements was added on the plates for 15 minutes. The medium was then removed and washed with PBS twice before adding lysis buffer. The lysates were then used for Western blotting.

3.2.2 Immunocytochemistry in primary neurons

Neurons from postnatal day 0 pups were prepared as mentioned in section 3.2.1. 100k neurons were seeded in one well of a 24-well plate containing coverslips coated with poly-D lysine (Corning Biocoat- 354086). The neurons were cultured for 10 days before the staining procedure. Subsequently, the Neurobasal medium was removed and the neurons were washed twice with PBS before fixing in 4% PFA in PBS for 10 minutes at room temperature (RT). The fixative was removed and the neurons were washed twice with PBS. Thereafter, they were treated with

0.1% Triton in PBS for 5 minutes to permeabilize the cells. To remove unspecific binding of antibodies, the neurons were incubated in 5% BSA in PBS (blocking solution) for 1 hour. The blocking solution was removed and the neurons were incubated with the respective primary antibodies (prepared in the blocking solution) overnight at 4°C. After washing in PBS twice, the fluorophore-labeled secondary antibody (diluted 1:1000 in blocking solution) was added for 1 hour at RT. The neurons were washed from unbound secondary antibodies in PBS (3x) with the pre-final wash including DAPI (1:5000 diluted in PBS) to label the nuclei. The coverslips were mounted onto glass slides using fluorescent mounting medium (Dako-S3023).

3.2.3 Colocalization studies and quantification

For quantifying the degree of colocalization between IR and cell compartment markers, the cells were stained as described in section 3.2.2. Images were acquired using a Leica SP8 laser scanning microscope. For quantification of colocalization, Colocalization Threshold plugin in the Fiji software was used. Manual selection was used to draw the region of interest encompassing the cells. Single z-plane images were used to calculate thresholded Mander's coefficient (tM) which measures the degree of colocalization in each channel with tM=0 representing no colocalization and tM=1 representing perfect colocalization.

3.2.4 ELISA for GLUT4

Lysates from neurons were prepared by adding lysis buffer directly into the cell culture dish. The protein quantity in the lysates were quantified using BCA assay and 30 µg lysate was used for the quantification of GLUT4 using the available enzyme-linked immunosorbent assay kit (Fine Test EM1079) according to manufacturer's recommendations.

3.2.5 Glucose uptake assay in primary neurons

Primary neuron-enriched cultures prepared from the brains of newborn mice (postnatal day 0-1) from WT and KO lines were cultured as described before for 10 days (section 3.2.1). The neurons were then incubated in medium without B27 supplement containing 1% BSA for 3 hours. Next, the neurons were further incubated in Neurobasal medium with 2.5 mM glucose with 1% BSA for 3 hours. Thereafter, 5 mM 6-NBDG glucose (Cayman Chemical 13961) with or without 250 nM insulin (prepared in 2.5 mM glucose Neurobasal medium) was added for 30 minutes. Finally, the cells were washed with PBS and lysed to quantify the cellular uptake of 6-NBDG by measuring the fluorescence at 535 nM. The glucose uptake in the neurons measured by total fluorescence units was normalised to the total protein content.

3.2.6 IDE enzyme activity assay

IDE enzyme activity in neurons and brain lysates were quantified as per the kit instructions (Anaspec SensoLyte 520 IDE activity assay kit; Catalog no: AS-72231). Briefly, the lysates were prepared by centrifuging neuronal cell suspension or homogenised brain samples in assay buffer at 10,000 g for 10 minutes at 4°C. The IDE substrate solution was prepared by a 100-fold dilution in the assay buffer. The protein content in the lysates were quantified using BCA assay (Thermo Scientific 23228) and equal amount of proteins were loaded in duplicates in a 96-well plate. The total volume of all the wells were brought to 50 µl using assay buffer. As a positive control, purified IDE enzyme solution (provided in the kit) was used and the assay buffer served as a negative control. The enzymatic reaction was set up by adding 50 µl of IDE substrate solution to each well followed by incubating the plates at 37°C for 30 minutes. The fluorescence intensity was measured by a spectrophotometer with excitation/emission at 490 nm/520 nm. The IDE enzyme activity in the samples were calculated from the standard curve and normalised to the protein content in the lysates.

3.2.7 Acute and chronic inhibitor treatments in primary neurons

Acute and chronic treatments of pharmacological inhibitors on primary neurons were done to evaluate the impact of insulin signaling on IDE levels. For acute inhibition of AKT, the neurons were either treated with 250 nM insulin for 15 minutes or with a combination of insulin (250 nM) and 50 µM LY294002 (Cell Signaling 9901S)- AKT inhibitor after preincubation with LY294002 for 1 hour. The treatments were followed by total lysate preparation for Western blotting. For acute inhibition of ERK and JNK, the neurons were incubated either with 20 µM of PD98059 (Cell Signaling 9900L)- ERK inhibitor or with 25 µM of SP600125 (Cell Signaling 8177S) JNK inhibitor for 1 hour followed by total lysate preparation for Western blotting. Chronic inhibition of insulin signaling was performed by treating neurons either with 100 nM Wortmannin (Cell Signaling 9951) an AKT inhibitor or 20 µM PD98059 for 2 hours, 6 hours or 24 hours followed by total lysate preparation for Western blotting.

3.2.8 Astrocyte cultures

Primary astrocyte cultures were prepared from brains of newborn mice (postnatal day 0-1). Cortex and hippocampus were dissected and subjected to enzymatic digestion by Trypsin/DNase solution. The tissues were then mechanically dissociated using a sterile plastic Pasteur pipette. The dissociated tissue along with the DMEM media was centrifuged at 200 g for 10 minutes at room temperature. The pellet was resuspended in DMEM media and plated on poly-D-lysine coated T75 flask. After 2 days, the flasks were washed rigorously with PBS to remove unattached and dead cells. Fresh DMEM was added to the cells which were cultured for 4 more days after which the lysates were prepared for Western blotting. Additionally, medium was collected for analysis of IDE expression.

3.2.9 Synaptosome preparations and treatments

Frozen cortex from mice (200 mg) were homogenised in 500 µl of SynPer reagent (Thermo Scientific 87793) with 1% protease and phosphatase cocktail. The homogenate was then centrifuged at 1200 g for 10 minutes at 4°C. The supernatant

was subsequently centrifuged at 15000 g for 20 minutes at 4°C. The pellet was then resuspended in HBK buffer and was divided into 4 separate fractions of equal volumes. The first fraction served as a control as no treatments were done. To the second fraction, 8 mM ATP was added. 250 nM insulin was added to the third fraction. A combination of 8 mM ATP and 250 nM insulin was added to the fourth fraction. These fractions were then incubated at 37°C for 15 minutes. Thereafter, these fractions were centrifuged at 10,000 g for 10 minutes at 4°C. Finally, the pellets were resuspended in 200 µl of RIPA buffer, protein content quantified by BCA and equal protein loaded onto gels for Western blotting.

3.3 Methods for *in vivo* experiments

3.3.1 Generation of cKO mouse line

Mice lacking SORLA (KO) were generated in the laboratory of Thomas Willnow. The scheme for generating this mouse line has been described previously (Andersen et al., 2005). For generation of neuron specific SORLA KO, Baf53b-Cre transgenic mice expressing Cre recombinase under the control of the mouse *Actl6b* gene promotor were purchased from Jackson Laboratories (Stock no. 027826) and has been described elsewhere (Zhan et al., 2015). Baf53b-Cre (*Cre* +/+; *Sorl1* +/+) mice were then bred with SORLA floxed mice (*Cre* -/-; *Sorl1* rec/rec) producing F1 generation mice (*Cre* +/-; *Sorl1* rec/+). The F1 mice was then bred with SORLA floxed mice to generate cKO (*Cre* +/-; *Sorl1* rec/rec) and WT (*Cre* -/-; *Sorl1* rec/rec) littermates. Animals were routinely genotyped by PCR using the primers listed in section 3.1.1 and the genotyping procedures are described in section 3.4.1. All animal experiments were approved by local ethics committees (LAGESO, Berlin, Germany). Animals were housed in the facility with controlled environmental parameters under a 12 hours light/12 hours dark cycle. Mice were either fed with standard chow (4.5% crude fat, 39% carbohydrates) or high-fat diet chow (34.6% crude fat, 10% carbohydrates) purchased from ssniff Spezialdiäten GmbH (E15741-347). Only male mice were used in all experiments at 10-25 weeks old, unless stated otherwise.

3.3.2 Mouse tissue collection for Western blot and qRT-PCR

Mice were sacrificed by cervical dislocation. Cortex, hippocampus, hypothalamus, liver, muscle and gonadal white adipose tissue were rapidly dissected and frozen in liquid nitrogen. The tissues were stored at -80°C until further processing.

3.3.3 Immunofluorescent stainings on brain sections

Brains were dissected and fixed with 4% paraformaldehyde (w/v) in PBS overnight at 4°C. They were further rinsed in PBS and transferred in 30% sucrose (w/v) in PBS. After being equilibrated in the sucrose solution, brains were frozen and sectioned (25 µm coronally) on a sliding microtome SM2000R (Leica Biosystems). Brain free-floating sections were stored at -20°C in cryoprotectant solution. For stainings, the sections were washed and fixed in 4% paraformaldehyde (w/v) in PBS for 10 minutes. Further, the sections were permeabilised in 0.5% Triton in PBS for 10 minutes followed by blocking in 5% donkey serum for 2 hours at room temperature. Thereafter, the sections were incubated overnight at 4°C in primary antibody diluted in blocking solution. After being washed in PBS-T(4x), the sections were transferred in the fluorophore-labeled secondary antibody solution (diluted in blocking buffer) and incubated for 2 hours at RT. The sections were washed from unbound secondary antibodies in PBS-T (4x) with the pre-final wash including DAPI (1:3000 diluted in PBS-T) to label the nuclei. The sections were mounted onto glass slides using fluorescent mounting medium (Dako).

3.3.4 Evaluation of insulin signaling and glucose uptake in mice brain

Intraperitoneal (i.p.) insulin injections were performed in mice to evaluate the activation of insulin signaling proteins in the brain. The mice were injected with 5 units of human recombinant insulin (Sigma- I9278) dissolved in PBS or saline. Thereafter, they were sacrificed by cervical dislocation after 15 minutes and total lysates were prepared from cortex, hippocampus and hypothalamus which were then subjected to protein quantification by Western blotting.

For the evaluation of glucose uptake, 100 µl of 5 mM 6-NBDG was injected i.p. in mice. After 20 minutes, the animals were sacrificed by cervical dislocation and total lysates were prepared from cortex, hippocampus and hypothalamus. The lysates were then subjected to spectrophotometric quantification of 6-NBDG with excitation/emission at 465/535 nm. The relative fluorescence units (rfu) measured were normalised to the total protein content.

3.3.5 Animal feeding studies and NMR measurements

Normal chow and high-fat diet feeding (diet composition mentioned in section 3.3.1) in mice were carried out from week 10 until week 20 of age. Body weight measurements were done weekly during this period on the same day of the week and at the same time. After the dietary intervention, body composition was determined by time-domain nuclear magnetic resonance imaging (NMR) in conscious mice post a 6-hour fasting period. NMR was done by the personnel from the Phenotyping platform at the Preclinical Research Centre (PRC) at MDC, Berlin.

3.3.6 Glucose and insulin tolerance tests

The glucose tolerance test (GTT) was performed to identify impaired glucose tolerance in mice. For GTT, the mice were fasted for 16 hours, their body weight measurements were taken and the blood glucose levels were measured from tail tip blood using a glucometer (time point 0 minutes). Thereafter, the mice were i.p. injected with D-glucose (dissolved in PBS) at a dose of 2 mg/kg of body weight. The blood glucose levels were measured every 20 minutes until 2 hours. For evaluation of GTT, the blood glucose levels were plotted against time and the area under the curve (AUC) was derived from the graph.

Insulin tolerance test (ITT) was performed to determine the sensitivity of insulin-responsive tissues in mice. For ITT, the mice were fasted for 6 hours, their body weight measurements were taken and the blood glucose levels were measured from tail tip blood using a glucometer (time point 0 minutes). Thereafter the mice were i.p. injected with human recombinant insulin (Sigma- I9278) dissolved in PBS at a dose of 0.75 U/kg of body weight. Blood glucose levels were measured every 20 minutes until 2 hours.

3.4 General methods

3.4.1 PCR for mouse genotyping

Genomic DNA for PCR genotyping was obtained from mouse ear. Biopsied tissue was incubated for 30 minutes at 95°C in base solution, followed by addition of the equal volume of neutralization solution. Extracted DNA was used for genotyping *Cre* with the following cycling conditions: (1) initial denaturation (2 minutes, 94°C), (2) denaturation (15 seconds, 94°C), (3) annealing (15 seconds, 60°C) (4) elongation (30 seconds, 72°C). Steps (2) to (4) were repeated 35 times in total. The cycle conditions for genotyping *Sorl1* were: (1) initial denaturation (2 minutes, 94°C), (2) denaturation (15 seconds, 94°C), (3) annealing (15 seconds, 63°C) (4) elongation (30 seconds, 72°C). Steps (2) to (4) were repeated 39 times in total. Primers used for PCR are listed in Table 3.1. The composition of the reaction mixture was as follows: Taq DNA polymerase (Biozym Scientific GmbH 0.025 U/µl), 1x Biozym Buffer, 0.2 mM of each deoxynucleotide triphosphates, 0.2 µM primers. PCR products were resolved on 2% agarose gels. Expected sizes of PCR products used for determination of mouse genotypes were -100 bp for Cre allele; sorla allele – 220 bp (WT) and 412 bp (rec).

3.4.2 SDS Polyacrylamide gel electrophoresis and Western blotting

Mouse tissue lysates were prepared by homogenizing the tissue in lysis buffer containing protease and phosphatase inhibitors. Primary neurons were directly lysed in the culture dish. The lysates were further incubated in lysis buffer for 1 hour at 4°C under constant rotation for efficient lysis. Lysates were cleared by centrifugation at 14000 x g, 4°C for 15 minutes. Protein concentration was determined using BCA assay. Lysates with adjusted protein concentration were mixed with 4x Laemmli sample buffer and boiled at 95°C for 5 minutes. Equal amount of proteins was resolved on 8-10 % polyacrylamide gels by means of SDS-PAGE. Gels were run in running buffer at 100 V using power supply from Biometra GmbH. Resolved proteins were transferred to nitrocellulose membrane with 0.22 µm pore size. Protein transfer was conducted in a transfer buffer at 125 mA for 90 minutes using the wet blotting system from Bio-Rad Laboratories. After the transfer,

membranes were blocked for 1 hour in 5% skimmed milk powder in TBS-T. Membranes were subsequently incubated overnight at 4°C in a primary antibody against the protein of interest diluted in blocking buffer. After extensive washing in TBS-T, the membranes were incubated for 1 hour in peroxidase-labeled secondary antibody recognizing immunoglobulin G (IgG) fragments of the primary antibody species. Secondary antibodies (Sigma-Aldrich) were diluted 1:10000 in blocking buffer. After washing in TBS-T, membranes were developed by enhanced chemiluminescence detection method using SuperSignal West Substrate (Thermo Scientific). Bands intensity was analyzed by densitometric scanning using Fiji software (ImageJ).

3.4.3 RNA isolation and quantitative real-time PCR (qRT-PCR)

For RNA isolation from mouse tissues, they were first homogenized in TRIzol reagent (AMBION GmbH 15596026). Chloroform was added to the homogenates at the ratio 1:5 (v/v). The mixture was subjected to centrifugation at 12000 x g, 4°C for 10 minutes. The upper, aqueous phase containing RNA was taken and gently mixed with 70% ethanol at the ratio 1:1 (v/v). The resulting solution was applied to silica-membrane column of RNeasy Mini Kit (Qiagen 74106). DNase treatment of the sample was performed directly on the purification column by addition of RNase-free DNase I (from the kit) and subsequently after a few washes the isolated RNA was suspended in 30 µl of RNAse free water.

RNA isolation from primary neurons was done according to the manufacturer's instruction from the RNeasy Mini Kit. In short, the neurons were lysed by lysis buffer (provided in the kit) in the dish. For a uniform cell suspension devoid of aggregates, the lysate was passed through a 30G needle 5 times. To the lysates, an equal amount of 70% ethanol was added and the resulting solution was then used for column-based isolation of RNA similar to what was done for tissues.

RNA concentrations were determined using the NanoDrop ND-1000 spectrophotometer. Equal amounts of purified RNA, 50 ng to 1 µg, were used for complementary DNA (cDNA) synthesis using High-Capacity RNA to cDNA Kit (Thermo Fisher 4368814). cDNA (in triplicates) concentrations were measured using the 7900 HT Fast Real time PCR System (Thermo Fisher).

Data were analysed using the cycle threshold (Ct) comparative method (2^{-ddCt}) normalizing to Ct values of housekeeping gene. The Ct value for a housekeeping mRNA was subtracted from the Ct value for the mRNA of interest to ensure equal amount of cDNA in each well (dCt). For comparison of multiple samples, the dCt value of the internal control was subtracted from the dCt values of the other samples (ddCt) and data were presented as $\log_2$ fold change in expression.

3.5 Statistics

Statistical analysis was performed using GraphPad Prism software (version 7.0). For comparison between two experimental groups, unpaired Student's t test was used. One- or two-way analysis of variance (ANOVA) with Bonferroni multiple comparison post-test was used to compare three or more experimental groups. A p value of less than 0.5 was considered to be statistically significant with * representing $p<0.05$, ** representing $p<0.01$, *** representing $p<0.001$ and **** representing $p<0.0001$. All quantitative data are shown as mean + standard error of the mean (SEM), if not otherwise stated.

4 Results

4.1 Studies in primary neuron-enriched cultures

4.1.1 SORLA deficiency impairs insulin signaling in primary neuron-enriched cultures

Impaired insulin signaling in the brain is a common feature in several neurodegenerative disorders. Previously, it has been shown that SORLA facilitates insulin signaling in adipocytes (Schmidt et al., 2016). A role for this receptor in the context of neuronal insulin signaling hasn't been examined yet.

To understand if SORLA regulates neuronal insulin signaling, I tested the levels of key insulin signaling proteins in primary neurons cultured from wildtype (WT) mice and from animals carrying a targeted disruption of the murine *Sorl1* gene (KO). For this, I generated primary neurons from the brains of postnatal day 0-1 mice (neonates) and cultured them for 10 days. Thereafter, total neuronal lysates were prepared and subjected to Western blot analysis to assess the total and phosphorylated levels of key insulin signaling proteins, including the insulin receptor (IR), protein kinase B (AKT) and glycogen synthase kinase 3β (GSK3β). Interestingly, the total levels of IR under basal condition were higher in WT neurons than in KO neurons (Figure 4.1A-B). Phosphorylation of the IR is detected only upon insulin stimulation, hence no bands for phosphorylated IR (pIR) were detected under the basal condition (data not shown). The total and phosphorylated levels of IR downstream proteins AKT and GSK3β, which regulate glucose uptake and glycogen synthesis, respectively, as well as the ratios of the phosphorylated to the total levels of these proteins were unaltered in WT and KO neurons.

Next, to understand whether increased IR protein levels in WT neurons were a consequence of altered transcription or post-transcriptional mechanisms, I performed quantitative real-time PCR to quantify the insulin receptor (*Insr*) transcript levels in WT and KO neurons under basal conditions. No significant differences in *Insr* transcript levels were observed comparing the two genotypes (Figure 4.1C), implicating post-transcriptional mechanisms in SORLA-dependent control of IR levels in WT neurons.

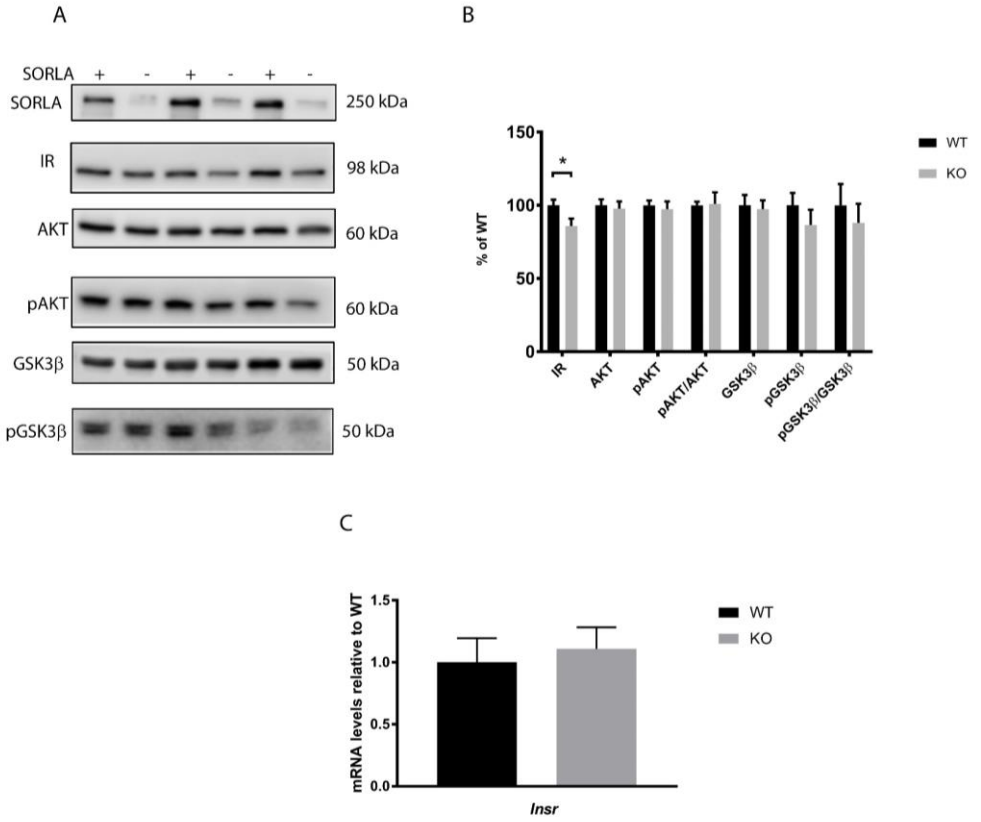

Figure 4.1: Basal levels of key proteins and their gene transcripts in the insulin signaling pathway in primary neurons. (**A-B**) Representative Western blots documenting basal levels of indicated proteins (A) and densitometric quantification of replicate Western blots (B) from primary neuron-enriched cultures prepared from brains of postnatal day 1 (P1) neonates of WT (SORLA +) and KO (SORLA -). Values are given as mean + SEM and presented as percentage of the WT (set to 100%). Unpaired Student's *t* test was used to calculate the significance of differences between the genotypes (*, $p<0.05$) (**C**) Quantitative real-time PCR for transcript levels of the insulin receptor (IR) encoding gene performed in primary neuron-enriched cultures prepared from brains of P1 neonates from WT and KO mice. The mRNA levels are expressed relative to the levels in WT (set to 1). Unpaired Student's *t* test was used to calculate the significance of differences between the genotypes. Three independent experiments in 3 mice per genotype were performed. (pAKT: phospho AKT; pGSK3β: phospho GSK3β)

SORLA regulates the post-transcriptional levels of several proteins by trafficking them to different intracellular compartments thereby determining their cellular fate. Previously, in adipocytes it has been shown that SORLA retrieves IR from early endosomes and brings it back to the *trans*-Golgi network (TGN), thereby preventing its lysosomal catabolism (Schmidt et al., 2016).

To understand if SORLA-dependent increase in IR levels in WT neurons was due to altered receptor trafficking, I performed co-immunofluorescence stainings for the

IR and different cell compartment markers in WT and KO neurons. Both in WT and KO neurons, IR molecules were co-stained with markers of the early endosome (EEA1), fast recycling endosome (RAB4), slow recycling endosome (RAB11), late endosome (RAB9), and Golgi compartment (VTI1A and VTI1B). In WT neurons, IR localized more to fast recycling endosomes (RAB4) and less to late endosomes (RAB9) as compared to the situation in KO neurons (Figure 4.2A-B). In absence of SORLA, IR preferentially trafficked to the late endosomal compartment as evidenced by its increased colocalization with RAB9. Increased targeting of the IR to late endosomes, followed by lysosomal catabolism, may explain the decreased levels of the IR seen in KO neurons (Figure 4.2C).

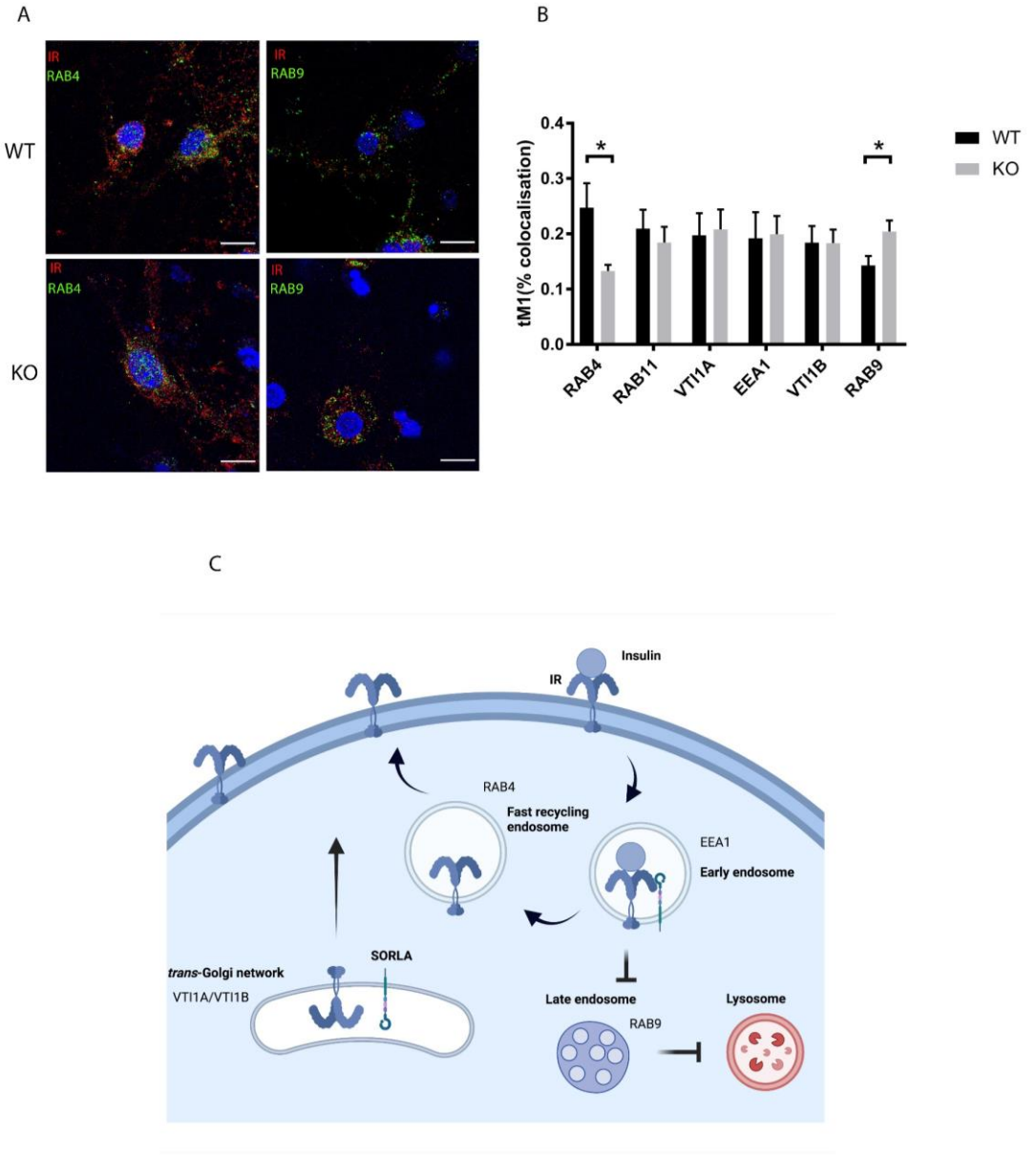

Figure 4.2: Insulin receptor (IR) trafficking in primary neurons. (A-B) Representative images (A) for co-immunostaining of the IR (red) with RAB4 and RAB9 (green) in WT and KO neurons and (B) the quantification of colocalisation using Mander's coefficient are shown. Nuclei were stained with DAPI (blue). Twenty-five cells were imaged from each genotype. Unpaired Student's *t* test was used to calculate the significance of differences between the genotypes (*, $p<0.05$). Scale bar: 20 µm. Values are given as mean + SEM. (**C)** Schematic of SORLA-mediated IR trafficking in neurons under basal condition. EEA1-early endosome; RAB4 and RAB11-recycling endosome; RAB9-late endosome/lysosome; VTI1A and VTI1B-Golgi.

I hypothesized that increased basal IR levels in WT neurons may lead to enhanced insulin signal reception in these cells. To examine this concept, I treated WT and KO neurons with 250 nM insulin for 15 minutes. Thereafter, total neuronal lysates were generated and subjected to Western blot analysis. Specifically, the activation

of key insulin signaling proteins was evaluated by quantifying the ratio of the phosphorylated to the total protein levels. In WT neurons, the total levels as well as levels of activated forms of the pIR and phosphorylated AKT (pAKT) were higher compared to KO neurons. However, there was no difference in the total as well as the activated levels of GSK3β comparing the two genotypes (Figure 4.3A-B). Still, these findings confirm a proposed role for SORLA in increasing IR activity in neurons in response to insulin.

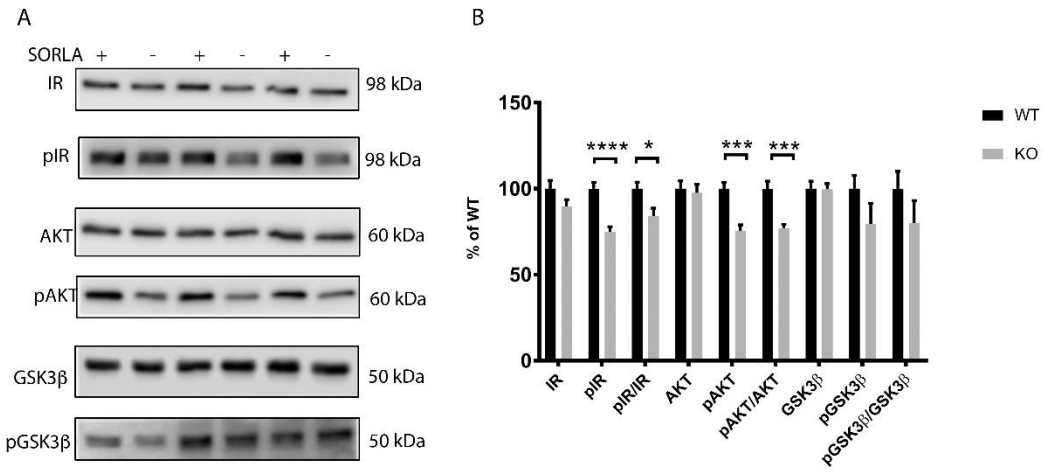

Figure 4.3: Levels of key proteins in the insulin signaling pathway in primary neurons treated with insulin. (**A-B**) Representative Western blots documenting levels of the indicated proteins (A) and densitometric quantification of replicate Western blots (B) from primary neuron-enriched cultures prepared from brains of postnatal day 1 neonates of WT (SORLA +) and KO (SORLA -) mice treated with 250 nM insulin for 15 minutes. Three independent experiments in cultures of 3 mice per genotype were performed. Values are given as mean + SEM and presented as percentage of the WT level (set to 100%). Unpaired Student's *t* test was used to calculate the significance of differences between the genotypes (*, $p<0.05$; ***, $p<0.001$; ****, $p<0.0001$). (pIR: phospho IR; pAKT: phospho AKT; pGSK3β: phospho GSK3β)

4.1.2 Loss of SORLA does not affect glucose uptake in neurons

Insulin signaling results in increased cellular uptake of glucose in skeletal muscle and adipose tissue (Boucher et al., 2014). To test whether an increase in neuronal insulin signaling in WT as compared to KO neurons affected glucose uptake concordantly, neurons of both genotypes were treated with 6-NBDG, a fluorescent glucose analog with or without the co-application of insulin. After the treatment, the glucose uptake was evaluated by measuring the fluorescence of 6-NBDG using a spectrophotometer, in neuronal lysates from WT and KO mice after normalising it to the total protein content.

In the absence of insulin, there was no difference in glucose uptake between the two genotypes (Figure 4.4A, condition: Insulin -). Following insulin treatment (Figure 4.4A, condition: Insulin +), there was neither an appreciable increase in glucose uptake when compared with the respective non-insulin treated condition, nor were there any genotype-dependent differences.

To mechanistically understand the glucose uptake process driven by the different glucose transporters in my primary neuron-enriched cultures, I evaluated the expression of GLUT3, which mediates basal glucose uptake, and of GLUT4, which mediates insulin-stimulated glucose uptake (Szablewski, 2017). When I tested the expression of GLUT3 in WT and KO neuronal cultures by Western blot, no genotype-dependent differences were observed (Figure 4.4B). To test the expression of GLUT4, I initially performed Western blot analysis on neuronal lysates from WT and KO neurons. However, due to its low neuronal expression levels, no immunoreactive bands for GLUT4 were detected (data not shown). Therefore, I used a commercial ELISA for quantification of GLUT4, hoping for an increased sensitivity for the detection of this low abundant protein. As a positive control, lysates from gonadal white adipose tissue (gWAT- tissue expressing high GLUT4 levels) from 20 weeks adult WT and KO mice were used. As expected, GLUT4 levels in the neuronal lysates were significantly lower as compared with gWAT (data not shown). This finding validated the assay performance. Interestingly, GLUT4 protein levels were significantly higher in KO neurons as compared to WT neurons (Figure 4.4C). Conceptually, an increased insulin signal reception in WT as compared to KO neurons is expected to lead to higher glucose uptake in cells expressing SORLA. However, the increased levels of GLUT4 seen in KO neurons may represent a compensatory mechanism, explaining comparable glucose uptake rates in the two genotypes.

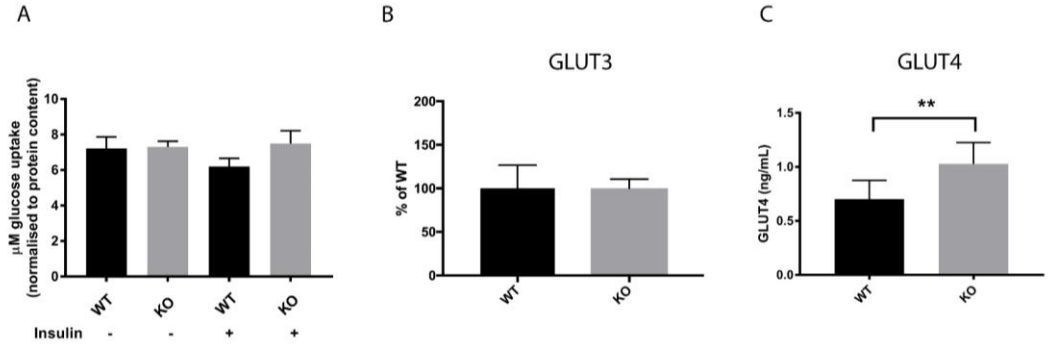

Figure 4.4: Loss of SORLA does not impact glucose uptake or levels of major glucose transporters in primary neurons. (A) Primary neuron-enriched cultures prepared from the brains of postnatal day 1 neonates (P1) from WT and KO lines were cultured for 10 days. The neurons were then incubated in medium without B27 supplement containing 1% BSA for 3 hours. Next, the neurons were further incubated in Neurobasal medium with 2.5 mM glucose with 1% BSA for 3 hours. Subsequently, 5 mM 6-NBDG glucose with or without 250 nM insulin (prepared in 2.5 mM glucose Neurobasal medium) was added for 30 minutes. Finally, the cells were washed with PBS and lysed to quantify the cellular uptake of 6-NBDG by measuring the fluorescence at 535 nm The glucose uptake normalised to total protein content is shown. **(B)** Densitometric quantification of replicate Western blots for detection of GLUT3 in WT and KO primary neuron-enriched cultures are shown. **(C)** GLUT4 protein levels in primary neuron-enriched cultures from P1 WT and KO mice was measured using ELISA. All the experiments were repeated thrice with 2-3 mice per genotype. All values are expressed as mean + SEM. Unpaired Student's *t* test was used to calculate the significance of differences between the genotypes (**, $p<0.01$).

4.1.3 Levels of insulin degrading enzyme (IDE) are reduced in SORLA-deficient neurons

Impaired insulin signaling affects the levels of several amyloid degrading enzymes responsible for clearance and degradation of Aβ (Carro & Torres-aleman, 2004; González-Casimiro et al., 2021). To understand whether SORLA-dependent IR activity in neurons has an impact on the levels of these amyloid degrading enzymes, I prepared lysates from WT and KO primary neurons and performed Western blot analysis for quantification of neprilysin, major amyloid degrading enzyme as well as IDE, a protease that degrades insulin but also Aβ (Jha et al., 2015). No differences in neprilysin levels were observed between the two genotypes (Figure 4.5A-B). However, levels of both IDE protein (Figure 4.5C-D) and *Ide* transcript (Figure 4.5E) were significantly higher in WT as compared to KO neurons. To confirm that increased IDE protein levels translated into an increased enzyme activity, the ability of IDE to cleave a fluorescently-labelled substrate was evaluated in neuronal lysates by spectrophotometric analysis. Indeed, the IDE activity was significantly higher in WT compared to KO neurons (Figure 4.5F).

Taken together, SORLA increases both expression and activity of IDE in neurons. These results are interesting as they suggest that SORLA decreases amyloid levels in the brain not only by preventing APP processing into Aβ (Andersen et al., 2005), but also by promoting amyloid degradation by IDE.

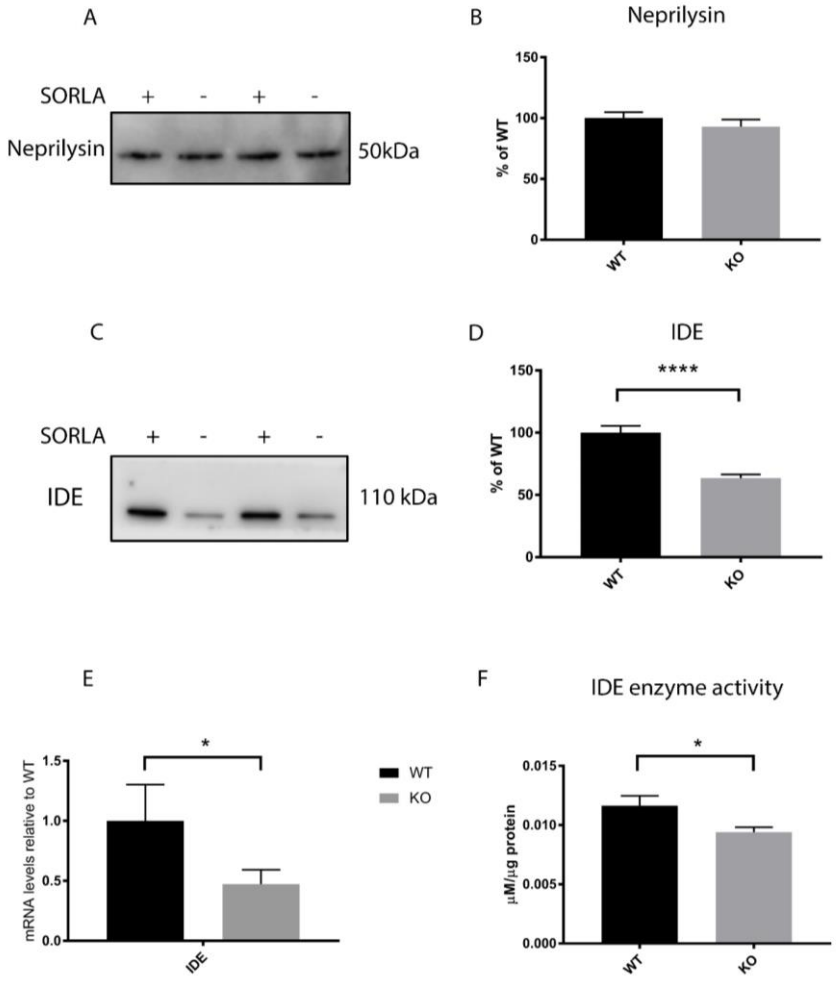

Figure 4.5: Levels of protein and transcript for amyloid degrading enzymes in primary neurons. (A-B) Representative Western blot scans of Neprilysin (A) and densitometric quantification of replicate Western blots (B) performed on primary neuronal cell lysates from WT and KO brains of postnatal day1 neonates are shown. (**C-D**) Western blot images of IDE levels (C) and densitometric quantification of replicate Western blots (D) show increased levels of IDE in WT compared to KO neurons. (**E**) Quantitative real-time PCR for *Ide* transcripts was performed in primary neuron-enriched cultures from P1 WT and KO mice. Transcript levels are expressed relative to the levels in WT (set to 1). **(F)** IDE activity in lysates from P1 WT and KO primary neuron-enriched cultures were quantified by measuring fluorescence upon cleavage of an IDE-specific FRET substrate. Levels were normalised to the total protein content (see method section for details). Three independent experiments with 3 mice per genotype were performed. All values are mean + SEM and are represented as percentage of the WT (set to 100%) in B and D or as relative levels to WT in E or as actual values in F. Unpaired Student's *t* test was used to calculate the significance of differences between the genotypes (*, $p<0.05$; ****, $p<0.0001$).

Primary neuron-enriched cultures used herein contain mainly neurons, but also contaminating astrocytes. To test the cell-specific expression pattern of IDE in my cultures, I performed co-immunofluorescent stainings of IDE with the neuronal marker microtubule associated protein 2 (MAP2) and the astrocytic marker glial fibrillary acidic protein (GFAP) in neuron-enriched cultures from WT and KO neonates. IDE immunosignals were not limited to neurons but also seen in astrocytes of WT and KO neuron-enriched cultures (Figure 4.6A).

To ascertain that the differences in IDE levels seen in neuron-enriched cultures from WT as compared to KO mice were a consequence of SORLA function specific to neurons and not in contaminating astrocytes, I prepared astrocyte cultures from WT and KO mice and tested for IDE expression by Western blot in total lysates prepared from these cultures. There was no difference in IDE expression levels comparing the two genotypes in these astrocytic cultures (Figure 4.6B-C). It has been reported that IDE is secreted by astrocytes in culture (Son et al., 2016). However, IDE was not detected in supernatant from WT and KO astrocytic cultures which further substantiates my findings that the difference observed in IDE protein levels in primary neuron-enriched cultures was due to SORLA action specific to neurons and not in contaminating astrocytes.

Taken together, these results confirmed that the impact of SORLA on promoting IDE expression and activity in neuron-enriched cultures is specific to neurons and operates through a transcriptional mechanism of IDE gene expression control.

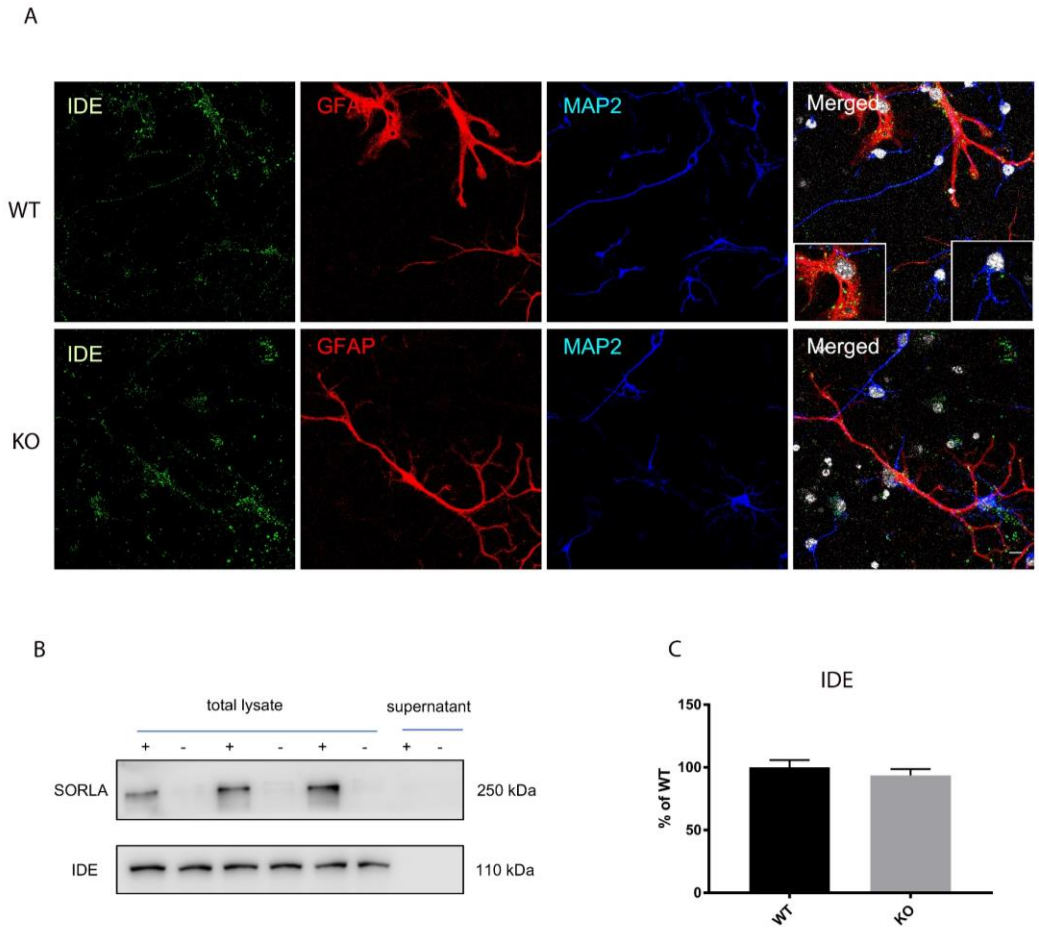

Figure 4.6: Insulin degrading enzyme (IDE) expression in neuron-enriched cultures and astrocytic cultures. (A) Co-immunofluorescent stainings of IDE (green) with GFAP (red) and MAP2 (blue) in neuron-enriched cultures from WT and KO neonates are shown. IDE expression is seen as distinct puncta in neuronal and astrocytic projections in the merged pictures (see insets for detail). Scale bar: 20 µm. **(B-C)** Representative Western blot images of IDE in total lysates and supernatant from astrocytic cultures prepared from brains of postnatal day 1 neonates from WT and KO lines (B) and densitometric quantification of replicate Western blots are shown (C). One experiment with 6 mice per genotype was performed. All values are mean + SEM and are given as percentage of the WT (set to 100%). Unpaired Student's *t* test was used to calculate the significance of differences between the genotypes.

4.1.4 IDE expression is not regulated by insulin signaling in neurons

Previously, chronic insulin treatment has been shown to upregulate IDE expression in neurons (L. Zhao et al., 2004). This report offered a possible mechanistic link between SORLA-dependent IR activity and IDE expression in neurons seen in my studies. However, in my studies, since acute insulin treatments (15 minutes) in neurons facilitated insulin signaling in presence of SORLA, I first investigated whether these treatments impacted IDE levels.

To do so, WT and KO neurons were either treated with insulin for 15 minutes or with a combination of insulin and LY294002, an inhibitor of AKT, a downstream effector of the insulin signaling pathway. Treatment was followed by total lysate preparation and Western blot analysis to test IDE expression. The assay worked as there was a substantial increase in pAKT levels in WT as well as KO neurons after insulin treatment when compared to their respective untreated controls. This increase in pAKT levels was completely abolished when the AKT inhibitor was added. However, neither insulin treatment nor the combination of insulin and LY294002 had any impact on IDE expression in WT (Figure 4.7A-B) or KO (Figure 4.7C-D) neurons.

In conclusion, my studies failed to corroborate a reported effect of insulin signaling on IDE expression in the acute time scale. Consistent with this observation, impaired insulin signaling through an effect on AKT cannot be held responsible for the decrease in IDE levels and activity in SORLA-deficient neurons.

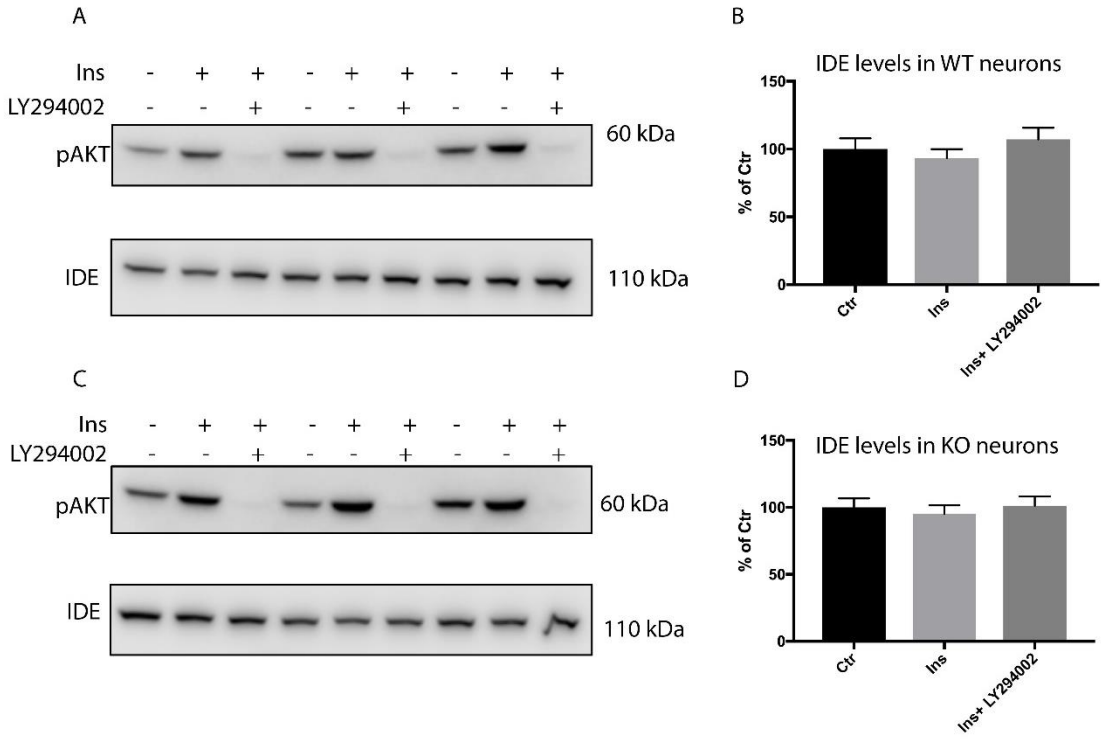

Figure 4.7: Acute insulin treatment does not affect insulin degrading enzyme (IDE) levels in primary neurons. (A-D) Primary neuron-enriched cultures from brains of postnatal day 1 WT and KO neonates were cultured for 10 days. The neurons were either treated with 250 nM insulin for 15 minutes (Ins+) or with a combination of insulin (250 nM) and 50 µM LY294002 (AKT inhibitor) after preincubation with LY294002 for 1 hour (Ins + LY294002). Representative Western blot images and densitometric quantification of replicate Western blots from WT (A and B) and KO (C and D) neurons are shown. Two independent experiments with 3 mice per genotype were performed. All values are

mean + SEM and are represented as percentage of control (set to 100%). One-way ANOVA was used to calculate the significance of differences between the treatments**.** (pAKT: phospho AKT)

The insulin signaling pathway consists of a metabolic arm regulated by AKT and a mitogenic arm regulated by extracellular signal-regulated kinases (ERK) and c-Jun-N-terminal kinase (JNK). Insulin-mediated upregulation of IDE expression via activation of ERK signaling pathway has been shown previously in astrocytes (Yamamoto et al., 2018). To understand whether the mitogenic arm of the insulin signaling pathway involving ERK and JNK has a similar effect on IDE expression in neurons, I inhibited the activity of these kinases in primary WT neuron-enriched cultures and tested the consequences for IDE levels. As expected, acute treatment with the ERK inhibitor PD98059 led to a substantial reduction in phospho ERK (pERK) levels when compared with untreated controls. However, an effect of these treatment on IDE expression was not observed (Figure 4.8A-B). In addition, to test whether JNK regulates IDE expression in neurons, acute treatment with the JNK inhibitor SP600125 were performed in WT neurons. A significant reduction in phospho JNK (pJNK) levels were observed after SP600125 treatment, when compared to untreated controls, but this had no impact on IDE expression (Figure 4.8C-D).

My studies involving pharmacological inhibition of AKT uncovered that acute insulin treatments does not regulate IDE levels in neurons. Additionally, inhibition of basal ERK and JNK did not impact IDE levels further substantiating our findings that SORLA-mediated IDE regulation in neurons is not insulin dependent on an acute time scale.

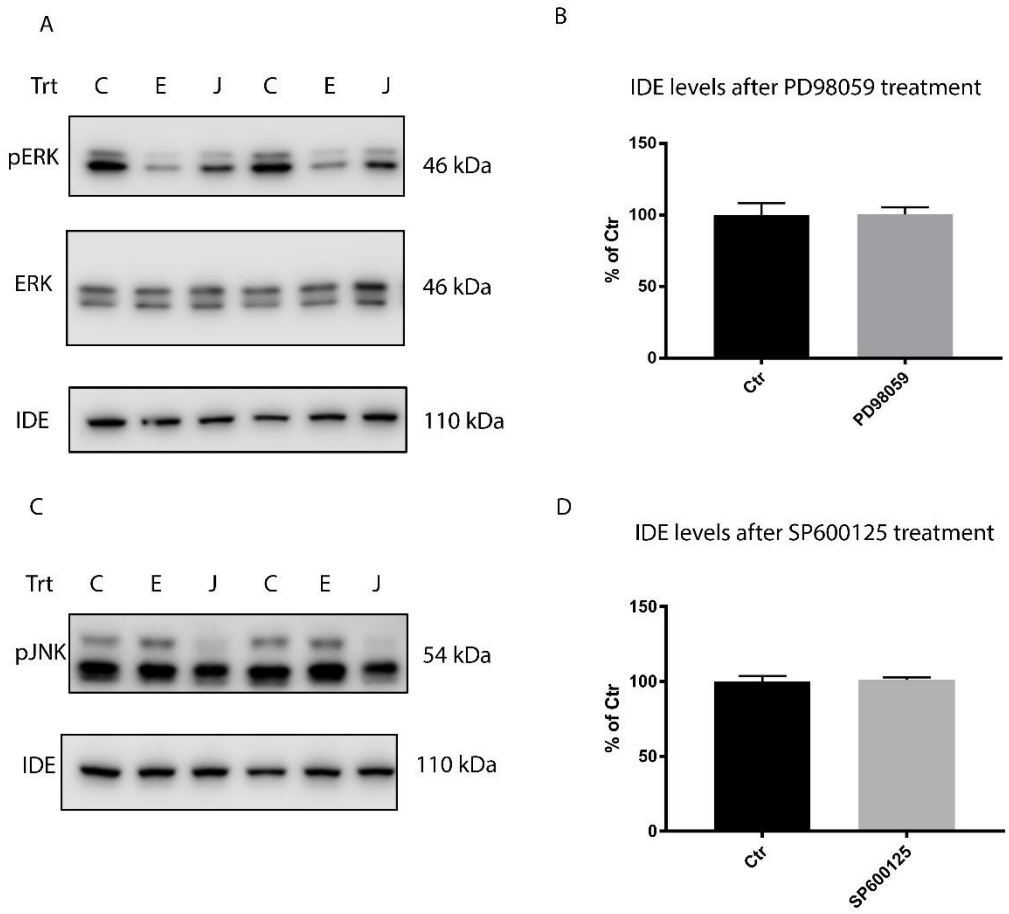

Figure 4.8: Insulin degrading enzyme (IDE) levels are unaffected by pharmacological inhibition of ERK and JNK. (A-D) Primary neuron-enriched cultures from brains of postnatal day 1 WT neonates were cultured for 10 days. The neurons were incubated either with 20 µM of PD98059 (ERK inhibitor) or with 25 µM of SP600125 (JNK inhibitor) for 1 hour followed by total lysate preparation. Representative Western blot images and densitometric quantification of replicate Western blots for ERK inhibitor treatments (A and B) and JNK inhibitor treatments (C and D) in WT neurons are shown. Two independent experiments with 3 mice per treatments were performed. All values are mean + SEM and are represented as percentage of the control (Ctr) (set to 100%). Unpaired Student's *t* test was used to calculate the significance of differences between the treatments**.** (Trt: Treatment; C: Control; E: ERK inhibitor; J: JNK inhibitor; pERK: phospho ERK; pJNK: phospho JNK)

Previously, all the studies that have shown insulin-mediated upregulation of IDE have employed chronic treatment of the hormone (Yamamoto et al., 2018; L. Zhao et al., 2004). To understand if chronic inhibition of AKT and ERK may affect the IDE levels in primary neurons, WT primary neuron-enriched cultures were subjected to treatment with Wortmannin (AKT inhibitor) or PD98059 (ERK inhibitor) for different time periods. In these experiments, I observed a substantial reduction in pAKT levels after Wortmannin treatment at all the time points when compared with the levels at time point 0 hours. However, chronic inhibition of AKT had no effect on

IDE levels in these neurons (Figure 4.9A-B). Similarly, PD98059 treatment in WT neurons led to a decrease in phosphorylated ERK compared to levels at time point 0 hours, but there was no effect of the treatments on IDE levels at any of the indicated time points (Figure 4.9C-D).

These results suggest that SORLA-mediated upregulation of IDE expression is independent of chronic insulin stimulation.

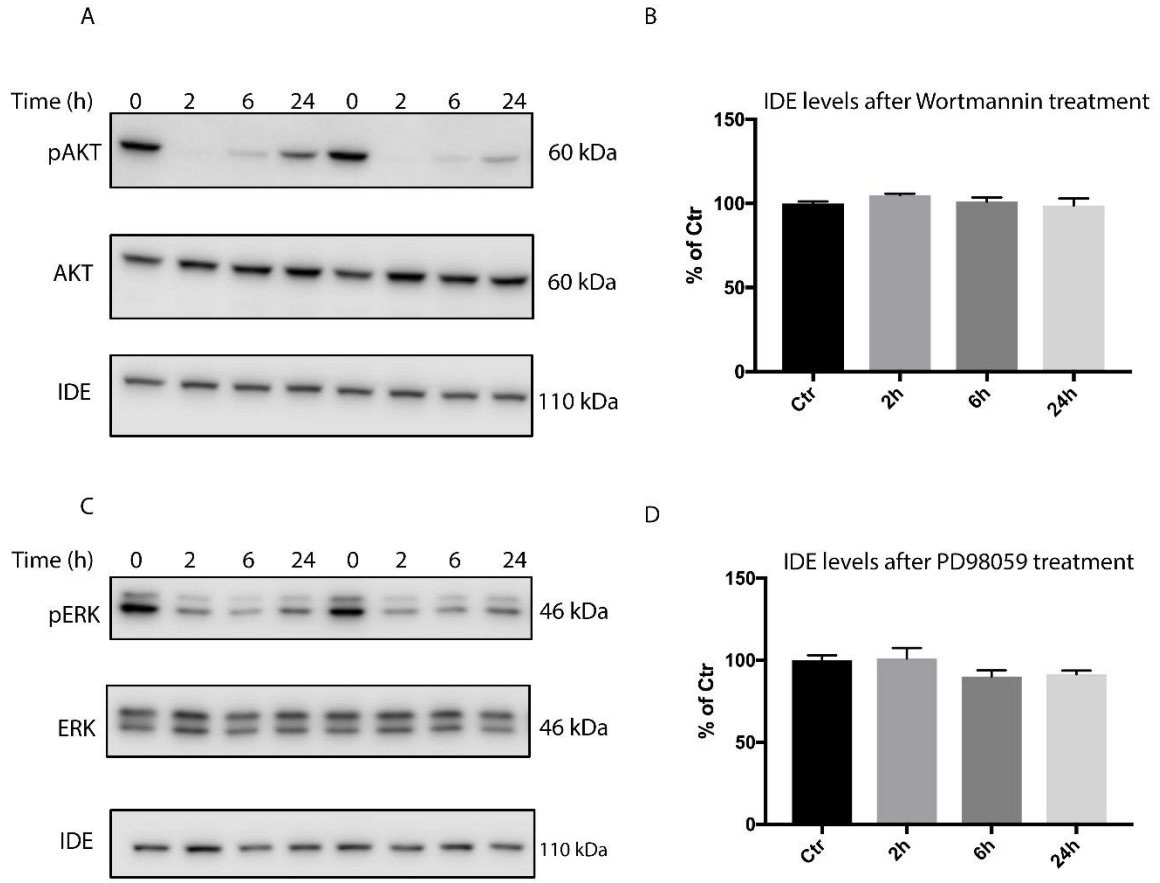

Figure 4.9: Chronic inhibition of AKT or ERK activity does not affect insulin degrading enzyme (IDE) levels in primary neurons. (A-D) Primary neuron-enriched cultures from brains of postnatal day 1 WT neonates were cultured for 10 days. The neurons were treated either with 100 nM Wortmannin (AKT inhibitor) or 20 µM of PD98059 (ERK inhibitor) for the indicated periods of time, followed by total lysate preparation. Representative Western blot images and densitometric quantification of replicate Western blots for Wortmannin treatments (A and B) and PD98059 treatments (C and D) in WT neurons are shown. Two independent experiments with 3 mice per treatments were performed. All values are mean + SEM and are represented as percentage of the control (Ctr) (set to 100%). One-way ANOVA was used to calculate the significance of differences between the treatments. (pERK: phospho ERK; pJNK: phospho JNK)

In conclusion, the studies in primary neurons showed that SORLA deficiency decreases insulin signaling possibly due to altered IR trafficking. However,

alterations in neuronal insulin signaling did not impact glucose uptake as it was comparable between the two genotypes. Defects in insulin signaling in SORLA KO neurons coincided with decreased levels of IDE, although neither acute nor chronic inhibition of insulin signaling had any impact on IDE levels in the neurons. Thus, the mechanism whereby neurons control expression of IDE in a SORLA-dependent manner remains to be elucidated.

4.2 Generation and validation of neuron-specific conditional SORLA KO (cKO) mouse model

My studies in primary neurons had established a so far unknown role for SORLA in enhancing neuronal insulin signaling and in increasing IDE expression in this cell type. To confirm this neuron-specific role for SORLA in the brain *in vivo*, a mouse model with loss of SORLA specific to neurons was required. Such a model had not been available and needed to be established as part of this thesis project.

For the generation of mice with a neuron-specific KO of SORLA, I purchased from the European Mouse Mutant Archives (EMMA) mice carrying a *Sorl1* gene wherein exon 5 was flanked by two loxP recombination sites (referred to as *Sorl1* lox/lox). Cre recombinase-mediated excision of exon 5 resulted in a premature stop codon preventing the translation of the full-length protein. In the course of this thesis project, *Sorl1* floxed mice were bred with several Cre transgenic strains (referred to as *Sorl1* wt/wt, *Cre* +/- mice) to investigate which Cre recombinase expression under the control of which different neuron-specific promotors leads to neuron-specific *Sorl1* deletion (Figure 4.10). After the first breeding round, mice expressing *Cre* and being heterozygous for the *Sorl1* floxed allele (*Sorl1* lox/wt, *Cre* +/-) were bred with *Sorl1* floxed mice. From these breedings, offsprings with Cre transgene and being homozygous for *Sorl1* floxed allele (*Sorl1* lox/lox, *Cre* +/-; **cKO**) and the control animals being homozygous for the *Sorl1* floxed allele but lacking *Cre* transgene (*Sorl1* lox/lox, *Cre* -/-; **WT**) were selected for validation of the neuron-specific loss of SORLA expression. These mice are referred to as cKO and WT, respectively. All subsequent studies were carried out with littermates.

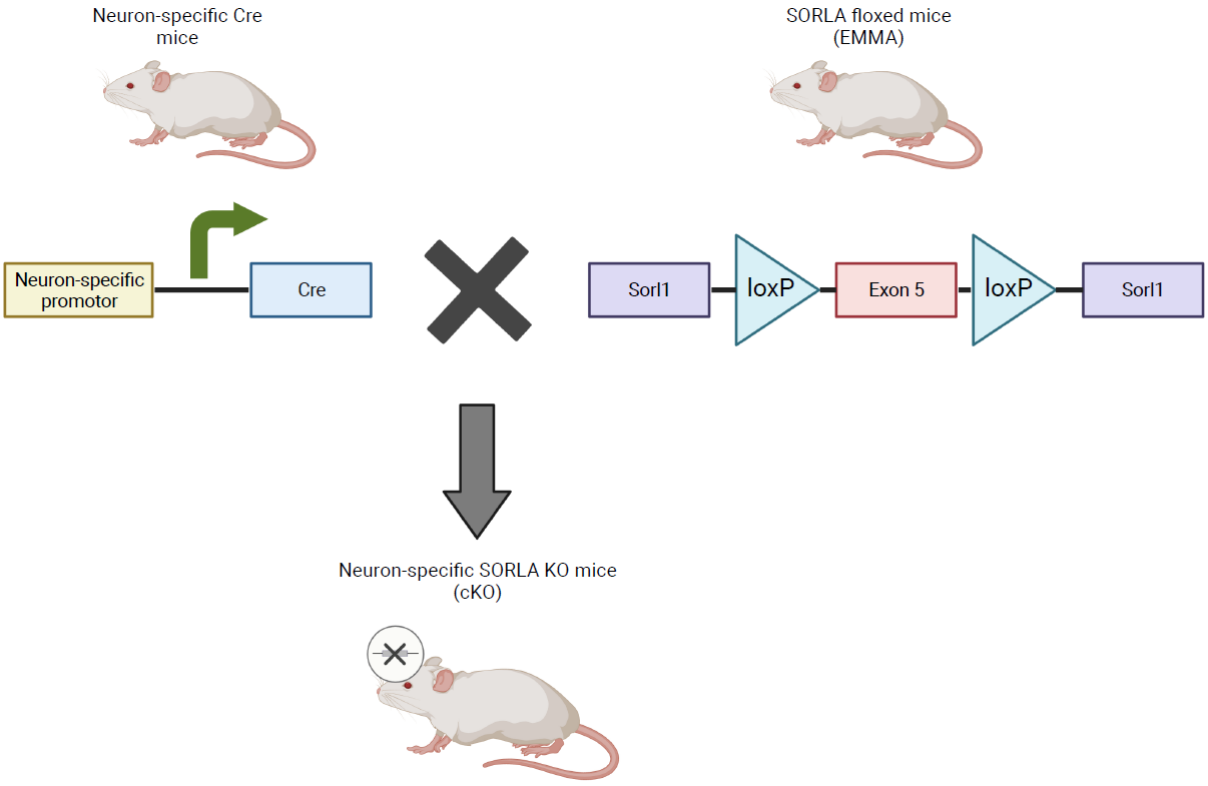

Figure 4.10: Strategy for the generation of a mouse strain with neuron-specific inactivation of *Sorl1 (cKO).* For generating cKO mice, animals expressing Cre recombinase under control of a neuron-specific promotor were bred with the SORLA floxed strain (exon 5 of *Sorl1* flanked by two loxP sites). Resulting mice having a floxed *Sorl1* gene but lacking Cre have normal SORLA expression and are referred to as WT (Cre -). Mice expressing Cre have a loss of SORLA expression in neurons and are referred to as cKO (Cre +). (Created with BioRender.com)

Several well-established neuron-specific Cre lines were used to test for generation and validation of cKO mice. These lines included Neurod6$^{tm1(cre)Kan}$ (**Nex-Cre)**, B6.129S2-*Emx1*$^{tm1(cre)Krj}$/J (**Emx-Cre),** and B6.Cg-Tg(Camk2a-cre)T29-1Stl/J (**CamKII-Cre**). Western blot analysis on total lysates prepared from brain, liver, muscle, and gonadal white adipose tissue (gWAT) of *Sorl1* lox/lox mice crossed with the various Cre lines were used to validate a neuron-specific loss of SORLA expression in these animals. As it turned out, all three cKO mouse lines showed either poor recombination efficiency (CamKII-Cre) or aberrant Cre activity in peripheral tissues, like liver and white adipose tissue (Nex-Cre and Emx-Cre) (data not shown). Thus, none of these Cre lines could be used for further studies and were discontinued.

Finally, I tried the Tg(Actl6b-Cre)4092Jiwu/J (**Baf53b-Cre**) strain of mice which hasn't been used extensively for generating neuron-specific gene knockouts,

although it has shown minimal recombination in peripheral tissues (Zhan et al., 2015). Baf53b is a subunit of the nucleosome remodelling complex Baf and is expressed exclusively in post-mitotic neurons.

To test if **Baf53b-Cre** mediated recombination led to a loss of SORLA expression specifically in the brains of the respective cKO mice, I prepared tissue lysates from WT (Cre -) and cKO (Cre +) mice for Western blot analysis to check for SORLA levels. cKO mice generated from the Baf53b-Cre line showed a significant reduction in SORLA expression in three brain regions (cortex, hippocampus and hypothalamus) compared to the WT littermates. By contrast, SORLA levels in liver, muscle, and gWAT were comparable between WT and cKO mice (Figure 4.11A-B). These results confirmed a brain-specific loss of SORLA expression in cKO mice, providing a suitable mouse model for my further investigations.

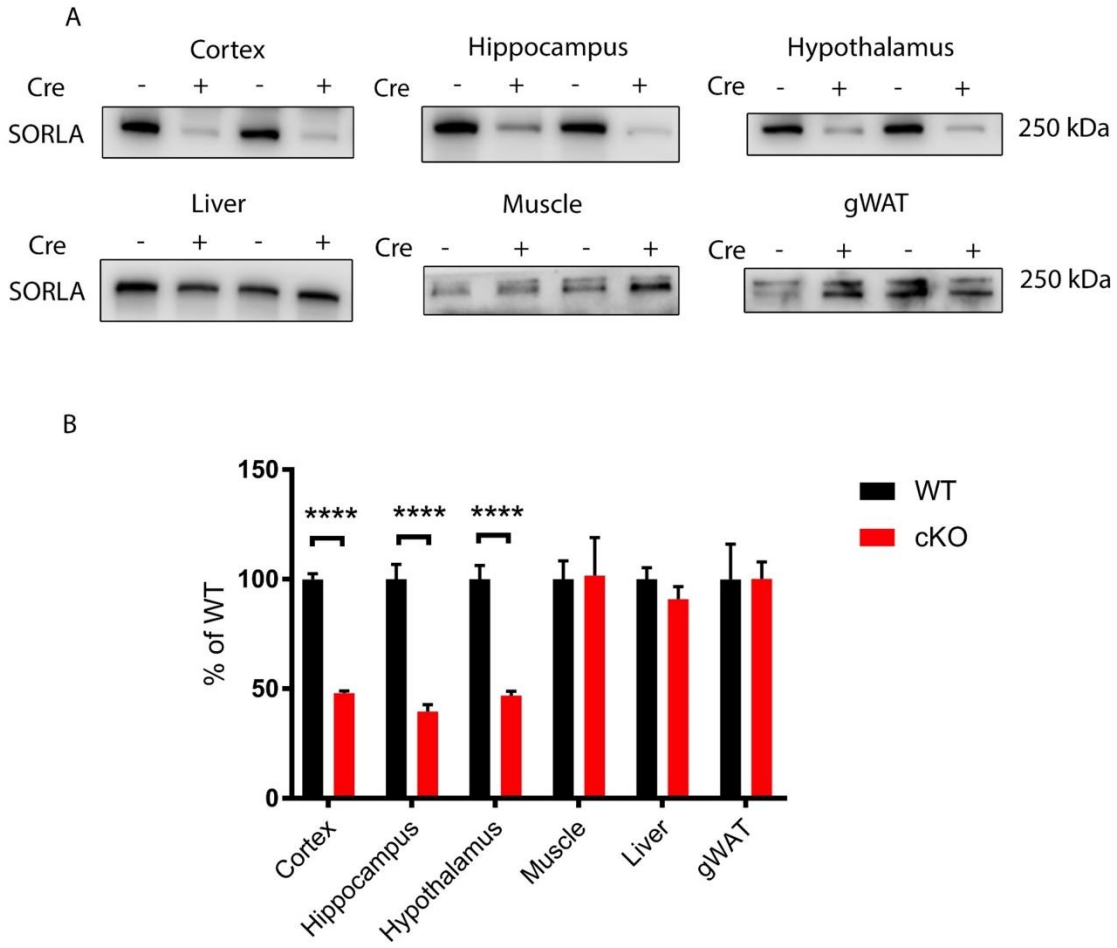

Figure 4.11: Neuron-specific loss of SORLA expression in conditional knockout (cKO) mice. (A-B) Representative Western blot analyses (A) and densitometric quantification of replicate Western blots (B) for immunodetection of SORLA in brain lysates and the indicated peripheral tissue from WT and cKO mice are shown. Six to 8 mice per genotype were used for quantification. All

values are mean + SEM and are given as percentage of the WT (set to 100%). Unpaired Student's *t* test was used to calculate the significance of differences between the genotypes (****, p<0.0001). (gWAT: gonadal white adipose tissue; Cre - : WT; Cre + : cKO)

To understand if the reduced expression of SORLA in the brains of cKO mice was due to a specific loss of SORLA in neurons rather than in other brain cell types, I performed co-immunofluorescent stainings on mouse brain sections for SORLA with different cell-specific markers. Specifically, I co-stained for neuronal marker NeuN, astrocyte marker GFAP, microglia marker Ionized calcium binding adapter molecule 1 (Iba1), as well as endothelial cell marker cluster of differentiation 31 (CD31) (not shown). In cKO mice, there was a complete loss of SORLA in the hippocampal CA2 neuronal layer when compared with WT mice (Figure 4.12A). No aberrant SORLA expression was detected in astrocytes, microglia, or endothelial cells of cKO mice. In addition, to validate the loss of SORLA expression from neurons in the cortex, I performed immunofluorescent stainings of SORLA with NeuN in WT and cKO mice. SORLA expression was not detected in the cortical neurons of the cKO mice. In comparison, perinuclear neuronal SORLA expression was detected in WT mice (Figure 4.12B).

Taken together, these results confirmed that loss of SORLA in cKO mouse brains was specific to neurons while its expression was intact in the peripheral tissues tested. Loss of neuronal expression of SORLA was seen equally in three brain regions of interest, confirming successful generation of a neuron-specific cKO mouse strain that could be used for subsequent *in vivo* studies.

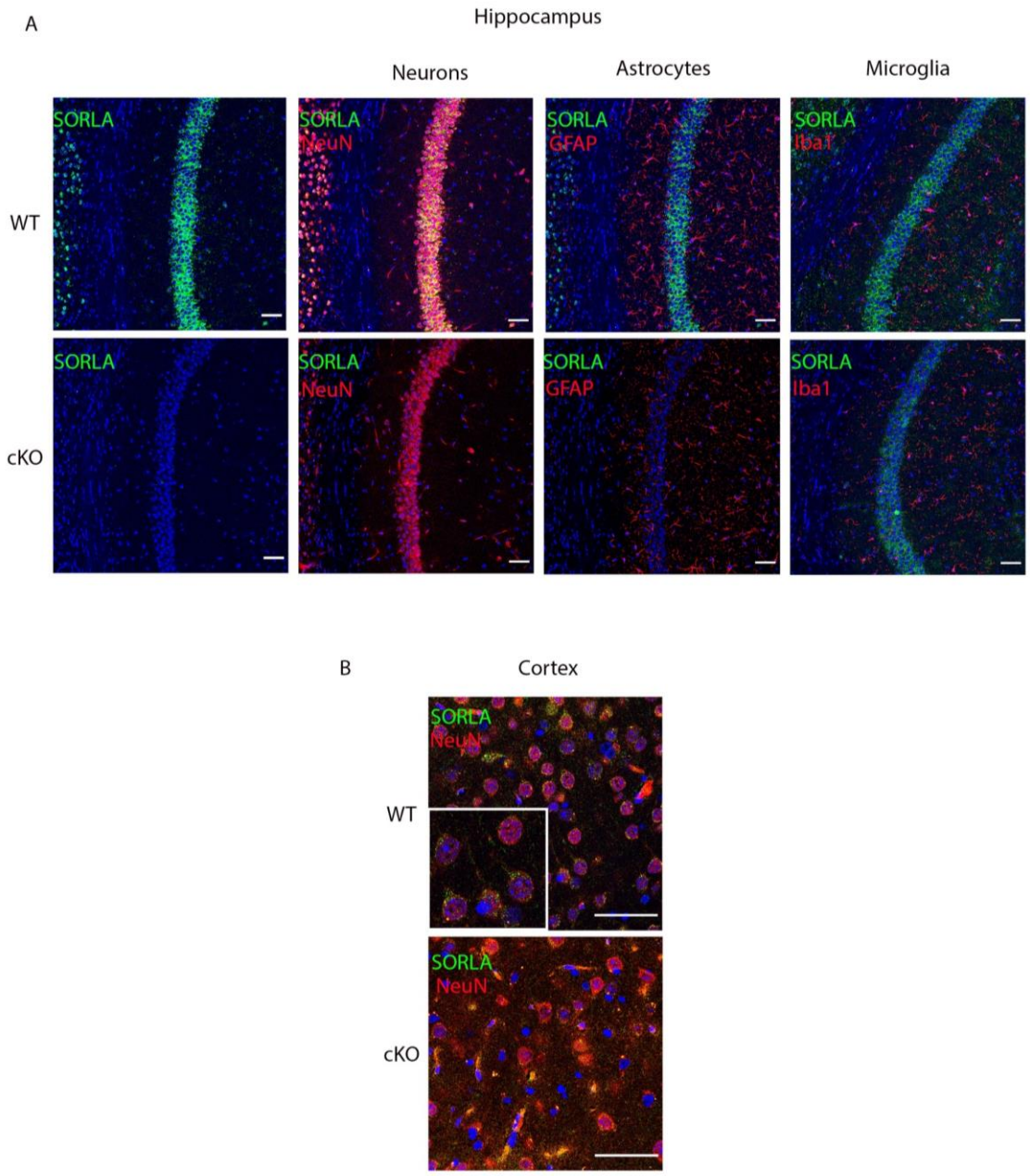

Figure 4.12: Validation of neuron-specific loss of SORLA expression in cKO mice. (A) Representative images of co-immunofluorescent detection of SORLA (green) with cell type-specific markers NeuN (neurons), GFAP (astrocytes), and Iba1 (microglia) in red on histological coronal sections (25 µm thick) from hippocampal CA2 layer of WT and cKO mice. Nuclei were counterstained with DAPI (blue). **(B)** Neuronal expression of SORLA (green) in WT cortex was confirmed by co-staining with Neun (red) (inset picture showing perinuclear neuronal expression of SORLA). No immunosignals for SORLA were seen in cKO sections. Scale bars: 50 µm.

4.3 Studies in cKO mice

4.3.1 Loss of SORLA does not impact insulin signaling or glucose uptake in cKO mouse brains

I had shown previously that SORLA potentiates insulin signaling in primary neuron-enriched cultures. To understand if SORLA has a similar activity in neurons in the brain *in vivo*, I prepared total lysates from hypothalami of WT and cKO mice and performed Western blot analysis to quantify key insulin signaling proteins. The hypothalamus was chosen to study SORLA-dependent IR activity in the brain as this is a region known to respond to insulin application in mice *in vivo*. Thus, such data may serve as an important control for insulin stimulation experiments to be performed later on. Moreover, previously I showed that there is a significant loss of SORLA expression in the hypothalamus of cKO mice compared to the WT mice.

In my Western blot analyses, the levels of IR, AKT, and GSK3β as well as the phosphorylated levels of AKT were comparable in hypothalamic protein lysates of WT and cKO mice, suggesting no defect in insulin signaling in the basal untreated condition (Figure 4.13A-B).

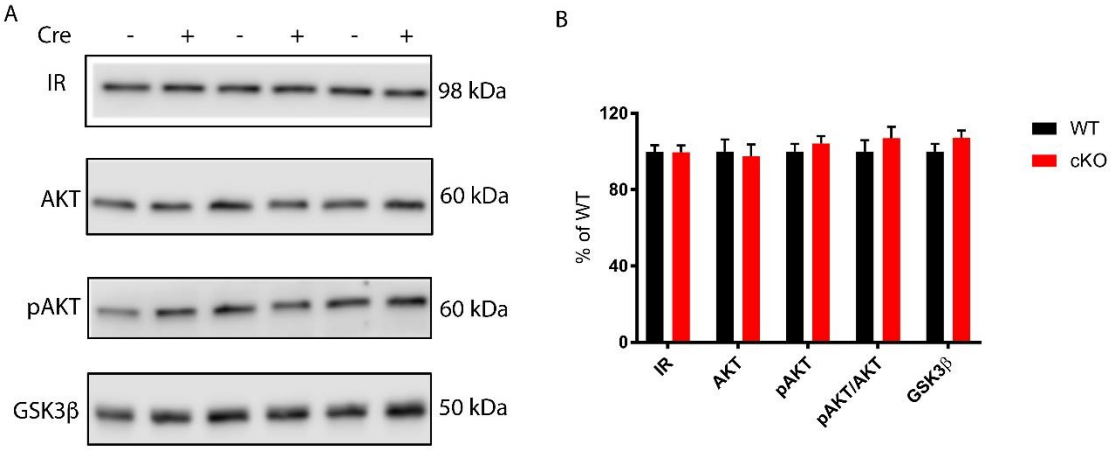

Figure 4.13: Levels of key proteins in the insulin signaling pathway in the hypothalamus of mice under basal conditions. (**A-B**) Representative Western blot images showing basal levels of insulin signaling proteins (A) and densitometric quantification of replicate Western blots (B) in hypothalami of WT and cKO mice. Nine to 10 mice per genotype were tested. All values are given as mean + SEM and are represented as percentage of the WT (set to 100%). Unpaired Student's *t* test was used to calculate the significance of differences between the genotypes. (Cre - : WT; Cre + : cKO; pAKT: phospho AKT; pGSK3β: phospho GSK3β)

Next, to investigate if insulin treatment affected brain insulin signaling differentially in WT versus cKO mice, I injected 5 units of insulin or saline (as a control) intraperitoneally (i.p.) in these animals. After 15 minutes, I dissected cortex, hippocampus, and hypothalamus for total lysate preparation and performed Western blot analysis to quantify the levels of key insulin signaling proteins. In cortex and hippocampus, activation of IR (i.e., an increase in pIR levels) in response to insulin treatment was not observed (data not shown). However, in hypothalamus, a significant increase in IR activation was observed in WT and cKO mice following insulin treatment (Figure 4.14A). Comparing the two genotypes, no differences were observed in total levels of IR, AKT and GSK3β in the hypothalamus (Figure 4.14A-B). Also, the levels of the phosphorylated forms of these proteins and the level of activation as quantified by the ratio of the phosphorylated to total protein levels were similar between WT and cKO mice (Figure 4.14A-B). These results indicated that neuron-specific loss of SORLA does not affect acute brain insulin signaling under the experimental conditions used here.

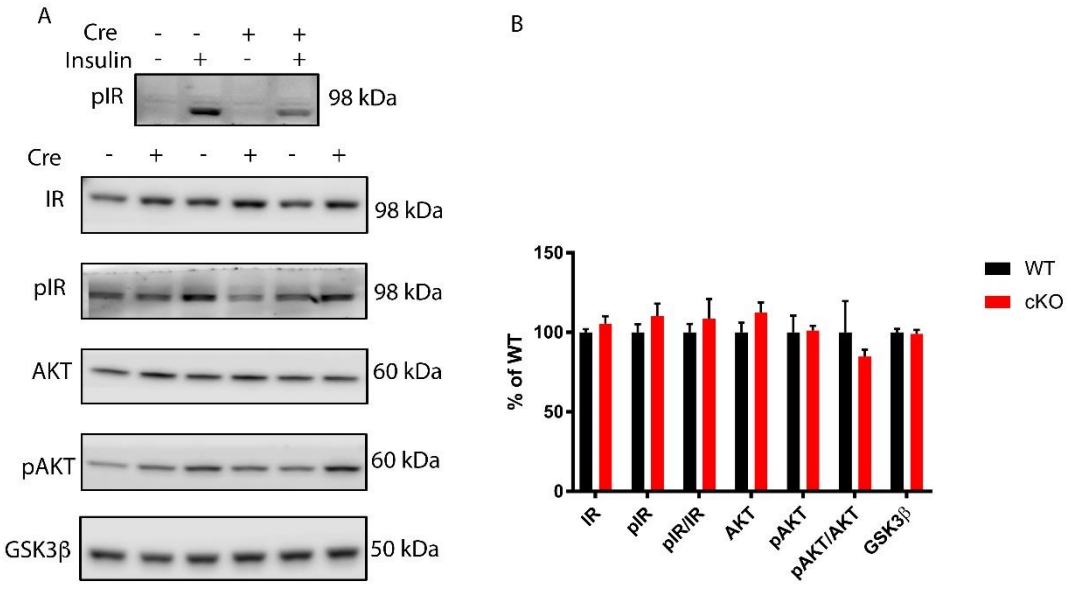

Figure 4.14: Levels of key proteins in the insulin signaling pathway in hypothalami of mice under insulin-stimulated conditions. (A-B) Insulin signaling in mice was evaluated by immunodetection of key insulin signaling proteins using Western blotting (A) and densitometric quantification of replicate Western blots (B) from WT and cKO mice following intraperitoneal (i.p) application of 5 units (U) of insulin. The upper most blot in panel A shows specific insulin-induced phosphorylation of the insulin receptor (IR) in WT and cKO mice. The blots below show the total and

phosphorylated levels of key insulin proteins after insulin stimulation in WT and cKO mice. Nine to 10 mice per genotype were tested. All values are given as mean + SEM and are represented as percentage of the WT (set to 100%). Unpaired Student's *t* test was used to calculate the significance of differences between the genotypes. (Cre - : WT; Cre + : cKO; pIR: phospho IR; pAKT: phospho AKT; pGSK3β: phospho GSK3β)

Brain glucose uptake depends both on insulin signaling and on the levels of glucose transporters (Milstein & Ferris, 2021). Although, there were no differences in insulin signaling observed between the two genotypes, it might still be possible that there are differences in glucose uptake based on altered glucose transporter levels. This assumption was supported by my earlier data on GLUT4 expression in primary neurons documenting its higher expression in KO neurons compared to WT neurons.

Hence, I examined if neuron-specific loss of SORLA affected brain glucose uptake in cKO mice, irrespective of having insulin signaling capacity similar to WT mice. For this, I i.p. injected 6-NBDG into WT and cKO mice, followed by dissection of cortex, hippocampus and hypothalamus at 20 minutes post-injection. The glucose uptake in the respective tissues was measured by spectrophotometric quantification of the fluorescent glucose analog in total lysates normalised to the total protein content.

No genotype-dependent differences were observed in the brain glucose uptake in all three brain regions tested (Figure 4.15A). I further checked the levels of the two main glucose transporters in the brain as SORLA may independently regulate their levels irrespective of insulin signaling, as seen in primary neurons. Accordingly, total lysates from WT and cKO hypothalami were prepared to quantify the expression levels of GLUT3 and GLUT4. GLUT4 was measured by a commercial ELISA kit as it offered improved sensitivity over Western blotting to detect this lowly expressed protein in the brain. GLUT3 was measured by Western blot analysis. Levels of GLUT4 (Figure 4.15B) and of GLUT3 (Figure 4.15C) were comparable in WT and cKO mice.

Taken together, these results failed to document any significant impact of neuronal SORLA deficiency on insulin signaling, glucose transporter expression, or glucose uptake in the brain of cKO mice.

.

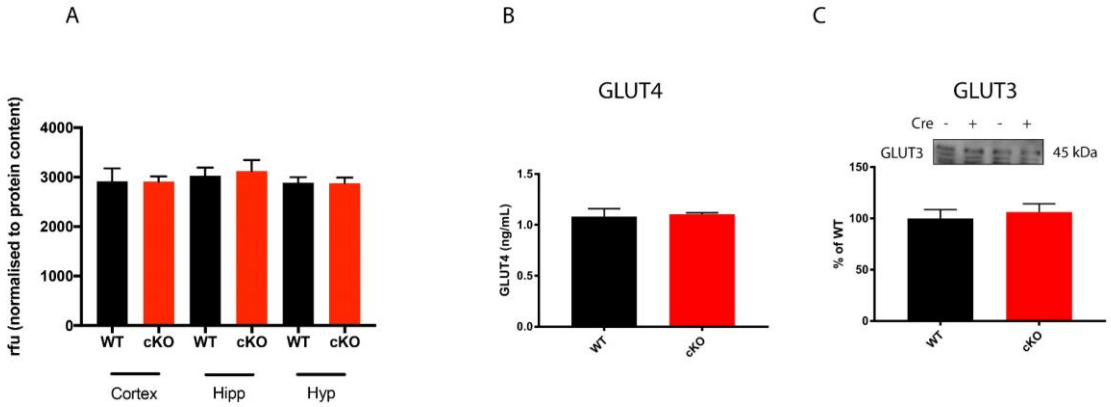

Figure 4.15: Glucose uptake and levels of major glucose transporters in the brains of WT and cKO mice. (A) 100 µl of 5 mM 6-NBDG was injected intraperitoneal (i.p) in WT and cKO mice. After 20 minutes, the animals were decapitated and the indicated brain regions were dissected for lysate preparations. The lysates were then subjected to spectrophotometric quantification of 6-NBDG with excitation/emission at 465/535 nm. The relative fluorescence units (rfu) were normalised to the total protein content. (**B**) GLUT4 protein levels in hypothalamus of WT and cKO mice were measured by commercial ELISA. (**C**) Exemplary Western blot analysis of GLUT3 levels in WT and cKO mouse hypothalami (inset) and densitometric quantification of replicate blots are shown. Six mice per genotype were tested and all values were expressed as mean + SEM. Unpaired Student's *t* test was used to calculate the significance of differences between the genotypes. (Cre - : WT; Cre + : cKO; Hipp: Hippocampus; Hyp: Hypothalamus)

4.3.2 Insulin signaling in synaptosomal preparations from the brain is identical in WT and cKO mice

Evaluating neuronal insulin signaling in total brain lysates can be challenging as IR expression is not just limited to neurons but to other brain cell types, like astrocytes and microglia (Pomytkin et al., 2018). Thus, any potential impact of SORLA deficiency in neurons of cKO mice may be obscured by normal insulin and glucose handling in other brain cell types when total brain lysates are studied.

Synaptosomes are enriched dendritic fractions of synaptic terminals containing mitochondria and synaptic vesicles. The presence of IR in these synaptosomal preparations make them ideal for studying insulin signaling in neurons as these preparations are devoid of any other cell type. To examine specifically if SORLA regulates neuronal insulin signaling in the brain, I made synaptosomal preparations from frozen cortices of WT and cKO mice as described previously (Franklin & Taglialatela, 2016).

To test the assay performance, synaptosomal lysates from WT brain cortices were subjected to treatments either with ATP or insulin separately, or with a combination of ATP and insulin. Extraneous ATP supplementation was needed to replenish the endogenous ATP depleted during synaptosomal preparations, essential for studying insulin signaling in these preparations.

After treatment, the lysates were subjected to Western blot analysis to test for the phosphorylation levels of IR and AKT. Faint immunoreactive bands for pIR and pAKT were observed when the lysates were treated with ATP, which mimics the *in vivo* condition when the mice were treated with saline, as shown by *in vivo* insulin treatment experiments. However, a significant increase in pIR and pAKT levels were observed when a combination of ATP and insulin was used, which mimics the situation of insulin treatments *in vivo* (Figure 4.16A).

To further investigate if there is an increased IR activity in synaptosomal preparations from WT compared to cKO mice, the ratio of pAKT/AKT was evaluated as a functional readout of insulin signaling post-treatment with ATP or a combination of ATP and insulin. No significant genotype-dependent differences were observed in pAKT/AKT ratio when the lysates were either treated with ATP (Figure. 4.16B-C) or with a combination of ATP and insulin (Figure 4.16D-E). These results further substantiated my findings *in vivo* that SORLA deficiency did not regulate insulin signaling in adult brain under the used experimental conditions.

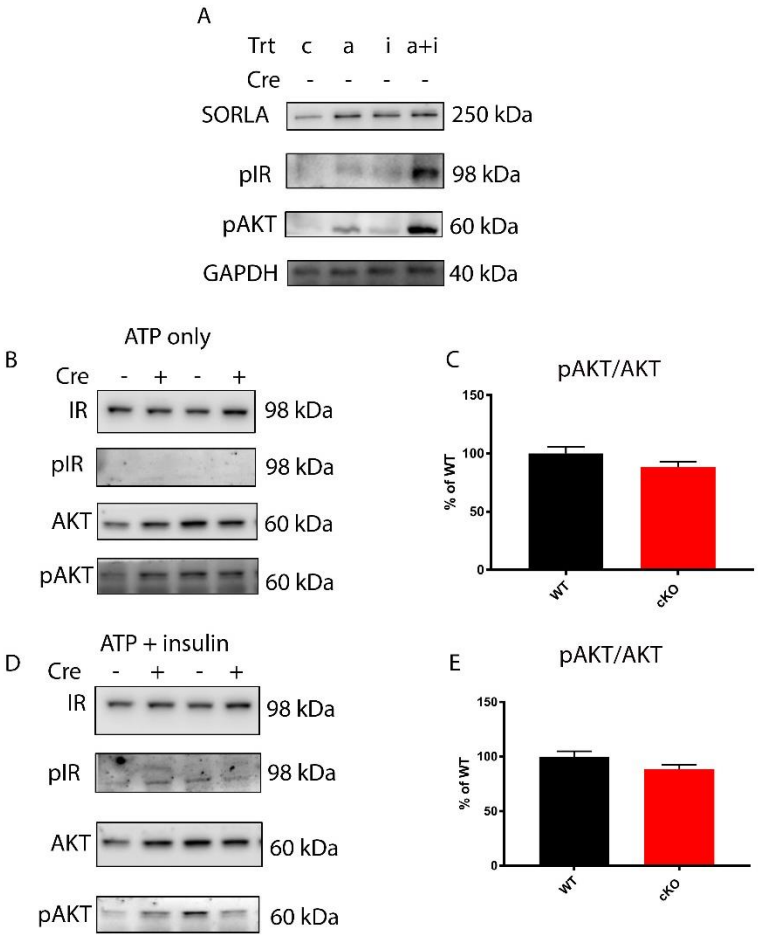

Figure 4.16: Insulin signaling is comparable in cortical synaptosomal preparations from WT and cKO mice. Synaptosomal preparations from WT and cKO mouse cortices were prepared as described previously. **(A)** Synaptosomal lysates were subjected to three different treatment conditions, namely 8 mM ATP for 15 minutes (a), 250 nM insulin for 15 minutes (i), or 8 mM ATP and 250 nM insulin for 15 minutes (a+i). Untreated synaptosomal lysates (c) served as control. The lysates were then probed for immunodetection of pIR and pAKT. GAPDH served as loading control. Increased rates of phosphorylation were observed for pIR and pAKT when a combination of ATP and insulin were added to the lysates (a+i). **(B-C)** Western blot analyses of key insulin signaling proteins in synaptosomal lysates from WT and cKO brain cortex following ATP treatment (B) and densitometric quantification of replicate Western blots (C) are shown. **(D-E)** Western blot scans of key insulin signaling proteins in synaptosomal lysates from WT and cKO brain cortex following combined ATP and insulin treatment (D) and densitometric quantification of replicate Western blots (E) are shown. Ten mice per genotype were tested. All values are given as mean + SEM and are represented as percentage of the WT (set to 100%). Unpaired Student's *t* test was used to calculate the significance of differences between the genotypes. (Cre - : WT; Cre + : cKO; pIR: phospho IR; pAKT: phospho AKT)

4.3.3 IDE levels are unchanged in cKO mouse brains

Previously, I had shown that SORLA promotes IDE expression in primary neurons. To understand if SORLA upregulates IDE expression also *in vivo*, I performed comparative immunofluorescent stainings, Western blot analysis, and enzyme activity assay in WT and cKO mouse brains.

Co-immunofluorescent stainings for IDE in WT and cKO hippocampal CA2 layer with cell-specific markers for neurons (NeuN), astrocytes (GFAP), microglia (Iba1), and endothelial cells (CD31) revealed its colocalization as mostly in endothelial cells while expression in neurons was minor (Figure 4.17A). Next, to compare IDE expression between the two *Sorl1* genotypes, total lysates were prepared from cortices of WT and cKO mice and subjected to Western blotting. In these experiments, the IDE levels were comparable between genotypes (Figure 4.17B-C). Additionally, I performed IDE enzyme activity assays to assess if there were differences in enzyme activity between the two genotypes. However, in line with comparable IDE expression levels, no genotype-dependent differences were observed in IDE enzyme activity (Figure 4.17D).

In summary, in primary neuron-enriched cultures, SORLA clearly promoted functional expression of IDE. However in the brain, no impact of neuronal receptor deficiency on IDE levels or activity was observed. This discrepancy is likely explained by the fact that expression of IDE in the brain is mainly seen in endothelial cells, which do not express SORLA. Therefore, SORLA-mediated induction of IDE expression in neurons might be obscured in brain lysates owing to its higher expression in the endothelial cells.

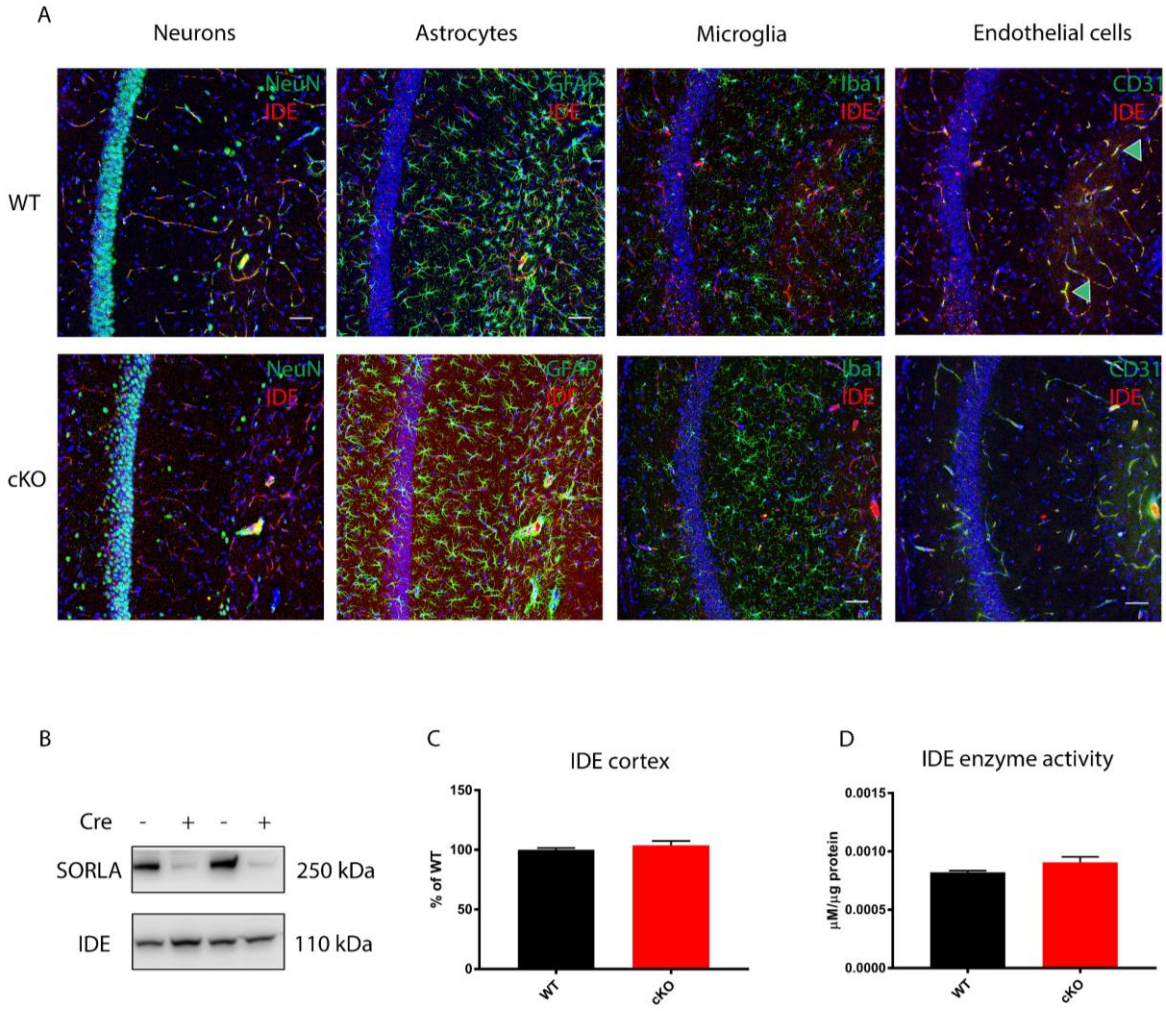

Figure 4.17: Levels and activity of insulin degrading enzyme (IDE) in the mouse brain (A) Representative images of 25 µm coronal sections of the hippocampal CA 2 regions from WT and cKO mice, immunofluorescent stained for IDE (red) and cell type-specific markers NeuN (neurons), GFAP (astrocytes), Iba1 (microglia), and CD31 (endothelial cells) (all in red). Nuclei were counterstained with DAPI (blue). IDE colocalising with endothelial cell markers is highlighted by green arrows in the WT panel. Scale bar: 50 µm. **(B-C)** Representative Western blot analyses of IDE levels in WT and cKO cortices (B) and densitometric quantification of replicate Western blots (C) are shown. **(D)** IDE enzyme activity in lysates from WT and cKO brain cortices were quantified by measuring fluorescence upon cleavage of an IDE-specific FRET substrate, values were normalised to the total protein content. Seven mice per genotype were tested in these experiments. All values are expressed as mean + SEM. Unpaired Student's *t* test was used to calculate the significance of differences between the genotypes. (Cre - : WT; Cre + : cKO)

4.3.4 Neuronal loss of SORLA results in reduced body weight and improved insulin sensitivity in cKO mice on normal chow

Brain insulin signaling is essential for whole-body energy homeostasis (Beddows & Dodd, 2021). Although I did not observe any significant differences in insulin signaling comparing WT and cKO mice brains, a role for SORLA in central

metabolic pathways impacting systemic energy homeostasis was still conceivable. Such activities may be dependent or independent of insulin signaling.

To examine a potential effect of neuronal loss of SORLA on systemic energy homeostasis, WT and cKO mice were fed a regular chow for 10 weeks and weekly body weight measurements were taken. Although, cKO mice showed a tendency for decreased weight gain over time, the difference in body weight over time was not statistically significant (Figure 4.18A). After the feeding period, the mice were analysed for body composition using Nuclear Magnetic Resonance (NMR). The total fat levels were comparable between WT and cKO mice (Figure 4.18B). By contrast, the lean (muscle) mass of cKO mice was significantly lower as compared to WT littermates (Figure 4.18C). Overall, cKO mice were lighter compared to WT mice as evidenced by a decreased body weight (Figure 4.18D). To rule out the possibility of a developmental growth defect in these animals, body length of the mice was measured using a flexible ruler. No genotype-dependent difference in body length was observed (Figure 4.18E).

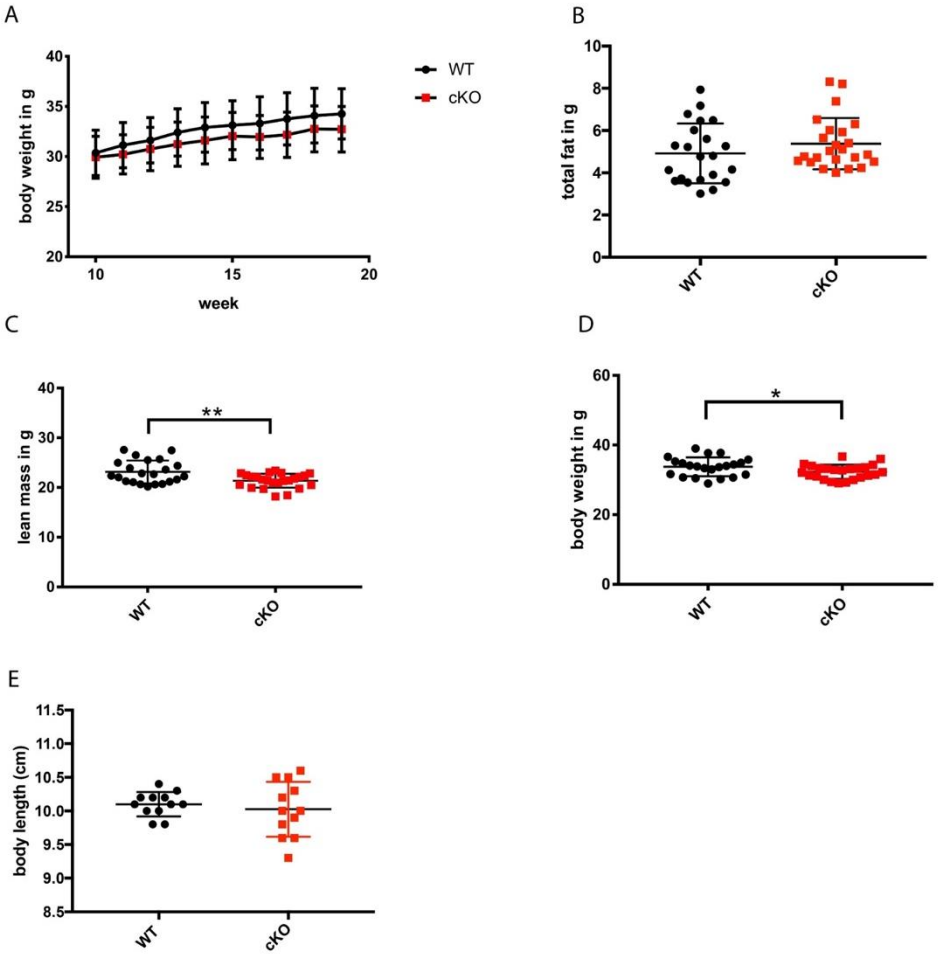

Figure 4.18: Neuronal loss of SORLA leads to decreased body weight in mice on normal chow. (A) WT and cKO mice were fed a normal chow from week 10 until week 20 of age and body weight was measured every week until the end of the feeding period. **(B-D)** After 10 weeks of feeding, NMR for body composition was performed to record total fat mass (B), lean mass (C), and body weight (D) in WT and cKO mice. **(E)** Additionally, the body length of the animals was measured using a flexible ruler (12 mice per genotype). Twenty-five mice per genotype were tested in the NMR experiments. All values are expressed as mean ± SEM. Unpaired Student's *t* test was used to calculate the significance of differences between the genotypes (*, $p<0.05$; **, $p<0.01$).

To understand if body weight changes were a consequence of altered glucose handling and insulin sensitivity, WT and cKO mice were subjected to glucose tolerance test (GTT) and insulin tolerance test (ITT). GTT and ITT are one of the first tests to be performed in mice to understand if there are any overt changes in systemic glucose homeostasis. These tests involve injecting the mice with a bolus of either glucose or insulin depending on their body weight followed by monitoring blood glucose levels over a course of 2 hours.

The area under the curve (AUC) is calculated in GTT which relates to the rate of glucose disposal in mice. Higher AUC implies a slower glucose disposal rate and glucose intolerance. Additional tests are needed to understand if the glucose intolerance is because of reduced insulin secretion from pancreas or decreased glucose disposal in peripheral tissues.

For GTT, the mice were starved for 16 hours and injected i.p. with 2 g glucose per kg body weight, and the blood glucose levels were monitored at regular intervals for 2 hours. There was no difference in fasting glucose levels comparing WT and cKO mice (Figure 4.19A). Also, blood glucose response profiles and area under the curve (AUC) during GTT were identical between the two genotype groups (Figure 4.19B-C), indicating comparable glucose disposal in peripheral tissues.

Next, I performed ITT to test for insulin sensitivity. In ITT, the percentage decrease in blood glucose levels from baseline is calculated for each mouse. The rate of glucose disposal from baseline is compared between the mutant and the control mice. Lower glucose disposal rate in mutant mice comparing control mice is indicative of insulin resistance. In contrast, a higher glucose disposal in mutant mice when compared to the control mice signifies that these mice are relatively more insulin sensitive.

WT and cKO mice were starved for 6 hours and injected i.p with 0.75 U insulin per kg body weight, and the blood glucose levels were monitored at regular intervals for 2 hours. The blood glucose levels in cKO mice dropped faster and stayed lower throughout the test period, indicating enhanced insulin sensitivity as compared with WT mice (Figure 4.19D).

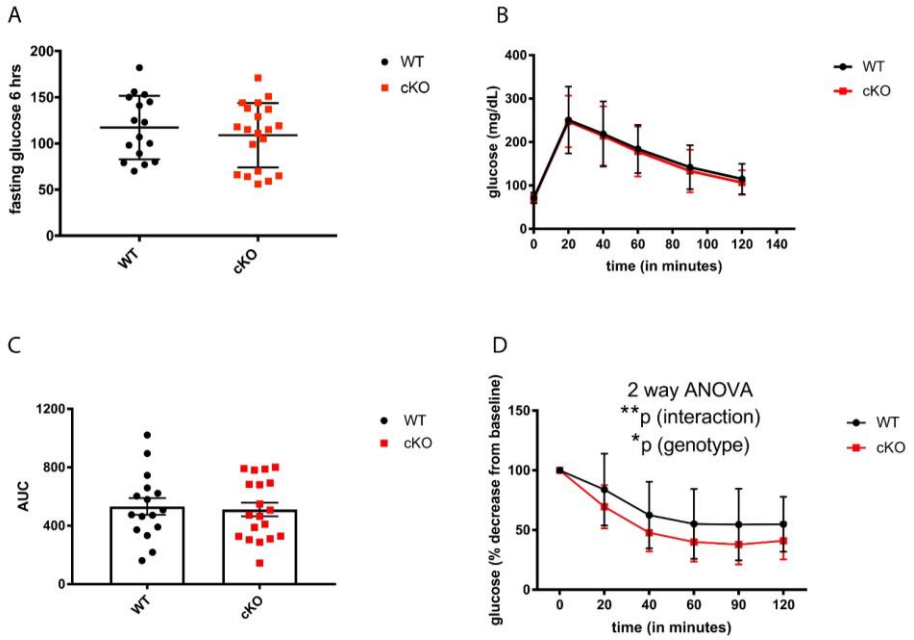

Figure 4.19: cKO mice have a normoglycemic response to glucose challenge but improved insulin sensitivity following 10 weeks of normal chow feeding. (**A**) Blood glucose levels from tail vein puncture were measured in WT and cKO mice after 6 hours of fasting using a standard glucometer. (**B-C**) Glucose tolerance test (GTT) was performed by intraperitoneal (i.p.) injecting 2 g/kg of body weight of glucose solution and then recording blood glucose levels at the indicated time points followed by the calculation of area under the curve (AUC) from the GTT plot. (**D**) For insulin tolerance test (ITT), 0.75 U/kg of body weight of insulin was injected i.p. and blood glucose levels were monitored over the course of 2 hours. Data for ITT are expressed as percent decrease in blood glucose levels from time point 0 hours. For fasting glucose levels, unpaired Student's *t* test was used to calculate the significance of differences between the genotypes (n=16-20 mice per genotype). 2-way ANOVA was used for analysis of GTT and ITT (n=14-18 mice per genotype; *, $p<0.05$; **, $p<0.01$).

The *in vivo* studies evaluating energy homeostasis in WT and cKO mice revealed that there is a decreased lean muscle mass in cKO mice which accounts for an overall decrease in total body weight compared to the WT mice. In addition, although the glucose sensitivity in WT and cKO mice were comparable, cKO mice were more insulin sensitive observed by an accelerated drop in blood glucose after insulin treatment.

4.3.5 The body composition, as well as glucose and insulin stress responses, are similar for WT and cKO mice on a high-fat diet

In the context of increasing global obesity, it is important to understand how physiological processes regulating energy homeostasis are affected by dietary

stress. Therefore, I decided to investigate if neuronal loss of SORLA aggravates changes in systemic energy homeostasis seen in cKO mice on normal chow. To do so, WT and cKO mice were fed a high-fat diet (HFD) for 10 weeks and weekly body weight measurements were taken. No differences in body weight gain were observed between WT and cKO mice, although towards the end of the feeding period, there was a tendency towards increased body weight for WT mice compared to cKO mice (Figure 4.20A). Unlike on normal chow diet, where the trend of increased body weight in WT mice compared to cKO mice was observable from the second week of dietary intervention, this increment in body weight comparing the two genotypes was delayed on HFD. WT and cKO mice had identical body weight curves until five weeks of HFD feeding, after which the two curves started to separate with WT mice gaining more weight each week thereafter until the end of the dietary intervention.

Also, WT and cKO mice were analysed for body composition using NMR after the dietary intervention. The overall body weight was comparable between WT and cKO mice as there was no difference in lean muscle mass and total fat (Figure 4.20B-D).

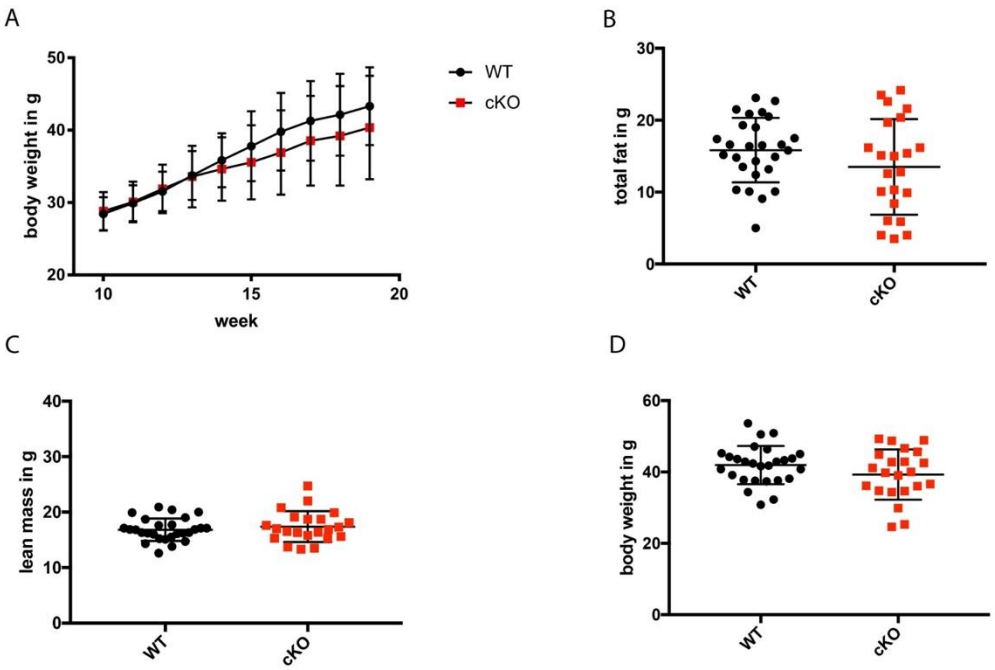

Figure 4.20: Body composition is comparable in WT and cKO mice after high fat diet feeding. (A) WT and cKO mice were fed high fat diet from week 10 until week 20 and the body weight was measured every week until the end of the feeding period. **(B-D)** After 10 weeks of feeding, NMR for body composition was performed to record total fat mass (B), lean mass (C), and body weight (D) in WT and cKO mice. Twenty-five mice per genotype were used in the NMR experiments. All values are expressed as mean ± SEM. Unpaired Student's *t* test was used to calculate the significance of differences between the genotypes.

Next, to understand if there were distinctions in glucose handling and insulin sensitivity between WT and cKO mice on HFD, I peformed GTT and ITT in fasted animals. For GTT, the mice were injected i.p. with 2 g glucose per kg body weight and the blood glucose levels were monitored at regular intervals for 2 hours. There was no difference in fasting glucose levels between WT and cKO mice (Figure 4.21A). Also, the glucose response profiles and AUC during GTT were identical between the two genotypes (Figure 4.21B-C).

Next, I performed ITT to test for insulin sensitivity. WT and cKO mice were injected i.p. with 0.75 U insulin per kg body weight and the blood glucose levels were monitored at regular intervals for 2 hours. No genotype-dependent differences in insulin sensitivity were observed in mice on HFD (Figure 4.21D).

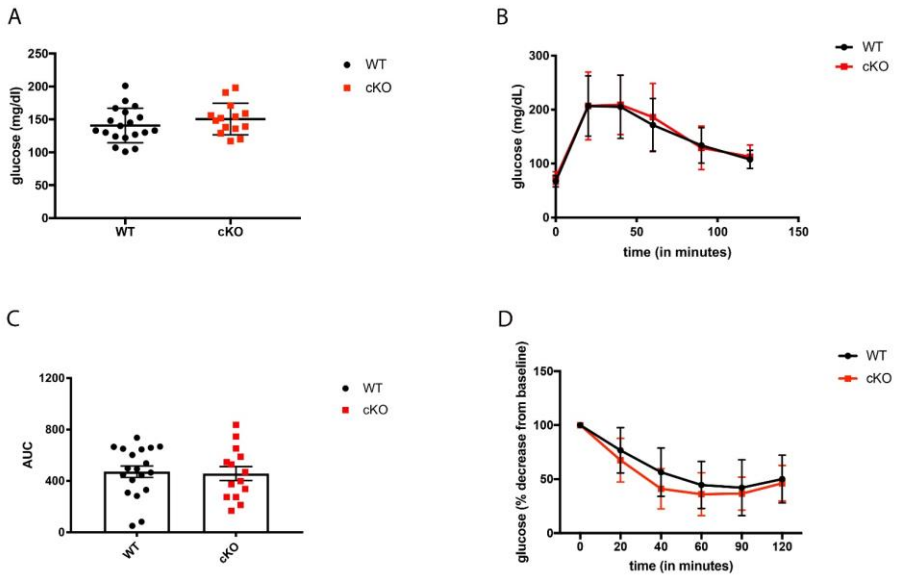

Figure 4.21: Glucose and insulin tolerance are comparable in WT and cKO mice after high-fat diet feeding. (A) Blood glucose levels from tail vein punctures were measured in WT and cKO mice after 6 hrs of fasting using a standard glucometer. **(B-C)** Glucose tolerance test (GTT) was performed by intraperitoneal (i.p.) injection of 2 g/kg of body weight of glucose solution and by

recording blood glucose at the indicated time points followed by AUC calculation from GTT plot. **(D)** For insulin tolerance test (ITT), 0.75 U/kg of body weight of insulin was injected i.p and the blood glucose levels were monitored over the course of 2 hours. Data for ITT are expressed as percent decrease in blood glucose levels from time point 0. For fasting glucose levels, unpaired Student's t test was used to calculate the significance of differences between the genotypes (n=16-20 mice per genotype). 2-way ANOVA was used for analysis of GTT and ITT (n=14-18 mice per genotype).

In conclusion, I generated a neuron-specific SORLA KO mouse model which was instrumental in studying a SORLA-specific role in neurons with relevance to brain insulin signaling, IDE expression and peripheral metabolism. My data showed that loss of SORLA in neurons did not impact brain insulin signaling and glucose uptake in mice *in vivo*. In contrast to the findings in primary neurons, neuronal loss of SORLA also did not affect global IDE levels in the brain of cKO mice. The metabolic phenotyping on these mice revealed no serious change in glucose and insulin utilization. Interestingly, on a normal chow diet, neuronal loss of SORLA in cKO mice led to a decreased body weight and improved insulin sensitivity, implicating neuronal receptor activity in central control of metabolism.

5 Discussion

5.1 Role of SORLA in insulin signaling and glucose homeostasis

5.1.1 SORLA alters IR localization and signaling in primary neurons

Receptors in the VPS10P family sort cargo proteins to different sub-cellular compartments and defects in sorting have been linked to neurodegenerative disorders (Hermey, 2009; Malik & Willnow, 2020b; Willnow et al., 2008). SORLA, a member of the VPS10P domain receptor family, facilitates insulin signaling in adipocytes and its expression correlates with the BMI in humans (Schmidt et al., 2016). It also prevents amyloidogenic processing of APP into Aβ in the brain and is therefore protective in AD (Andersen et al., 2005). Metabolic disorders, like T2D and obesity, greatly increase the risk of neurodegenerative disorders like AD (Chatterjee & Mudher, 2018; Kang et al., 2017). Aberrations in neuronal insulin signaling have been linked to both AD and T2D (Blázquez et al., 2014; Kullmann et al., 2015). However, a role of this receptor in neuronal insulin signaling and the relevance of this activity for AD related processes hasn't been explored. This important question has been the central topic in my thesis project.

To address this question, I used different cell culture and animal models to understand the role of SORLA in brain insulin signaling. Initially, I queried whether loss of SORLA activity had any impact on the expression and activity of proteins in the insulin signaling pathway in primary neuron-enriched cultures. As it turned out, loss of SORLA in neurons led to a 20% decrease in total IR levels (Figure 4.1). The post-transcriptional regulation of IR expression, as evidenced by similar WT and KO *Insr* transcript levels suggested alterations in IR trafficking in neurons. Indeed, SORLA prevented trafficking of IR to the late endosome/lysosome compartment where it is degraded (Figure 4.2). SORLA-dependent trafficking of IR has also been studied previously in Chinese hamster ovary (CHO) cells. In CHO cells overexpressing SORLA, IR was targeted less to the late endosome/lysosome compartment suggesting identical trafficking routes of IR in the two cell models expressing SORLA (Schmidt et al., 2016).

These results are comparable with a study where neuronal low-density lipoprotein receptor 1 (LRP1) deficiency resulted in a substantial decrease in total IR levels (Liu et al., 2015). LRP1 is an endocytic receptor and, just like SORLA, regulates the expression levels of several cell-surface receptors, including the IR. Although the mechanism for IR regulation by LRP1 was not investigated in the study, they found that LRP1 directly interacts with IR in neuronal cells. SORLA and LRP1 share structural similarities and probably IR binds to a conserved domain in these receptors (Gliemann et al., 2004). Also, insulin increased the cell surface expression of LRP1 and hence facilitated insulin signaling in neurons. Compared to my neuronal model where loss of SORLA led to trafficking of IR to the late endosome/lysosome, the intracellular trafficking of IR in LRP1 deficient neurons was not studied and hence the mechanism remains elusive.

Neuronal insulin signaling is evaluated by acute stimulation (15 minutes) of neurons with insulin followed by checking the activated levels of key insulin signaling proteins (B. Kim et al., 2011; Krasil'nikova et al., 2019; Peng et al., 2016). The activation of these proteins is measured by quantifying the ratio of the phosphorylated to total protein levels. As expected, SORLA-mediated increase in total IR levels led to increased activation of IR and AKT upon insulin stimulation (Figure 4.3). Surprisingly, SORLA deficiency did not impact the activation of GSK3β. One plausible explanation for this can be that the regulation of GSK3β is not only controlled by insulin, but also by other growth factors affecting different signaling pathways (Jope & Johnson, 2004; B. D. Manning & Toker, 2017b). Overall, these results are in line with other receptor knockout models which regulate insulin signaling. In primary neurons, loss of LRP1 resulted in a decreased activation of AKT upon insulin stimulation (Liu et al., 2015). Also, SORLA overexpression in adipocytes cells led to enhanced insulin signaling and lipid accumulation (Schmidt et al., 2016). My results substantiate the role of SORLA as an important regulator of neuronal insulin signaling.

One of the most important metabolic functions of insulin is to increase glucose uptake in insulin-sensitive tissues (Boucher et al., 2014; Leto & Saltiel, 2012). This process is driven by activation of AKT which mobilises GLUT4 vesicles from the cytosol to the plasma membrane thereby increasing the number of these glucose transporters for increased glucose uptake in cells (Eyster et al., 2006; Stöckli et al.,

2012). However, neuronal glucose uptake is mainly regulated by GLUT3 which does not translocate to the plasma membrane in response to an insulin stimulus like GLUT4 (Agrawal et al., 2019). Moreover, the kinetics and the distribution of these two key glucose transporters are different and they regulate different aspects of neuronal glucose uptake. GLUT3 is the major neuronal glucose transporter and is widely distributed across the brain including cortex, olfactory bulb, hippocampus, hypothalamus, and cerebellum (Apelt et al., 1999; Vannucci et al., 1997). Among all the glucose transporters, it has a very high affinity for glucose and regulates basal glucose transport, the rate of which is independent of plasma glucose levels when it exceeds the physiological range of 4-10 mM ("Human Biochemistry.," 2018). By contrast, the localization of GLUT4 in the brain is mostly restricted to the hypothalamus, although it is also found in neurons of cortex and hippocampus albeit at low levels (Agrawal et al., 2019; Vannucci et al., 1997). The affinity of GLUT4 for glucose is lower than that of GLUT3 but by virtue of its translocation to the plasma membrane, it increases the glucose uptake several folds upon an insulin stimulus ("Human Biochemistry.," 2018).

As SORLA facilitates insulin signaling in neurons, I hypothesized that it may also promote glucose uptake in neurons. There are different methods to measure glucose uptake in cells (Yamamoto et al., 2015). Conventionally, glucose uptake was measured by enzymatic oxidation of glucose within cells followed by its conversion into a coloured product which was spectrophotometrically quantified (Ngo & Lenhoff, 1980). This assay was less sensitive and was subsequently replaced by a more widely used assay for measuring glucose uptake involving the use of a radiolabelled glucose analog (Dienel et al., 1997; Lange et al., 1990; Pauwels et al., 1998). On the one hand, this assay is sensitive as it offers a high signal to background ratio. On the other hand, it requires multiple washing steps and handling of radioactive tracer. Subsequently, the use of fluorescent glucose analogs, such as 2- [N-(7-nitrobenz-2-oxa-1,3-diazol-4-yl) amino]-2-deoxy-D-glucose (2-NBDG) and 6-NBDG, became more popular due to their ease of handling and sensitivity. One study compared glucose uptake sensitivity in 3T3-L1 cells and found that the fluorescent method was the most sensitive and offered a greater increase in GLUT4-mediated glucose uptake than the radioactive method (Vishwanath et al., 2013). The two fluorescent analogs developed are used for

studying different aspects of glucose homeostasis. 2-NBDG is used to study glucose metabolism within the cell as it is phosphorylated at C-6 by hexokinase and then undergoes degradation into non-fluorescent products. 6-NBDG is used for glucose uptake studies as C-6 cannot be phosphorylated and hence it starts accumulating within the cell which can be spectrophotometrically quantified (W. H. Kim et al., 2012). Therefore, for my studies, I used 6-NBDG to measure glucose uptake in neurons.

In my studies, SORLA did not impact basal glucose uptake in neurons (Figure 4.4). These results were expected as there was no genotype-dependent difference in GLUT3 levels, which mediates the basal glucose uptake. Insulin increases glucose uptake by several folds in adipocytes and skeletal muscle (Boucher et al., 2014). Also, insulin induced increase in glucose uptake has been observed in mouse hypothalamic neuronal cell line (Liu et al., 2015). However, in my primary neuron-enriched culture model, I failed to observe such an insulin-dependent increase in glucose uptake (Figure 4.4). My uptake studies were conducted at a wide range of 6-NBDG concentrations, none of which led to an insulin-dependent increase in glucose uptake (data not shown). The concentration of 6-NBDG used for my studies was 5 mM, which was much higher than the concentration used in other studies typically in the range of µM (Jakoby et al., 2017; Vishwanath et al., 2013). The reason for my choice of such high 6-NBDG concentration relates to the kinetics of glucose uptake in neurons. I hypothesized that at high 6-NBDG concentrations, glucose uptake by the GLUT3 receptor may be saturated, facilitating glucose uptake by the insulin-dependent GLUT4 in presence of insulin. However, this strategy did not increase glucose uptake upon insulin stimulation (Figure 4.4). A recent study showed similar results where insulin failed to increase glucose uptake in neurons. In this study, neurons were either treated individually with insulin/IGF-1 or a combination thereof. Neither of these interventions had any impact on glucose uptake (Fernandez et al., 2017). In the same study, astrocytes were treated with insulin/IGF-1 or their combination. Only the latter combination led to a substantial increase in glucose uptake in these cells. It was further shown that synergistic/cooperation of insulin and IGF-1 was required for translocation of GLUT1 to the cell membrane to facilitate glucose uptake. Thus, the failure to elicit insulin-induced glucose uptake in neurons in our model are in line with these findings as the results from the mentioned study argue a role for astrocytes in

handling glucose uptake under insulin stimulated conditions, whereas neurons regulate the basal glucose uptake. I did not specifically look into astrocytic glucose uptake as the expression of SORLA is mainly neuronal and the effect of contaminating astrocytes on glucose uptake would be marginal when compared with the neuronal glucose uptake.

5.1.2 Neuronal loss of SORLA does not affect brain insulin signaling

Insulin action in the brain is not just limited to neurons but the hormone acts in different cell types, such as astrocytes, microglia and endothelial cells effecting different functions. For example, loss of IR in astrocytes leads to behavioral deficits in mice with anxiety and depressive-like behavior (Cai et al., 2018). Deletion of IR in brain endothelial cells causes an increase in food intake along with hyperinsulinemia (Konishi et al., 2017). Therefore, to study the role of SORLA in neuronal insulin signaling in the brain *in vivo*, there was a need to generate a neuron-specific SORLA KO (cKO) mouse model. Cre-LoxP technique is a standard technology used to generate such a cell-type specific gene defect in mice (H. Kim et al., 2018). In the past, several Cre lines have been used to specifically achieve neuron-specific gene deletion. However, most of the Cre lines were not specific to neurons and led to aberrant gene deletion in peripheral tissues as well. For example, in the Nestin-Cre mice, the expression of Cre recombinase is driven by the Nestin promotor. Nestin is an intermediate filament protein implicated in axonal growth in neurons. Interestingly, these mice have recombinase Cre activity not just in the central nervous system (CNS), but also in peripheral tissues such kidney, heart, lung and muscle (Nicole et al., 2006). Another Cre line which was used for the generation of neuron-specific gene deletion is the Camk2a-Cre. The expression of Cre recombinase was driven by calcium/calmodulin-dependent protein kinase II alpha (Camk2a) promotor. The calcium/calmodulin-dependent protein kinase type II subunit alpha protein regulates synaptic plasticity, neurotransmission and long-term potentiation in neurons. The recombinase activity in the Camk2a-Cre mice was limited to pyramidal neurons in the hippocampus and a few other neuronal populations in the forebrain (Dragatsis & Zeitlin, 2000). While searching for a pan-neuronal Cre line, I came across a recent publication where the promoter of

Actl6b/Baf53b was used to create a cKO mice. Baf53b, an actin-related protein, is a subunit of the nucleosome remodelling complex Baf and is expressed exclusively in post-mitotic neurons. It is essential for maintaining synaptic plasticity and memory consolidation. These mice had recombinase activity in neuronal populations across the different brain regions with no Cre expression in the peripheral tissues (Zhan et al., 2015). Also, recombinase expression was limited to mature neurons and no expression was observed in neuronal progenitor cells and glia cells. I decided to use these mice for generating neuron-specific SORLA KO mice. In the cKO mice, SORLA expression was substantially reduced in the brain, whereas SORLA expression was preserved in peripheral tissues, such as liver, adipose tissue, and muscle (Figure 4.11). Additionally, immunostainings revealed that SORLA expression was completely gone in the neurons of the cortex and hippocampus (Figure 4.12). These results confirm my successful generation of a pan-neuron specific SORLA KO mice. In full SORLA knockout mice, cell-specific mechanisms resulting in a phenotype would be difficult to explain as it could result from loss of SORLA activity in multiple cell-types. Using a cell-specific gene deletion approach as the one used here will help us understand the function of a specific protein in a certain cell-type. For example, the neuronal cKO mouse model will help elucidate the neuronal role of SORLA in brain metabolism as well as its implication in peripheral metabolism.

In my hands, this model was ideal to study the relevance of SORLA for neuronal insulin signaling in the brain. As done with the primary neurons, my first approach for characterization of the cKO mouse model was to test for changes in the basal level of insulin signaling proteins as compared to control mice. SORLA deletion in the neurons did not affect the basal levels of insulin signaling proteins (Figure 4.13). These results are in contrast with the findings in the primary neuronal cultures where SORLA deficiency led to a slight decrease in IR levels. This discrepancy could result from the fact that IR levels in total brain lysates represents its expression in all the brain cell types and not just neurons. So, due to technical limitations of detecting subtle differences in protein expression by Western blotting, small differences in IR levels observed in neuron-enriched cultures would be difficult to appreciate in the total brain lysates. Other possibility can be an induction of IR

expression in other brain cell types in cKO mice to compensate for a possible decrease in IR levels in neurons.

Studying brain insulin signaling is challenging due to several technical limitations such as route of insulin administration, method of evaluation and isolation of pure neuronal fraction. However, a few alternatives such as evaluating the expression of insulin signaling proteins in sorted neurons postmagnetic sorting (Anderson, Deborah K., Liang, 2017; Pan & Wan, 2020) and studying insulin signaling in synaptosomal fractions provide an indirect method of evaluating insulin signaling in the brain (Franklin & Taglialatela, 2016; Kulas et al., 2019).

In a recent study, neuronal insulin signaling was evaluated by isolating synaptosomes (isolated synaptic terminals of neurons) from frozen brain, followed by *ex vivo* treatment with a combination of ATP and insulin (Franklin & Taglialatela, 2016). Although the reason for the use of ATP is obscure, it was deemed essential for the activation of insulin signaling proteins in synaptosomal fraction. The advantage of using synaptosomes for assessing insulin signaling is that they constitute a purely neuron-enriched tissue fraction with robust expression of IR. Accordingly, I adopted this method to ask whether loss of SORLA in synaptosomal fractions affects insulin signaling. Again, analysis of insulin signaling in synaptosomal fraction failed to document an impact of SORLA on IR levels (Figure 4.16). Furthermore, insulin treatments in these isolated fractions revealed that insulin signaling, as evidenced by AKT activation, was not altered by loss of SORLA in neurons (Figure 4.16). This apparent discrepancy in the results between primary neuron-enriched cultures and synaptosomes hint a different regulation of IR by SORLA *ex vivo* and *in vivo,* which warrants further investigation.

Next, to understand the differences in activation of brain insulin signaling in SORLA WT and cKO mice, I performed exogenous insulin application in these mice. To study brain insulin signaling, different routes of insulin administration have been tried, each offering their own benefits and limitations. Intracerebroventricular (i.c.v) injections involves injecting insulin directly in the cerebral ventricles bypassing the BBB (Gelling et al., 2006; Perrin et al., 2004). This method offers the advantage of rapid distribution of insulin across the different brain regions and is a more direct way of measuring brain insulin signaling. However, this intervention can be

performed only under the influence of anesthesia, the use of which has been shown to induce neuronal insulin resistance (Hölscher, 2014). To avoid the use of anesthesia and bypass the BBB, intranasal (IN) insulin application has become the route of choice for insulin administration (Akinola et al., 2018; Grillo et al., 2017). For my studies, I also employed IN injections to induce insulin signaling in the brain. However, weak IR activation was observed only in the olfactory bulb of the mice as evidenced by a weak signal to background ratio of pIR by Western blotting (data not shown). By contrast, no IR activation was observed in cortex, hippocampus and hypothalamus. Dose and time optimization for IN insulin administration did not improve the outcome significantly. Therefore, I decided to switch to intraperitoneal (i.p) insulin administration although using this route leads to a substantial loss of insulin at the BBB and through an uptake of insulin by peripheral tissues. This method for studying brain insulin signaling has been used previously and offers improved resolution of measuring subtle protein differences due to better signal to background ratio (Konishi et al., 2017) . In my hands, i.p. insulin administration resulted in IR activation in the hypothalamus due to its proximity to the third ventricle where the BBB is sparse ensuring adequate insulin delivery. Unfortunately, IR activation was not observed in other brain regions, such as cortex and hippocampus. Probably, in the short duration of 15 minutes i.e., the time from insulin administration to organ collection, insulin in the peripheral circulation cannot penetrate into the deeper cortical layers and the hippocampus to activate the IR.

Still, given the ability to stimulate the IR in the hypothalamus of my mice, I evaluated the impact of SORLA deficiency on this tissue. However, SORLA deficiency in the hypothalamus did not result in differential activation of IR as compared to control mice (Figure 4.14). These results were in line with comparable total IR levels in WT and cKO mice. Again, as these analyses were carried out in total brain lysates and not in a pure neuronal fraction, it is still conceivable that subtle differences in neuronal IR activation existed in SORLA mutant mice maybe have been diluted out in the total brain lysate.

Despite a failure to detect an impact of SORLA activity on insulin action in the mouse brain, I investigated whether loss of neuronal receptor activity may still change brain glucose uptake. Brain glucose uptake is facilitated by GLUT receptors as well as insulin and IGF-1 (Camandola, 2017). Initial studies investigating the

effect of insulin on brain glucose uptake revealed that the hormone did not increase glucose uptake in rodent models and humans (reviewed in (Beddows & Dodd, 2021; Milstein & Ferris, 2021). Studies, using more sensitive fluorodeoxyglucose-positron emission tomography (FDG-PET), have shown that insulin increases brain glucose utilization by as much as 15% in humans (Bingham et al., 2002; Hirvonen et al., 2011). Another study correlated higher insulin resistance indicated by higher Homeostatic Model Assessment of Insulin Resistance (HOMA-IR) score in individuals with lower brain glucose metabolism measured by FDG-PET (Hahn et al., 2015). These studies argued for a role of insulin in brain glucose metabolism. In my studies of brain glucose uptake, I used *in vivo* application of 6-NBDG, as done for primary neuron-enriched cultures before. Neuronal SORLA deficiency did not impact glucose uptake in cortex, hippocampus and hypothalamus when compared with WT mice (Figure 4.15). These results are consistent as SORLA neither affects basal insulin signaling nor the levels of the two neuronal GLUT receptors- GLUT3 and GLUT4 in cKO as compared with WT mice. In summary, in the studies presented here, neuronal loss of SORLA in cKO mouse brains had no impact on brain insulin signaling and glucose uptake.

5.1.3 Neuronal loss of SORLA affects peripheral metabolism

Although SORLA did not affect overall insulin signaling in the hypothalamus in my studies, it was still probable that this receptor might regulate insulin signaling in specific hypothalamic neuronal populations. Insulin signaling in the hypothalamus regulates several aspects of energy balance, such as food intake, glucose homeostasis and energy expenditure (Loh et al., 2017; Puente et al., 2016a). The functional relevance of insulin signaling on peripheral metabolism has been demonstrated by loss of function studies in mice. For example, mice with pan-neuronal loss of IR developed diet-induced obesity with an increase in body fat mass and raise in plasma insulin levels . Additionally, these mice developed mild insulin resistance and elevated plasma triglyceride levels. Lack of neuronal insulin signaling also caused impaired spermatogenesis and maturation of ovarian follicles leading to defects in reproduction (Bru et al., 2000).

To understand if neuronal loss of SORLA affects peripheral metabolism, I fed WT and cKO mice normal-chow diet for 10 weeks followed by evaluation of body composition. The weight gain for cKO mice over the feeding period was comparable to that of WT animals suggesting no overt metabolic defects as a consequence of receptor deficiency (Figure 4.18). Interestingly, at the end of the feeding period the cKO mice were slightly lighter than their WT littermates. Reduced body weight was not due to a developmental delay as the body length was comparable between the two genotype groups. Instead, the cKO mice had decreased lean muscle mass which led to an overall decrease in body weight. Neuronal SORLA loss did not impact total fat mass in these mice. On comparing these results with the phenotype observed in a full KO mice, an interesting observation can be made. In the full KO mice, there was no difference in total body weight, although these mice had increased lean muscle mass and decreased adiposity when compared with the WT mice. Whereas, in the cKO mice, there was a decrease in lean muscle mass consequently leading to decreased body weight when compared with WT mice. These contrasting results in the two different mouse models (KO vs cKO) argue a role of SORLA in muscle mass development, although to dissect the specific role of SORLA in the muscle, a conditional KO mouse with loss of SORLA in the muscle is needed.

Until now, aberrant brain insulin signaling has not been linked to peripheral defects in muscle mass development. Also, since SORLA does not impact hypothalamic insulin signaling, the decrease in muscle mass in cKO mice hints at a different regulatory mechanism which needs to be further investigated. One possible avenue to look into and better understand the differences in muscle mass between WT and cKO mice is mTOR signaling which is essential for maintaining skeletal muscle mass (Sanchez et al., 2020). mTOR deficiency in skeletal muscle leads to severe myopathy (Risson et al., 2009). Possibly, loss of SORLA in neurons affects the mTOR pathway, and this signal is relayed to the muscle by nerve innervations affecting muscle development.

The hypothalamus contains neurons which are either activated or inhibited by glucose (McCrimmon, 2008; Routh, 2002; Waterson & Horvath, 2015). These neuronal populations sense glucose concentration in the brain interstitial fluid and regulate peripheral glucose levels by signaling through nerve innervations to liver

and other organs. To understand if SORLA expression in these glucosensory neuronal populations may impact overall glucose homeostasis, I performed glucose and insulin tolerance test to investigate any defects in glucose handling in these mice. Fasting plasma glucose (FPG) levels were similar in WT and cKO mice (Figure 4.19). FPG is elevated in diabetics as inefficient pancreatic insulin secretion coupled with insulin resistance which leads to a decrease in glucose disposal in these tissues causing hyperglycemia (American Diabetes Association, 2005; Khan, 2001; Mozaffary et al., 2016). Comparable FPG levels in cKO and control mice indicated no overall defect in systemic glucose uptake. Glucose disposal following a glucose challenge in these mice were identical possibly suggesting no defects in pancreatic insulin secretion and tissue glucose uptake. However, the glucose disposal rate after insulin challenge in cKO mice was much higher when compared to WT littermates indicating that these mice were more insulin sensitive. These results are counterintuitive as cKO mice have a decreased lean mass which should lead to an inefficient glucose disposal and, subsequently, to elevated plasma glucose levels. One possible explanation for the results may be that, to compensate for a loss of muscle mass in cKO mice, these mice upregulate the IR at the cell surface in muscle facilitating increased insulin signaling. Although such a mechanism has not been proposed before, mice which have mTOR deficiency in the muscle exhibit increased basal uptake of glucose, despite developing severe myopathy (Risson et al., 2009). The increased glucose uptake was attributed to increased activation of AKT, a key regulator mediating cellular glucose uptake. Whether the loss of muscle in my cKO mouse model leads to increased glucose uptake and consequently improved insulin sensitivity is not known and needs to be investigated further.

In the context of increasing incidence of obesity and T2D globally, research efforts in the recent years have entailed high-fat diet (HFD) studies to see whether this dietary intervention aggravates phenotypes further as compared to normal chow (Buettner et al., 2007; Hariri & Thibault, 2010). Thus, I performed HFD intervention in mice to understand if this dietary intervention had any impact on the whole-body glucose metabolism. WT and cKO mice had identical weight gain curves until week 5 of HFD feeding (Figure 4.20). Thereafter, there was a decreased tendency for weight gain in cKO mice as compared with their WT littermates. This decreased

tendency for weight gain in cKO mice may be due to altered feeding, energy expenditure or physical activity. However, since the weight gain was not statistically significant during the feeding intervention, no further analysis was performed to follow up on this trend. Body composition analysis showed no difference in overall body weight between WT and cKO mice. Individually as well, lean muscle mass and total fat were comparable between the two genotypes (Figure 4.20). These results contrast the findings on normal chow with respect to body weight and lean muscle mass. Possibly, the functional activity of SORLA may be lost upon massive metabolic stress induced by HFD feeding.

5.2 SORLA: linking insulin signaling and AD?

5.2.1 SORLA deficiency in neurons decreases IDE expression

Aggregation of extracellular amyloid plaques and intracellular neurofibrillary tau tangles are the two main pathologies associated with AD. Insulin regulates the levels of both tau and Aβ directly. It inhibits the activation of GSK3β, the main enzyme which phosphorylates tau and prevents its aggregation (Avila et al., 2012; Gratuze et al., 2018). Also, insulin upregulates the levels of IDE, an enzyme which degrades Aβ (L. Zhao et al., 2004). Insulin and Aβ compete for the same enzyme for their degradation. When the levels of insulin are high in the brain, less of Aβ is degraded and hence it accumulates as plaques (Pivovarova et al., 2016; Qiu & Folstein, 2006). Therefore, IDE acts as an important molecular link between metabolism and neurodegeneration.

In my thesis, I uncovered that SORLA potentiates insulin signaling in neurons. However, whether SORLA controls IDE levels through insulin signaling or whether these actions represent two independent SORLA activities, remained unclear. In detail, in primary neuron-enriched cultures, loss of SORLA led to a substantial decrease in IDE levels (Figure 4.5). The levels of neprilysin, another major amyloid degrading enzyme were unaltered in neurons, which means that the SORLA action is specific to IDE. Interestingly, the transcript levels of *Ide* were also reduced. These results were surprising as SORLA typically acts as a sorting receptor for ligands,

impacting post-translational aspects of protein expression control. Alterations in *Ide* transcript levels suggests that SORLA may indirectly sort a protein which, in turn, regulates the transcription of *Ide*. The IDE protein levels correlated with its enzyme activity with neuronal loss of SORLA leading to a substantial decrease in IDE activity.

IDE was initially identified as an extracellular Aβ degrading enzyme secreted by microglia (Qiu et al., 1997) and by astrocytes (Son et al., 2016). These studies confirmed the extracellular release of IDE in the medium for degradation of Aβ. However, a recent study argued that IDE is not secreted from cultured cells and the extracellular IDE results from a loss of cell membrane integrity (Song et al., 2018). Earlier studies evaluating IDE expression in neurons showed that it was localized at the cell surface and was capable of degrading extracellular Aβ in the medium (Vekrellis et al., 2000). Immunostainings of IDE in my primary neuron-enriched cultures confirmed prior reports that IDE expression was not limited to neurons, but was seen in contaminating astrocytes (Figure 4.6). However, the difference in IDE levels in primary neuron-enriched cultures was not because of contaminating astrocytes cells as the IDE protein levels were comparable in astrocyte cultures from the two genotypes. Also, since IDE was not secreted in my astrocyte cultures, the difference in primary neuron-enriched cultures resulted from loss of SORLA in neurons and not because of difference in IDE secreted from contaminating astrocytes. These results confirm that the SORLA-mediated regulation of IDE expression is specific to neurons. Specifically, in my primary-neuron enriched culture model, SORLA regulates the transcription of *Ide* and thereby its protein levels.

Previously, it has been shown that chronic insulin treatment upregulates IDE levels in primary neurons (L. Zhao et al., 2004). This increase in IDE levels was abolished upon addition of PI3K inhibitors confirming the involvement of the metabolic arm of the insulin signaling pathway in this process. Since my studies in primary neurons involved acute insulin treatments and an effect of such treatments on IDE levels in neurons or any other cell type hasn’t been investigated yet, I performed pharmacological inhibition of different components of the insulin signaling pathway to see whether they affect IDE levels. Acute insulin treatments followed by pharmacological inhibition of PI3K did not affect IDE levels in neurons (Figure 4.7).

Similarly, acute inhibition of ERK and JNK did not impact IDE levels (Figure 4.8). These results confirm that acute insulin treatments do not affect IDE levels in primary neurons. Probably, the short duration of treatments was not sufficient to affect changes in IDE levels, as none of the previous studies have recapitulated an effect of insulin on IDE on an acute time scale (Tanokashira et al., 2017; Yamamoto et al., 2018; L. Zhao et al., 2004). Since previous studies on IDE expression control involved chronic inhibition of components of the insulin signaling pathway, I decided to perform time-course inhibition of AKT and ERK to evaluate their impact on IDE levels in neurons. Surprisingly, neither inhibition of AKT nor ERK for any the time periods investigated impacted IDE levels (Figure 4.9). These results contrast the findings where insulin increased IDE levels in neurons via the PI3K-AKT pathway (L. Zhao et al., 2004). Also, a recent study reported that the regulation of IDE expression in astrocytes is mediated by ERK signaling (Yamamoto et al., 2018). The differences can likely be explained by the dose of insulin as well as the type of neuronal cultures used in the previous study. For my studies, I used insulin at a dose of 250 nM because there was an appreciable increase in activation of AKT at this dose. By contrast, a much lower dose range of 20-100 nM was used in other studies (Yamamoto et al., 2018; L. Zhao et al., 2004). Also, the difference in the results in the two models may be explained by the type of neuronal cultures used. In my studies, mouse primary neuronal cultures from cortical and hippocampal areas were used, whereas the other study used rat primary neuronal cultures from the hippocampus for studying insulin -mediated regulation of IDE. Future studies involving either pure hippocampal or cortical neuronal cultures may give better insights into whether SORLA regulates insulin-mediated IDE levels in a brain region-specific manner. IDE protein expression levels are regulated by metabolites such as glucose (Pivovarova et al., 2009), insulin (L. Zhao et al., 2004), glucagon (González-Casimiro et al., 2021; Li et al., 2018) and fatty acids (Li et al., 2018). Among other known regulators of IDE, PPARγ transcriptionally induces IDE expression in neurons (Du et al., 2009). Interestingly, insulin treatment in kidney proximal tubular cells (Al-Rasheed et al., 2004) and human adipocytes (Rieusset et al., 1999) stimulates PPARγ transcriptional activity. Whether insulin-mediated PPARγ activation in neurons induces IDE transcription is not known and needs further evaluation.

5.2.2 Neuronal loss of SORLA does not impact brain IDE expression

My studies showed that loss of SORLA in primary neurons led to a substantial decrease in IDE protein and enzyme activity levels, although this effect was not dependent on insulin. Earlier studies have shown that the brain IDE levels in AD patients were lower as compared with control subjects (Cook et al., 2003; Moriel et al., 2019). Also, SORLA levels in brains of AD patients was significantly lower than in control subjects (Andersen et al., 2005; Dodson et al., 2006; Scherzer et al., 2004). However, the impact of neuronal loss of SORLA on IDE levels in an *in vivo* model hasn't been investigated. I set out to understand if neuronal loss of SORLA affected brain IDE levels in my cKO mouse model.

Immunostainings of IDE in the mouse brain revealed that it is majorly expressed in endothelial cells (Figure 4.17A). These findings are in line with other studies where IDE was shown to localize with endothelial cells in the brain (Morelli et al., 2004). Although IDE expression was also confirmed in the neuronal hippocampal CA2 layer, levels were much lower as compared with the levels in endothelial cells. Protein quantification failed to reveal any changes in IDE levels in mouse brains upon neuronal loss of SORLA. These findings were further validated using an IDE enzyme activity assay which showed a comparable IDE activity in the brain lysates from WT and cKO mice (Figure 4.17D). So, unlike in primary neuronal cultures, neuronal loss of SORLA did not affect the IDE levels globally in the brain. Perhaps, these results are not too surprising as IDE was expressed majorly in the brain endothelial cells, a cell type which does not express SORLA. So, SORLA-mediated induction of IDE levels in primary neurons would be difficult to observe in brain lysates owing to much higher expression of IDE in endothelial cells which would obscure any difference observed in the neurons. Still, control of IDE levels or activity in neurons may represent an important novel model of action whereby this receptor controls local catabolism of Aβ.

5.3 Outlook

In summary, I have studied the role of SORLA in neuronal insulin signaling and its impact on glucose uptake, peripheral glucose metabolism, and AD-related processes. I have shown that SORLA promotes neuronal insulin signaling (Figure 5.1A) and also increases the expression levels and activity of IDE, potentially important for Aβ degradation (Figure 5.1B). Also, speculative at present these novel findings suggest a potential mechanism whereby SORLA controls Aβ level through insulin action.

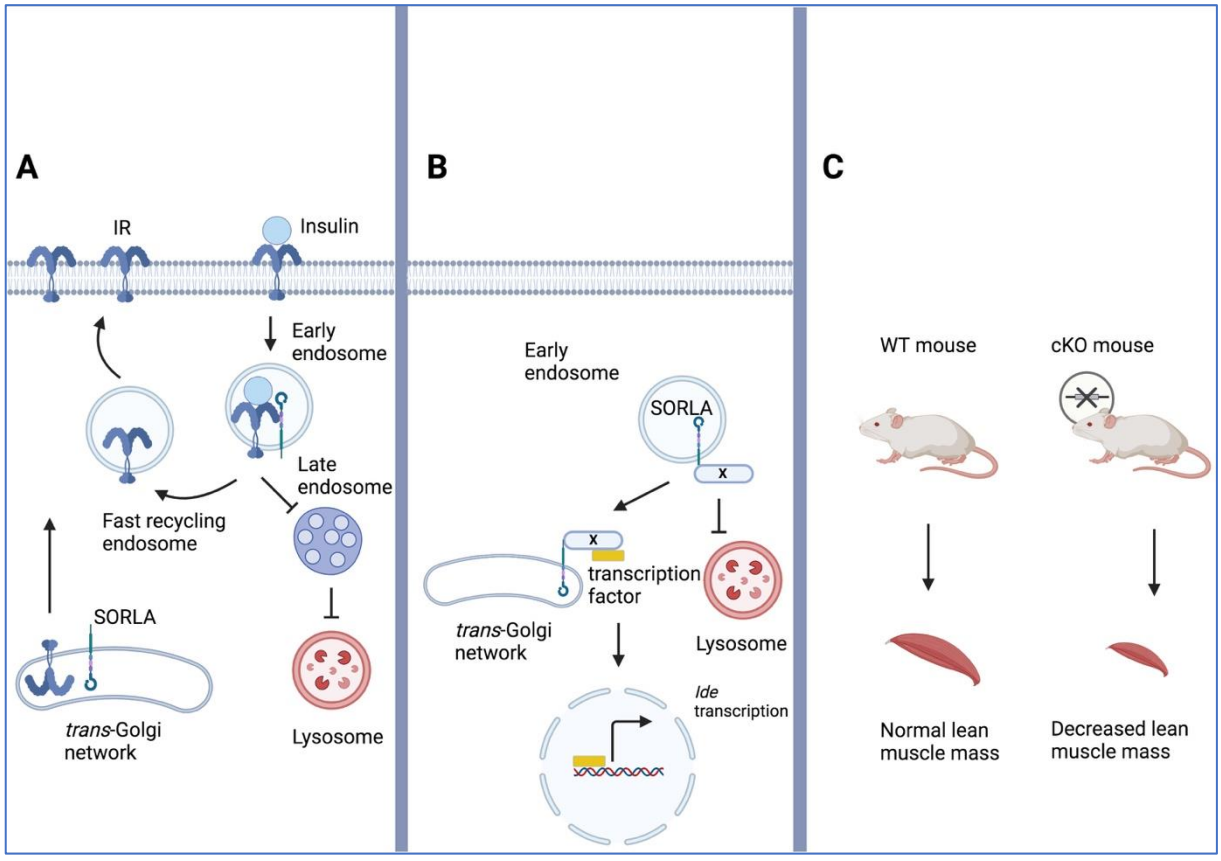

Figure 5.1: Proposed model for SORLA action in neurons in cell and animal models. (A) SORLA prevents lysosomal targeting of IR thereby increasing total IR levels and facilitating insulin signaling in neurons. **(B)** SORLA potentially stabilizes and prevents lysosomal degradation of a ligand which binds to a transcription factor. This transcription factor then translocates to the nucleus and binds to the promotor region of *Ide* and initiates transcription. Loss of SORLA would lead to the degradation of the ligand which would prevent the translocation of the transcription factor essentially preventing transcription of *Ide*. **(C)** Neuronal loss of SORLA in cKO mice causes a decrease in lean muscle mass when compared with WT littermates along with an increase in insulin sensitivity. (Created with BioRender.com)

In my thesis, I focused on the role of SORLA in regulating metabolic aspects of the insulin signaling in neurons to investigate a link between (brain) metabolism and amyloidogenesis converging on this receptor. Still, other aspects of neuronal insulin signaling may also be controlled by SORLA action on the IR. In a recent study, SORLA-mediated activation of ERK in neurons improved neurite outgrowth and regeneration. (Stupack et al., 2020). This study showed the relevance of SORLA in regulating mitogenic arm of the insulin signaling pathway. Insulin action in neurons prevents apoptosis and is essential for synaptogenesis (Chiu & Cline, 2010). Whether SORLA mediated insulin action in neurons has any role in control of apoptosis, synapse formation, or synaptic transmission is not known but constitute interesting new ideas for future AD-relevant research.

Another interesting aspect for future research based on my findings herein is the role of SORLA in central control of body weight. Loss of key metabolic proteins in the brain can have implications on peripheral handling of glucose and lipids, and hence whole-body homeostasis (Bru et al., 2000; Kappeler et al., 2008; Puente et al., 2016b). In my studies, neuronal loss of SORLA led to a decrease in body weight due to a decrease in muscle mass. In-depth analysis regarding the food intake, locomotor activity, metabolic fuel usage, and energy expenditure may provide more insights into the metabolism of these mice explaining the observed phenotype. In support of a role for SORLA in central metabolic control, cKO mice were more insulin-sensitive, possibly hinting at alterations in the brain-muscle axis caused by neuronal loss of SORLA. This aspect needs to be further explored by specifically looking at the mTOR signaling both in the brain as well as the muscle as this pathway regulates protein synthesis essential for muscle mass.

Although there are several open questions that need to be addressed for a complete understanding of the role of SORLA in neuronal insulin signaling in the context of AD, my findings lay the foundation for further research to explore the mechanistic underpinnings of SORLA-mediated insulin action in neurons.

6 Bibliography

2021 Alzheimer's disease facts and figures. (2021). *Alzheimer's and Dementia*, *17*(3), 327–406. https://doi.org/10.1002/alz.12328

Abdul-Hay, S. O., Kang, D., McBride, M., Li, L., Zhao, J., & Leissring, M. A. (2011). Deletion of Insulin-degrading enzyme elicits Antipodal, age-dependent effects on glucose and insulin tolerance. *PLoS ONE*, *6*(6), 2–7. https://doi.org/10.1371/journal.pone.0020818

Agrawal, R., Vieira-de-abreu, A., Durupt, G., Taylor, C., Chan, O., Fisher, S. J., Agrawal, R., Durupt, G., Taylor, C., & Chan, O. (2019). Insulin regulates GLUT4 in the ventromedial hypothalamus to restore the sympathoadrenal response to hypoglycemia in diabetic rats. *American Journal of Physiology*, 1286–1295. https://doi.org/10.1152/ajpendo.00324.2018

Akinola, O., Amin, A., Olorundare, O. E., Fatigun, C. O., Alli-Oluwafuyi, A.-M., Afolabi, O. S., & Njan, A. A. (2018). Effect of intranasal insulin on peripheral glucose profile in dexamethasone-induced insulin resistance in Wistar rats. *Beni-Suef University Journal of Basic and Applied Sciences*, *7*(4), 516–524. https://doi.org/10.1016/j.bjbas.2018.06.003

Al-Rasheed, N. M., Chanai, R. S., Baines, R. J., Willars, G. B., & Brunskill, N. J. (2004). Ligand-independent activation of peroxisome proliferator-activated receptor-γ by insulin and C-peptide in kidney proximal tubular cells: Dependent on phosphatidylinositol 3-kinase activity. *Journal of Biological Chemistry*, *279*(48), 49747–49754. https://doi.org/10.1074/jbc.M408268200

American Diabetes Association. (2005). Diagnosis and Classification of Diabetes Mellitus. *Diabetes Care*, *28*(1), S 37-S42.

Andersen, O. M., Reiche, J., Schmidt, V., Gotthardt, M., Spoelgen, R., Behlke, J., von Arnim, C. A. F., Breiderhoff, T., Jansen, P., Wu, X., Bales, K. R., Cappai, R., Masters, C. L., Gliemann, J., Mufson, E. J., Hyman, B. T., Paul, S. M., Nykjsær, A., & Willnow, T. E. (2005). Neuronal sorting protein-related receptor sorLA/LR11 regulates processing of the amyloid precursor protein. *Proceedings of the National Academy of Sciences of the United States of America*, *102*(38), 13461–13466. https://doi.org/10.1073/pnas.0503689102

Anderson, Deborah K., Liang, J. W. and C. L. (2017). Magnetic cell sorting for in vivo and in vitro astrocyte, neuron, and microglia analysis. *Physiology & Behavior*, *176*(5), 139–148. https://doi.org/10.1002/cpns.71.

Andrews, S. J., Fulton-Howard, B., O'Reilly, P., Marcora, E., Goate, A. M., Farrer, L. A., Haines, J. L., Mayeux, R., Naj, A. C., Pericak-Vance, M. A., Schellenberg, G. D., & Wang, L. S. (2020). Causal Associations Between Modifiable Risk Factors and the Alzheimer's Phenome. *Annals of Neurology*. https://doi.org/10.1002/ana.25918

Apelt, J., Mehlhorn, G., & Schliebs, R. (1999). Insulin-Sensitive GLUT4 Glucose Transporters Are Colocalized With GLUT3-Expressing Cells and Demonstrate a Chemically Distinct Neuron-Specific Localization in Rat Brain. *Journal of Neuroscience Research*, 57(5), 693–705.

Asaro, A., Carlo-Spiewok, A. S., Malik, A. R., Rothe, M., Schipke, C. G., Peters, O., Heeren, J., & Willnow, T. E. (2020). Apolipoprotein E4 disrupts the neuroprotective action of sortilin in neuronal lipid metabolism and endocannabinoid signaling. *Alzheimer's and Dementia*, *16*(9), 1248–1258. https://doi.org/10.1002/alz.12121

Ashrafi, G., & Ryan, T. A. (2017). Glucose metabolism in nerve terminals. *Current Opinion in Neurobiology*, *45*, 156–161. https://doi.org/10.1016/j.conb.2017.03.007

Ashrafi, G., Wu, Z., Farrell, R. J., & Ryan, T. A. (2017). GLUT4 Mobilization Supports Energetic Demands of Active Synapses. *Neuron*, *93*(3), 606-615.e3. https://doi.org/10.1016/j.neuron.2016.12.020

Avila, J., León-Espinosa, G., García, E., García-Escudero, V., Hernández, F., & DeFelipe, J. (2012). Tau Phosphorylation by GSK3 in Different Conditions. *International Journal of Alzheimer's Disease*, *2012*(May 2014), 1–7. https://doi.org/10.1155/2012/578373

Beddows, C. A., & Dodd, G. T. (2021). Insulin on the brain: The role of central insulin signalling in energy and glucose homeostasis. *Journal of Neuroendocrinology*, *33*(4), 1–20. https://doi.org/10.1111/jne.12947

Bergström, P., Agholme, L., Nazir, F. H., Satir, T. M., Toombs, J., Wellington, H., Strandberg, J., Bontell, T. O., Kvartsberg, H., Holmström, M., Boreström, C., Simonsson, S., Kunath, T., Lindahl, A., Blennow, K., Hanse, E., Portelius, E., Wray, S., & Zetterberg, H. (2016). Amyloid precursor protein expression and processing are differentially regulated during cortical neuron differentiation. *Scientific Reports*, *6*(July), 1–14. https://doi.org/10.1038/srep29200

Bernstein, H. G., Ansorge, S., Riederer, P., Reiser, M., Frölich, L., & Bogerts, B. (1999). Insulin-degrading enzyme in the Alzheimer's disease brain: Prominent localization in neurons and senile plaques. *Neuroscience Letters*, *263*(2–3), 161–164. https://doi.org/10.1016/S0304-3940(99)00135-4

Bertram, L., McQueen, M. B., Mullin, K., Blacker, D., & Tanzi, R. E. (2007). Systematic meta-analyses of Alzheimer disease genetic association studies: The AlzGene database. *Nature Genetics*, *39*(1), 17–23. https://doi.org/10.1038/ng1934

Biessels, G. J., & Reagan, L. P. (2015). Hippocampal insulin resistance and cognitive dysfunction. *Nature reviews. Neuroscience*,*16*(11), 660-671. https://doi.org/10.1038/nrn4019

Bingham, E., Hopkins, D., Smith, D., Pernet, A., Hallett, W., Reed, L., Paul, M. K., & Amiel, S. A. (2002). The role of insulin in human brain glucose metabolism. *Diabetes*, *51*(December), 3384–3390. https://doi.org/10.2337/diabetes.51.12.3384

Blázquez, E., Velázquez, E., & Hurtado-carneiro, V. (2014). Insulin in the brain : its pathophysiological implications for states related with central insulin resistance , type 2 diabetes and alzheimer ' s disease. *Frontiers in endocrinology*, 5,161. 1–21. https://doi.org/10.3389/fendo.2014.00161

Boucher, J., Kleinridders, A., & Kahn, C. R. (2014). Insulin Receptor Signaling in Normal. *Cold Spring Harb Perspect Biol 2014*, *6*, a009191. https://doi.org/10.1101/cshperspect.a009191

Braak, H., & del Tredici, K. (2012). Where, when, and in what form does sporadic Alzheimer's disease begin? *Current Opinion in Neurology*, *25*(6), 708–714. https://doi.org/10.1097/WCO.0b013e32835a3432

Braak, H., & del Tredici, K. (2015). The preclinical phase of the pathological process underlying sporadic Alzheimer's disease. *Brain*, *138*(10), 2814–2833. https://doi.org/10.1093/brain/awv236

Brito-Moreira, J., Lourenco, M. v., Oliveira, M. M., Ribeiro, F. C., Ledo, J. H., Diniz, L. P., Vital, J. F. S., Magdesian, M. H., Melo, H. M., Barros-Aragão, F., de Souza, J. M., Alves-Leon, S. v., Gomes, F. C. A., Clarke, J. R., Figueiredo, C. P., de Felice, F. G., & Ferreira, S. T. (2017). Interaction of amyloid-β (Aβ) oligomers with neurexin 2α and neuroligin 1 mediates synapse damage and memory loss in mice. *Journal of Biological Chemistry*, *292*(18), 7327–7337. https://doi.org/10.1074/jbc.M116.761189

Brown, M. R., Radford, S. E., & Hewitt, E. W. (2020). Modulation of β-Amyloid Fibril Formation in Alzheimer's Disease by Microglia and Infection. *Frontiers in Molecular Neuroscience*, *13*(November). https://doi.org/10.3389/fnmol.2020.609073

Bru, J. C., Gautam, D., & Burks, D. J. (2000). Role of Brain Insulin Receptorin Control of Body Weight and Reproduction. *Science*, 289(5487), 2122-2125. https://doi.org/10.1126/science.289.5487.2122 Buettner, R., Schölmerich, J., & Bollheimer, L. C. (2007). High-fat diets: Modeling the metabolic disorders of human obesity in rodents. *Obesity*, *15*(4), 798–808. https://doi.org/10.1038/oby.2007.608

Burillo, J., Marqués, P., Jiménez, B., González-Blanco, C., Benito, M., & Guillén, C. (2021). Insulin resistance and diabetes mellitus in alzheimer's disease. *Cells*, *10*(5). https://doi.org/10.3390/cells10051236

Caglayan, S., Bauerfeind, A., Schmidt, V., Carlo, A. S., Prabakaran, T., Hübner, N., & Willnow, T. E. (2012). Identification of Alzheimer disease risk genotype that predicts efficiency of SORL1 expression in the brain. *Archives of Neurology*, *69*(3), 373–379. https://doi.org/10.1001/archneurol.2011.788

Caglayan, S., Takagi-Niidome, S., Liao, F., Carlo, A. S., Schmidt, V., Burgert, T., Kitago, Y., Fuĉhtbauer, E. M., Fuĉhtbauer, A., Holtzman, D. M., Takagi, J., & Willnow, T. E. (2014). Lysosomal sorting of amyloid-β by the SORLA receptor is impaired by a familial Alzheimer's disease mutation. *Science Translational Medicine*, *6*(223). https://doi.org/10.1126/scitranslmed.3007747

Cai, W., Xue, C., Sakaguchi, M., Konishi, M., Shirazian, A., Ferris, H. A., Li, M. E., Yu, R., Kleinridders, A., Pothos, E. N., & Kahn, C. R. (2018). Insulin regulates astrocyte gliotransmission and modulates behavior. *Journal of Clinical Investigation*, *128*(7), 2914–2926. https://doi.org/10.1172/JCI99366

Camandola, S. (2017). Brain metabolism in health , aging , and neurodegeneration. *The EMBO Journal*, *36*(11), 1474–1492. https://doi.org/10.15252/embj.201695810

Carro, E., & Torres-aleman, I. (2004). The role of insulin and insulin-like growth factor I in the molecular and cellular mechanisms underlying the pathology of Alzheimer ' s disease. *European Journal of Pharmacology, 490*, 127–133. https://doi.org/10.1016/j.ejphar.2004.02.050

Chatterjee, S., & Mudher, A. (2018). Alzheimer's disease and type 2 diabetes: A critical assessment of the shared pathological traits. *Frontiers in Neuroscience*, *12*(JUN). https://doi.org/10.3389/fnins.2018.00383

Chen, G. F., Xu, T. H., Yan, Y., Zhou, Y. R., Jiang, Y., Melcher, K., & Xu, H. E. (2017). Amyloid beta: Structure, biology and structure-based therapeutic development. *Acta Pharmacologica Sinica*, *38*(9), 1205–1235. https://doi.org/10.1038/aps.2017.28

Chiu, S. L., & Cline, H. T. (2010). Insulin receptor signaling in the development of neuronal structure and function. *Neural Development*, *5*(1), 1–18. https://doi.org/10.1186/1749-8104-5-7

Cook, D. G., Leverenz, J. B., McMillan, P. J., Kulstad, J. J., Ericksen, S., Roth, R. A., Schellenberg, G. D., Jin, L. W., Kovacina, K. S., & Craft, S. (2003). Reduced hippocampal insulin-degrading enzyme in late-onset Alzheimer's disease is associated with the apolipoprotein E-ε4 allele. *American Journal of Pathology*, *162*(1), 313–319. https://doi.org/10.1016/S0002-9440(10)63822-9

Darocha-Souto, B., Scotton, T. C., Coma, M., Serrano-Pozo, A., Hashimoto, T., Serenó, L., Rodríguez, M., Sánchez, B., Hyman, B. T., & Gómez-Isla, T. (2011). Brain oligomeric β-amyloid but not total amyloid plaque burden correlates with neuronal loss and astrocyte inflammatory response in amyloid precursor protein/tau transgenic mice. *Journal of Neuropathology and Experimental Neurology*, *70*(5), 360–376. https://doi.org/10.1097/NEN.0b013e318217a118

de Wilde, M. C., Vellas, B., Girault, E., Yavuz, A. C., & Sijben, J. W. (2017). Lower brain and blood nutrient status in Alzhiemer's disease: Results from meta-analyses. *Alzheimer's and Dementia: Translational Research and Clinical Interventions*, *3*(3), 416–431. https://doi.org/10.1016/j.trci.2017.06.002

Dienel, G. A. (2019). BRAIN GLUCOSE METABOLISM : INTEGRATION OF ENERGETICS WITH FUNCTION. *Physiological Reviews,* 99(1), 949–1045. https://doi.org/10.1152/physrev.00062.2017

Dienel, G. A., Cruz, N. F., Adachi, K., Sokoloff, L., & Holden, J. E. (1997). Determination of local brain glucose level with [14C]methylglucose: Effects of glucose supply and demand. *American Journal of Physiology - Endocrinology and Metabolism*, *273*(5 36-5), 839–849. https://doi.org/10.1152/ajpendo.1997.273.5.e839

Dodd, G. T., & Tiganis, T. (2017). Insulin action in the brain: Roles in energy and glucose homeostasis. *Journal of Neuroendocrinology*, *29*(10), 1–13. https://doi.org/10.1111/jne.12513

Dodson, S. E., Gearing, M., Lippa, C. F., Montine, T. J., Levey, A. I., & Lah, J. J. (2006). LR11/SorLA expression is reduced in sporadic Alzheimer disease but not in familial Alzheimer disease. *Journal of Neuropathology and Experimental Neurology*, *65*(9), 866–872. https://doi.org/10.1097/01.jnen.0000228205.19915.20

Donovan, C. M., & Watts, A. G. (2014). Peripheral and central glucose sensing in hypoglycemic detection. *Physiology*, *29*(5), 314–324. https://doi.org/10.1152/physiol.00069.2013

Dragatsis, I., & Zeitlin, S. (2000). CaMKIIα-cre transgene expression and recombination patterns in the mouse brain. *Genesis*, *26*(2), 133–135.

https://doi.org/10.1002/(SICI)1526-968X(200002)26:2<133::AID-GENE10>3.0.CO;2-V

Du, J., Zhang, L., Liu, S., Zhang, C., Huang, X., Li, J., Zhao, N., & Wang, Z. (2009). Biochemical and Biophysical Research Communications PPAR c transcriptionally regulates the expression of insulin-degrading enzyme in primary neurons. *Biochemical and Biophysical Research Communications*, *383*(4), 485–490. https://doi.org/10.1016/j.bbrc.2009.04.047

Dumanis, S. B., Burgert, T., Caglayan, S., Füchtbauer, A., Füchtbauer, E. M., Schmidt, V., & Willnow, T. E. (2015). Distinct functions for anterograde and retrograde sorting of SORLA in amyloidogenic processes in the brain. *Journal of Neuroscience*, *35*(37), 12703–12713. https://doi.org/10.1523/JNEUROSCI.0427-15.2015

E. H. Corder, A. M. Saunders, W. J. S., & D. E. Schmechel, P. C. Gaskell, G. W. Small, A. D. Roses, J. L. Haines, M. A. P.-V. (1993). Gene Dose of Apolipoprotein E Type 4 Allele and the Risk of Alzheimer's Disease in Late Onset Families. *Science*, *261*(3), 921–923. http://doi.wiley.com/10.1002/ana.24454%0Ahttp://www.ncbi.nlm.nih.gov/pubmed/24655651%0Ahttp://www.pubmedcentral.nih.gov/articlerender.fcgi?artid=PMC4126411%0Ahttp://dx.doi.org/10.1016/S1474-4422(10)70325-2%0Ahttp://dx.doi.org/10.1038/nrneurol.2012.263%0Aw

Eckman, E. A., Reed, D. K., & Eckman, C. B. (2001). Degradation of the Alzheimer's Amyloid β Peptide by Endothelin-converting Enzyme. *Journal of Biological Chemistry*, *276*(27), 24540–24548. https://doi.org/10.1074/jbc.M007579200

Edwards, G. A., Gamez, N., Escobedo, G., Calderon, O., & Moreno-Gonzalez, I. (2019). Modifiable risk factors for Alzheimer's disease. *Frontiers in Aging Neuroscience*, *11*(JUN), 1–18. https://doi.org/10.3389/fnagi.2019.00146

Eyster, C. A., Duggins, Q. S., Gorbsky, G. J., & Olson, A. L. (2006). Microtubule Network Is Required for Insulin Signaling through Activation of Akt/Protein Kinase B. *Journal of Biological Chemistry*, *281*(51), 39719–39727. https://doi.org/10.1074/jbc.m607101200

Fan, L., Mao, C., Hu, X., Zhang, S., Yang, Z., Hu, Z., Sun, H., Fan, Y., Dong, Y., Yang, J., Shi, C., & Xu, Y. (2020). New Insights Into the Pathogenesis of Alzheimer's Disease. *Frontiers in Neurology*, *10*(January), 1–12. https://doi.org/10.3389/fneur.2019.01312

Farris, W., Mansourian, S., Chang, Y., Lindsley, L., Eckman, E. A., Frosch, M. P., Eckman, C. B., Tanzi, R. E., Selkoe, D. J., & Guénette, S. (2003). Insulin-degrading enzyme regulates the levels of insulin, amyloid β-protein, and the β-amyloid precursor protein intracellular domain in vivo. *Proceedings of the National Academy of Sciences of the United States of America*, *100*(7), 4162–4167. https://doi.org/10.1073/pnas.0230450100

Fernandez, A. M., Hernandez-garzón, E., Perez-domper, P., Perez-alvarez, A., Mederos, S., Matsui, T., Santi, A., Trueba-saiz, A., García-guerra, L., Pose-utrilla, J., Fielitz, J., Olson, E. N., Fernandez, R., Rosa, D., Garcia, L. G., Pozo, M. A., Iglesias, T., Araque, A., & Soya, H. (2017). *Insulin Regulates Astrocytic Glucose Handling Through Cooperation With IGF-I*. *66*(January), 64–74. https://doi.org/10.2337/db16-0861

Ferreira, S. T., Lourenco, M. v., Oliveira, M. M., & de Felice, F. G. (2015). Soluble amyloid-β oligomers as synaptotoxins leading to cognitive impairment in Alzheimer's disease. *Frontiers in Cellular Neuroscience*, *9*(MAY), 1–17. https://doi.org/10.3389/fncel.2015.00191

Festa, G., Mallamace, F., Sancesario, G. M., Corsaro, C., Mallamace, D., Fazio, E., Arcidiacono, L., Sakai, V. G., Senesi, R., Preziosi, E., Sancesario, G., & Andreani, C. (2019). Aggregation states of Aβ1-40, Aβ1-42 and Aβp3-42 amyloid beta peptides: A SANS study. *International Journal of Molecular Sciences*, *20*(17), 1–9. https://doi.org/10.3390/ijms20174126

Fiory, F., Perruolo, G., Cimmino, I., Cabaro, S., Pignalosa, F. C., Miele, C., Beguinot, F., Formisano, P., & Oriente, F. (2019). The Relevance of Insulin Action in the Dopaminergic System. *Frontiers in Neuroscience*, *13*(August), 1–16. https://doi.org/10.3389/fnins.2019.00868

Flowers, S. A., & Rebeck, G. W. (2020). APOE in the normal brain. *Neurobiology of Disease*, *136*, 104724. https://doi.org/10.1016/j.nbd.2019.104724

Franklin, W., & Taglialatela, G. (2016). A method to determine insulin responsiveness in synaptosomes isolated from frozen brain tissue. *Journal of Neuroscience Methods*, *261*, 128–134. https://doi.org/10.1016/j.jneumeth.2016.01.006

Gabbouj, S., Natunen, T., Koivisto, H., Jokivarsi, K., Takalo, M., Marttinen, M., Wittrahm, R., Kemppainen, S., Naderi, R., Posado-Fernández, A., Ryhänen, S., Mäkinen, P., Paldanius, K. M. A., Doria, G., Poutiainen, P., Flores, O., Haapasalo, A., Tanila, H., & Hiltunen, M. (2019). Intranasal insulin activates Akt2 signaling pathway in the hippocampus of wild-type but not in APP/PS1 Alzheimer model mice. *Neurobiology of Aging*, *75*, 98–108. https://doi.org/10.1016/j.neurobiolaging.2018.11.008

Gabbouj, S., Ryhänen, S., Marttinen, M., Wittrahm, R., Takalo, M., Kemppainen, S., Martiskainen, H., Tanila, H., & Haapasalo, A. (2019). *Altered Insulin Signaling in Alzheimer ' s Disease Brain – Special Emphasis on PI3K-Akt Pathway*. *13*(June), 1–8. https://doi.org/10.3389/fnins.2019.00629

Gasparini, L., Gouras, G. K., Wang, R., Gross, R. S., Beal, M. F., Greengard, P., & Xu, H. (2001). Stimulation of β-amyloid precursor protein trafficking by insulin reduces intraneuronal β-amyloid and requires mitogen-activated protein kinase signaling. *Journal of Neuroscience*, *21*(8), 2561–2570. https://doi.org/10.1523/jneurosci.21-08-02561.2001

Gelling, R. W., Morton, G. J., Morrison, C. D., Niswender, K. D., Myers, M. G., Rhodes, C. J., & Schwartz, M. W. (2006). Insulin action in the brain contributes to glucose lowering during insulin treatment of diabetes. *Cell Metabolism*, *3*(1), 67–73. https://doi.org/10.1016/j.cmet.2005.11.013

Glerup, S., Lume, M., Olsen, D., Nyengaard, J. R., Vaegter, C. B., Gustafsen, C., Christensen, E. I., Kjolby, M., Hay-Schmidt, A., Bender, D., Madsen, P., Saarma, M., Nykjaer, A., & Petersen, C. M. (2013). SorLA Controls Neurotrophic Activity by Sorting of GDNF and Its Receptors GFRα1 and RET. *Cell Reports*, *3*(1), 186–199. https://doi.org/10.1016/j.celrep.2012.12.011

Gliemann, J., Hermey, G., Nykjær, A., Petersen, C. M., Jacobsen, C., & Andreasen, P. A. (2004). The mosaic receptor sorLA/LR11 binds components of the plasminogen-activating system and platelet-derived growth factor-BB similarly to LRP1 (low-

density lipoprotein receptor-related protein), but mediates slow internalization of bound ligand. *Biochemical Journal*, *381*(1), 203–212. https://doi.org/10.1042/BJ20040149

González-Casimiro, C. M., Merino, B., Casanueva-álvarez, E., Postigo-Casado, T., Cámara-Torres, P., Fernández-Díaz, C. M., Leissring, M. A., Cózar-Castellano, I., & Perdomo, G. (2021). Modulation of insulin sensitivity by insulin-degrading enzyme. *Biomedicines*, *9*(1), 1–38. https://doi.org/10.3390/biomedicines9010086

Götz, J., Bodea, L. G., & Goedert, M. (2018). Rodent models for Alzheimer disease. *Nature Reviews Neuroscience*, *19*(10), 583–598. https://doi.org/10.1038/s41583-018-0054-8

Gratuze, M., Joly-Amado, A., Vieau, D., Buée, L., & Blum, D. (2018). Mutual relationship between tau and central insulin signalling: Consequences for ad and tauopathies? *Neuroendocrinology*, *107*(2), 181–195. https://doi.org/10.1159/000487641

Gray, S. M., Aylor, K. W., & Barrett, E. J. (2017). Unravelling the regulation of insulin transport across the brain endothelial cell. *Diabetologia*, 60(8), 1512–1521. https://doi.org/10.1007/s00125-017-4285-4

Grillo, C. A., Benedict, C., Chapman, C. D., & Schi, H. B. (2017). Intranasal insulin in Alzheimer ' s disease : Food for thought. *Neuropharmacology*, 196-201 . https://doi.org/10.1016/j.neuropharm.2017.11.037

Gustavsson, A., Pemberton-Ross, P., Gomez Montero, M., Hashim, M., & Thompson, R. (2020). Challenges in demonstrating the value of disease-modifying therapies for Alzheimer's disease. *Expert Review of Pharmacoeconomics and Outcomes Research*, *20*(6), 563–570. https://doi.org/10.1080/14737167.2020.1822738

Habib, A., Sawmiller, D., Tan, J., Child, S., & Neurosciences, B. (2018). Restoring sAPPα functions as a potential treatment for Alzheimer's disease. *Journal of neuroscience research*, *95*(4), 973–991. https://doi.org/10.1002/jnr.23823.Restoring

Haeusler, R. A., Mcgraw, T. E., & Accili, D. (2017). Biochemical and cellular properties of insulin receptor signalling. *Nature Publishing Group*, *19*(1), 31–44. https://doi.org/10.1038/nrm.2017.89

Hahn, C. S., Scott, D. W., Xu, X., Roda, M. A., Gregory, A., Wells, J. M., Viera, L., Winstead, C. J., Bratcher, P., Sparidans, R. W., Redegeld, F. A., Jackson, P. L., Folkerts, G., & Edwin, J. (2015). Association of insulin resistance with cerebral glucose uptake in late middle-aged adults at risk for Alzheimer's disease. *JAMA Neurology*, *1*(3), 1–21. https://doi.org/10.1001/jamaneurol.2015.0613.Association

Hariri, N., & Thibault, L. (2010). High-fat diet-induced obesity in animal models. *Nutrition Research Reviews*, *23*(2), 270–299. https://doi.org/10.1017/S0954422410000168

Harold, D., Abraham, R., Hollingworth, P., Sims, R., Gerrish, A., Hamshere, M. L., Pahwa, J. S., Moskvina, V., Dowzell, K., Williams, A., Jones, N., Thomas, C., Stretton, A., Morgan, A. R., Lovestone, S., Powell, J., Proitsi, P., Lupton, M. K., Brayne, C., … Williams, J. (2009). Genome-wide association study identifies variants at CLU and PICALM associated with Alzheimer's disease. *Nature Genetics*, *41*(10), 1088–1093. https://doi.org/10.1038/ng.440

Hassan, A., Sharma Kandel, R., Mishra, R., Gautam, J., Alaref, A., & Jahan, N. (2020). Diabetes Mellitus and Parkinson's Disease: Shared Pathophysiological Links and

Possible Therapeutic Implications. *Cureus*, *12*(8). https://doi.org/10.7759/cureus.9853

He, Y., Wei, M., Wu, Y., Qin, H., Li, W., Ma, X., Cheng, J., Ren, J., Shen, Y., Chen, Z., Sun, B., Huang, F. de, Shen, Y., & Zhou, Y. D. (2019). Amyloid β oligomers suppress excitatory transmitter release via presynaptic depletion of phosphatidylinositol-4,5-bisphosphate. *Nature Communications*, *10*(1). https://doi.org/10.1038/s41467-019-09114-z

Heni, M., Kullmann, S., Preissl, H., Fritsche, A., & Häring, H. U. (2015). Impaired insulin action in the human brain: Causes and metabolic consequences. *Nature Reviews Endocrinology*, *11*(12), 701–711. https://doi.org/10.1038/nrendo.2015.173

Hermey, G. (2009). The Vps10p-domain receptor family. *Cellular and Molecular Life Sciences*, *66*(16), 2677–2689. https://doi.org/10.1007/s00018-009-0043-1

Hirvonen, J., Virtanen, K. A., Nummenmaa, L., Hannukainen, J. C., Honka, M. J., Bucci, M., Nesterov, S. v., Parkkola, R., Rinne, J., Iozzo, P., & Nuutila, P. (2011). Effects of insulin on brain glucose metabolism in impaired glucose tolerance. *Diabetes*, *60*(2), 443–447. https://doi.org/10.2337/db10-0940

Hölscher, C. (2014). First clinical data of the neuroprotective effects of nasal insulin application in patients with Alzheimer's disease. *Alzheimer's and Dementia*, *10*(1 SUPPL.), 33–37. https://doi.org/10.1016/j.jalz.2013.12.006

Holtzman, D. M., Herz, J., & Bu, G. (2012). Apolipoprotein E and Apolipoprotein E Receptors: Normal Biology and Roles in Alzheimer Disease. *Online*, 1–24.

Hulse, R. E., Ralat, L. A., & Wei-Jen, T. (2009). Structure, Function, and Regulation of Insulin-Degrading Enzyme. In *Vitamins and Hormones* (1st ed., Vol. 80, Issue C). Elsevier Inc. https://doi.org/10.1016/S0083-6729(08)00622-5

Human Biochemistry. (2018). In *Annals of Internal Medicine* (Vol. 31, Issue 6). https://doi.org/10.7326/0003-4819-31-6-1134

Jakoby, P., Schmidt, E., Ruminot, I., Gutiérrez, R., Barros, L. F., & Deitmer, J. W. (2017). Higher Transport and Metabolism of Glucose in Astrocytes Compared with Neurons : A Multiphoton Study of Hippocampal and Cerebellar Tissue Slices. *Cerebral cortex*, 24(1), 222-231. https://doi.org/10.1093/cercor/bhs309

Jansen, I. E., Savage, J. E., Watanabe, K., Bryois, J., Williams, D. M., Steinberg, S., Sealock, J., Karlsson, I. K., Hägg, S., Athanasiu, L., Voyle, N., Proitsi, P., Witoelar, A., Stringer, S., Aarsland, D., Almdahl, I. S., Andersen, F., Bergh, S., Bettella, F., … Posthuma, D. (2019). Genome-wide meta-analysis identifies new loci and functional pathways influencing Alzheimer's disease risk. *Nature Genetics*, *51*(3), 404–413. https://doi.org/10.1038/s41588-018-0311-9

Janson, J., Laedtke, T., Parisi, J. E., O'Brien, P., Petersen, R. C., & Butler, P. C. (2004). Increased Risk of Type 2 Diabetes in Alzheimer Disease. *Diabetes*, *53*(2), 474–481. https://doi.org/10.2337/diabetes.53.2.474

Jha, N. K., Jha, S. K., Kumar, D., Kejriwal, N., Sharma, R., Ambasta, R. K., & Kumar, P. (2015). Impact of insulin degrading enzyme and neprilysin in Alzheimer's disease biology: Characterization of putative cognates for therapeutic applications. *Journal of Alzheimer's Disease*, *48*(4), 891–917. https://doi.org/10.3233/JAD-150379

Jope, R. S., & Johnson, G. V. W. (2004). The glamour and gloom of glycogen synthase kinase-3. *Trends in Biochemical Sciences*, *29*(2), 95–102. https://doi.org/10.1016/j.tibs.2003.12.004

Kamenetz, F., Tomita, T., Hsieh, H., Seabrook, G., Borchelt, D., Iwatsubo, T., Sisodia, S., & Malinow, R. (2003). APP Processing and Synaptic Function. *Neuron*, *37*(6), 925–937. https://doi.org/10.1016/S0896-6273(03)00124-7

Kang, S., Lee, Y. H., & Lee, J. E. (2017). Metabolism-centric overview of the pathogenesis of Alzheimer's disease. *Yonsei Medical Journal*, *58*(3), 479–488. https://doi.org/10.3349/ymj.2017.58.3.479

Kappeler, L., de Magalhaes Filho, C., Dupont, J., Leneuve, P., Cervera, P., Périn, L., Loudes, C., Blaise, A., Klein, R., Epelbaum, J., le Bouc, Y., & Holzenberger, M. (2008). Brain IGF-1 receptors control mammalian growth and lifespan through a neuroendocrine mechanism. *PLoS Biology*, *6*(10), 2144–2153. https://doi.org/10.1371/journal.pbio.0060254

Kedia, N., Almisry, M., & Bieschke, J. (2017). Glucose directs amyloid-beta into membrane-active oligomers. *Physical Chemistry Chemical Physics*, *19*(27), 18036–18046. https://doi.org/10.1039/C7CP02849K

Kellar, D., & Craft, S. (2020). Brain insulin resistance in Alzheimer's disease and related disorders: mechanisms and therapeutic approaches. *The Lancet Neurology*, *19*(9), 758–766. https://doi.org/10.1016/S1474-4422(20)30231-3

Ketterer, C., Tschritter, O., Preissl, H., Heni, M., Häring, H. U., & Fritsche, A. (2011). Insulin sensitivity of the human brain. *Diabetes Research and Clinical Practice*, *93*(SUPPL. 1), S47–S51. https://doi.org/10.1016/S0168-8227(11)70013-4

Khan, R. (2001). Postprandial blood glucose. *Diabetes Care*, *24*(4), 775–778. https://doi.org/10.2337/diacare.24.4.775

Kim, B., Backus, C., Oh, S. S., Hayes, J. M., & Feldman, E. L. (2009). Increased tau phosphorylation and cleavage in mouse models of type 1 and type 2 diabetes. *Endocrinology*, *150*(12), 5294–5301. https://doi.org/10.1210/en.2009-0695

Kim, B., McLean, L. L., Philip, S. S., & Feldman, E. L. (2011). Hyperinsulinemia induces insulin resistance in dorsal root ganglion neurons. *Endocrinology*, *152*(10), 3638–3647. https://doi.org/10.1210/en.2011-0029

Kim, H., Kim, M., Im, S.-K., & Fang, S. (2018). Mouse Cre-LoxP system: general principles to determine tissue-specific roles of target genes. *Laboratory Animal Research*, *34*(4), 147. https://doi.org/10.5625/lar.2018.34.4.147

Kim, W. H., Lee, J., Jung, D. W., & Williams, D. R. (2012). Visualizing sweetness: Increasingly diverse applications for fluorescent-tagged glucose bioprobes and their recent structural modifications. *Sensors*, *12*(4), 5005–5027. https://doi.org/10.3390/s120405005

Kleinridders, A., & Ferris, H. (2014). Insulin Action in Brain Regulates Systemic Metabolism and Brain Function. *Diabetes*, 63(7), 2232-2243. https://doi.org/10.2337/db14-0568

Klip, A., McGraw, T. E., & James, D. E. (2019). Thirty sweet years of GLUT4. *Journal of Biological Chemistry*, *294*(30), 11369–11381. https://doi.org/10.1074/jbc.REV119.008351

Ko, S. Y., Ko, H. A., Chu, K. H., Shieh, T. M., Chi, T. C., Chen, H. I., Chang, W. C., & Chang, S. S. (2015). The possible mechanism of advanced glycation end products (AGEs) for Alzheimer's disease. *PLoS ONE*, *10*(11), 1–16. https://doi.org/10.1371/journal.pone.0143345

Konishi, M., Sakaguchi, M., Lockhart, S. M., Cai, W., Ella, M., & Homan, E. P. (2017). Endothelial insulin receptors differentially control insulin signaling kinetics in peripheral tissues and brain of mice. *Proceedings of the National Academy of Sciences of the United States of America, 114*(40), E8478–E8487. https://doi.org/10.1073/pnas.1710625114

Krasil'nikova, I., Surin, A., Sorokina, E., Fisenko, A., Boyarkin, D., Balyasin, M., Demchenko, A., Pomytkin, I., & Pinelis, V. (2019). Insulin Protects Cortical Neurons Against Glutamate Excitotoxicity. *Frontiers in Neuroscience*, *13*(September), 1–12. https://doi.org/10.3389/fnins.2019.01027

Kulas, J. A., Franklin, W. F., Smith, N. A., Manocha, G. D., Puig, K. L., Nagamoto-Combs, K., Hendrix, R. D., Taglialatela, G., Barger, S. W., & Combs, C. K. (2019). Ablation of amyloid precursor protein increases insulin-degrading enzyme levels and activity in brain and peripheral tissues. *American Journal of Physiology - Endocrinology and Metabolism*, *316*(1), E106–E120. https://doi.org/10.1152/ajpendo.00279.2018

Kullmann, S., Heni, M., Fritsche, A., & Preissl, H. (2015). Insulin Action in the Human Brain: Evidence from Neuroimaging Studies. *Journal of Neuroendocrinology*, *27*(6), 419–423. https://doi.org/10.1111/jne.12254

Kunkle, B. W., Grenier-Boley, B., Sims, R., Bis, J. C., Damotte, V., Naj, A. C., Boland, A., Vronskaya, M., van der Lee, S. J., Amlie-Wolf, A., Bellenguez, C., Frizatti, A., Chouraki, V., Martin, E. R., Sleegers, K., Badarinarayan, N., Jakobsdottir, J., Hamilton-Nelson, K. L., Moreno-Grau, S., … Pericak-Vance, M. A. (2019). Genetic meta-analysis of diagnosed Alzheimer's disease identifies new risk loci and implicates Aβ, tau, immunity and lipid processing. *Nature Genetics*, *51*(3), 414–430. https://doi.org/10.1038/s41588-019-0358-2

Lange, K., Brandt, U., & Zimmermann, B. (1990). Relationship between insulin stimulation and endogenous regulation of 2-deoxyglucose uptake in 3T3-L1 adipocytes. *Journal of Cellular Physiology*, *142*(1), 1–14. https://doi.org/10.1002/jcp.1041420102

Larsen, J. V., & Petersen, C. M. (2017). SorLA in Interleukin-6 Signaling and Turnover. *Molecular and Cellular Biology*, *37*(11). https://doi.org/10.1128/MCB.00641-16

Lee, C. W. C., Lau, K. F., Miller, C. C. J., & Shaw, P. C. (2003). Glycogen synthase kinase-3β-mediated tau phosphorylation in cultured cell lines. *NeuroReport*, *14*(2), 257–260. https://doi.org/10.1097/00001756-200302100-00020

Lee, J. H., Barral, S., & Reitz, C. (2008). The neuronal sortilin-related receptor gene SORL1 and late-onset Alzheimer's disease. *Current Neurology and Neuroscience Reports*, *8*(5), 384–391. https://doi.org/10.1007/s11910-008-0060-8

Lee, S. H., Zabolotny, J. M., Huang, H., Lee, H., & Kim, Y. B. (2016). Insulin in the nervous system and the mind: Functions in metabolism, memory, and mood. *Molecular Metabolism*, *5*(8), 589–601. https://doi.org/10.1016/j.molmet.2016.06.011

Leto, D., & Saltiel, A. R. (2012). Regulation of glucose transport by insulin : traffic control of GLUT4. *Nature Reviews Molecular Cell Biology*, *13*(6), 383–396. https://doi.org/10.1038/nrm3351

Li, H., Yang, S., Wu, J., Ji, L., Zhu, L., Cao, L., Huang, J., Jiang, Q., Wei, J., Liu, M., Mao, K., Wei, N., Xie, W., & Yang, Z. (2018). cAMP/PKA signaling pathway contributes to neuronal apoptosis via regulating IDE expression in a mixed model of type 2 diabetes and Alzheimer's disease. *Journal of Cellular Biochemistry*, *119*(2), 1616–1626. https://doi.org/10.1002/jcb.26321

Liu, C.-C., Yue, M., Melrose, H. L., Tsai, C.-W., Bu, G., Hu, J., & Kanekiyo, T. (2015). Neuronal LRP1 Regulates Glucose Metabolism and Insulin Signaling in the Brain. *Journal of Neuroscience*, *35*(14), 5851–5859. https://doi.org/10.1523/jneurosci.5180-14.2015

Loh, K., Zhang, L., Brandon, A., Wang, Q., Begg, D., Qi, Y., Fu, M., Kulkarni, R., Teo, J., Baldock, P., Brüning, J. C., Cooney, G., Neely, G., & Herzog, H. (2017). Insulin controls food intake and energy balance via NPY neurons. *Molecular Metabolism*, *6*(6), 574–584. https://doi.org/10.1016/j.molmet.2017.03.013

Long, J. M., & Holtzman, D. M. (2019). Alzheimer Disease: An Update on Pathobiology and Treatment Strategies. *Cell*, *179*(2), 312–339. https://doi.org/10.1016/j.cell.2019.09.001

Lu, X.-Y., Huang, S., Chen, Q.-B., Zhang, D., Li, W., Ao, R., Leung, F. C.-Y., Zhang, Z., Huang, J., Tang, Y., & Zhang, S.-J. (2020). Metformin Ameliorates A β Pathology by Insulin-Degrading Enzyme in a Transgenic Mouse Model of Alzheimer's Disease. *Oxidative Medicine and Cellular Longevity*, *2020*, 1–10. https://doi.org/10.1155/2020/2315106

Luchsinger, J. A., Tang, M. X., Shea, S., & Mayeux, R. (2004). Hyperinsulinemia and risk of Alzheimer disease. *Neurology*, *63*(7), 1187–1192. https://doi.org/10.1212/01.WNL.0000140292.04932.87

Ma, Q. L., Teter, B., Ubeda, O. J., Morihara, T., Dhoot, D., Nyby, M. D., Tuck, M. L., Frautschy, S. A., & Cole, G. M. (2007). Omega-3 fatty acid docosahexaenoic acid increases SorLA/LR11, a sorting protein with reduced expression in sporadic Alzheimer's disease (AD): Relevance to AD prevention. *Journal of Neuroscience*, *27*(52), 14299–14307. https://doi.org/10.1523/JNEUROSCI.3593-07.2007

Malik, A. R., Szydlowska, K., Nizinska, K., Asaro, A., van Vliet, E. A., Popp, O., Dittmar, G., Fritsche-Guenther, R., Kirwan, J. A., Nykjaer, A., Lukasiuk, K., Aronica, E., & Willnow, T. E. (2019). SorCS2 Controls Functional Expression of Amino Acid Transporter EAAT3 and Protects Neurons from Oxidative Stress and Epilepsy-Induced Pathology. *Cell Reports*, *26*(10), 2792-2804.e6. https://doi.org/10.1016/j.celrep.2019.02.027

Malik, A. R., & Willnow, T. E. (2020a). VPS10P Domain Receptors: Sorting Out Brain Health and Disease. *Trends in Neurosciences*, *43*(11), 870–885. https://doi.org/10.1016/j.tins.2020.08.003

Malik, A. R., & Willnow, T. E. (2020b). VPS10P Domain Receptors: Sorting Out Brain Health and Disease. *Trends in Neurosciences*, *43*(11), 870–885. https://doi.org/10.1016/j.tins.2020.08.003

Manning, A. M., & Davis, R. J. (2003). Targeting JNK for therapeutic benefit: From junk to gold? *Nature Reviews Drug Discovery*, *2*(7), 554–565. https://doi.org/10.1038/nrd1132

Manning, B. D., & Toker, A. (2017a). AKT/PKB Signaling: Navigating the Network. *Cell*, *169*(3), 381–405. https://doi.org/10.1016/j.cell.2017.04.001

Manning, B. D., & Toker, A. (2017b). AKT/PKB Signaling: Navigating the Network. *Cell*, *169*(3), 381–405. https://doi.org/10.1016/j.cell.2017.04.001

Marcusson, E. G., Horazdovsky, B. F., Cereghino, J. L., Gharakhanian, E., & Emr, S. D. (1994). The sorting receptor for yeast vacuolar carboxypeptidase Y is encoded by the VPS10 gene. *Cell*, *77*(4), 579–586. https://doi.org/10.1016/0092-8674(94)90219-4

Marioni, R. E., Harris, S. E., Zhang, Q., McRae, A. F., Hagenaars, S. P., Hill, W. D., Davies, G., Ritchie, C. W., Gale, C. R., Starr, J. M., Goate, A. M., Porteous, D. J., Yang, J., Evans, K. L., Deary, I. J., Wray, N. R., & Visscher, P. M. (2018). GWAS on family history of Alzheimer's disease. *Translational Psychiatry*, *8*(1), 0–6. https://doi.org/10.1038/s41398-018-0150-6

Márquez, F., & Yassa, M. A. (2019). Neuroimaging Biomarkers for Alzheimer ' s Disease. *Molecular neurodegeneration 5*, 1–14. https://doi.org/10.1186/s13024-019-0325-5

Martins, R. N. (2019). The Link Between Diabetes , Glucose Control , and Alzheimer ' s Disease and Neurodegenerative Diseases*. Neurodegeneration and Alzheimer's disease*, 89–115. https://doi.org/10.1002/9781119356752.ch4

McCrimmon, R. (2008). The mechanisms that underlie glucose sensing during hypoglycaemia in diabetes. *Diabetic Medicine*, *25*(5), 513–522. https://doi.org/10.1111/j.1464-5491.2008.02376.x

Mehta, D., Jackson, R., Paul, G., Shi, J., & Sabbagh, M. (2017). Why do trials for Alzheimer's disease drugs keep failing? *Expert Opinion on Investigational Drugs*, *26*(6), 735–739. https://doi.org/10.1080/13543784.2017.1323868.Why

Mergenthaler, P., Lindauer, U., Dienel, G. A., & Meisel, A. (2013). Sugar for the brain : the role of glucose in physiological and pathological brain function. *Trends in Neurosciences*, *36*(10), 587–597. https://doi.org/10.1016/j.tins.2013.07.001

Michaelson, D. M. (2014). APOE ε4: The most prevalent yet understudied risk factor for Alzheimer's disease. *Alzheimer's and Dementia*, *10*(6), 861–868. https://doi.org/10.1016/j.jalz.2014.06.015

Milstein, J. L., & Ferris, H. A. (2021). The brain as an insulin-sensitive metabolic organ. *Molecular Metabolism*, *52*(April), 101234. https://doi.org/10.1016/j.molmet.2021.101234

Monte, S. M. de. (2015). Type 3 Diabetes is Sporadic Alzheimer ' s disease : Mini-Review. *European neuropsychopharmacology* 24(12), 1954–1960. https://doi.org/10.1016/j.euroneuro.2014.06.008.Type

Monti, G., & Andersen, O. M. (2018). 20 Years Anniversary for SORLA/SORL1 (1996-2016). *Receptors & Clinical Investigation*, *4*, 1–10. https://doi.org/10.14800/rci.1611

Morelli, L., Llovera, R. E., Mathov, I., Lue, L. F., Frangione, B., Ghiso, J., & Castaño, E. M. (2004). Insulin-degrading enzyme in brain microvessels: Proteolysis of amyloid β vasculotropic variants and reduced activity in cerebral amyloid angiopathy. *Journal of Biological Chemistry*, *279*(53), 56004–56013. https://doi.org/10.1074/jbc.M407283200

Moriel, N., Tong, M., & Gallucci, G. (2019). Altered expression of insulin-degrading enzyme and regulator of calcineurin in the rat intracerebral streptozotocin model and human apolipoprotein E- ε 4 – associated Alzheimer ' s disease. *Alzheimer's and dementia, 11*, 392–404. https://doi.org/10.1016/j.dadm.2019.03.004

Motoi, Y., Aizawa, T., Haga, S., Nakamura, S., Namba, Y., & Ikeda, K. (1999). Neuronal localization of a novel mosaic apolipoprotein E receptor, LR11, in rat and human brain. *Brain Research*, *833*(2), 209–215. https://doi.org/10.1016/S0006-8993(99)01542-5

Mozaffary, A., Asgari, S., Tohidi, M., Kazempour-Ardebili, S., Azizi, F., & Hadaegh, F. (2016). Change in fasting plasma glucose and incident type 2 diabetes mellitus: Results from a prospective cohort study. *BMJ Open*, *6*(5), 1–7. https://doi.org/10.1136/bmjopen-2015-010889

Müller, T., Meyer, H. E., Egensperger, R., & Marcus, K. (2008). The amyloid precursor protein intracellular domain (AICD) as modulator of gene expression, apoptosis, and cytoskeletal dynamics-Relevance for Alzheimer's disease. *Progress in Neurobiology*, *85*(4), 393–406. https://doi.org/10.1016/j.pneurobio.2008.05.002

Naj, A. C., & Schellenberg, G. D. (2017). Genomic variants, genes, and pathways of Alzheimer's disease: An overview. *American Journal of Medical Genetics, Part B: Neuropsychiatric Genetics*, *174*(1), 5–26. https://doi.org/10.1002/ajmg.b.32499

Nalivaeva, N. N., & Turner, A. J. (2019). Targeting amyloid clearance in Alzheimer ' s disease as a therapeutic strategy. *British journal of pharmacology,176(18)*, 3447–3463. https://doi.org/10.1111/bph.14593

Ngo, T. T., & Lenhoff, H. M. (1980). A Sensitive and Versatile Chromogenic and Peroxidase-Coupled. *Analytical Biochemistry*, *397*, 389–397.

Nicole, D., Denise, H., Kostas, K., M, B. J., & Andreas, T. (2006). Nestin-Cre Transgenic Mouse Line Nes-Cre1 Mediates Highly Efficient Cre/loxP Mediated Recombination in the Nervous System, Kidney, and Somite-Derived Tissues. *Genesis*, *44*(2), 355–360. https://doi.org/10.1002/dvg

Offe, K., Dodson, S. E., Shoemaker, J. T., Fritz, J. J., Gearing, M., Levey, A. I., & Lah, J. J. (2006). The lipoprotein receptor LR11 regulates amyloid β production and amyloid precursor protein traffic in endosomal compartments. *Journal of Neuroscience*, *26*(5), 1596–1603. https://doi.org/10.1523/JNEUROSCI.4946-05.2006

Pan, J., & Wan, J. (2020). Methodological comparison of FACS and MACS isolation of enriched microglia and astrocytes from mouse brain. *Journal of Immunological Methods*, *486*(February), 112834. https://doi.org/10.1016/j.jim.2020.112834

Pandini, G., Pace, V., Copani, A., Squatrito, S., Milardi, D., & Vigneri, R. (2013). Insulin has multiple antiamyloidogenic effects on human neuronal cells. *Endocrinology*, *154*(1), 375–387. https://doi.org/10.1210/en.2012-1661

Parks, B. W., Nam, E., Org, E., Kostem, E., Norheim, F., Hui, S. T., Pan, C., Civelek, M., Rau, C. D., Bennett, B. J., Mehrabian, M., Ursell, L. K., He, A., Castellani, L. W., Zinker, B., Kirby, M., Drake, T. A., Drevon, C. A., Knight, R., … Lusis, A. J. (2013). Genetic control of obesity and gut microbiota composition in response to high-fat, high-sucrose diet in mice. *Cell Metabolism*, *17*(1), 141–152. https://doi.org/10.1016/j.cmet.2012.12.007

Pauwels, E. K. J., Ribeiro, M. J., Stoot, J. H. M. B., McCready, V. R., Bourguignon, M., & Mazière, B. (1998). FDG accumulation and tumor biology. *Nuclear Medicine and Biology*, *25*(4), 317–322. https://doi.org/10.1016/S0969-8051(97)00226-6

Peng, Y., Liu, J., Shi, L., Tang, Y., Gao, D., Long, J., & Liu, J. (2016). Mitochondrial dysfunction precedes depression of AMPK/AKT signaling in insulin resistance induced by high glucose in primary cortical neurons. *Journal of Neurochemistry*, *137*(5), 701–713. https://doi.org/10.1111/jnc.13563

Perrin, C., Knauf, C., & Burcelin, R. (2004). Intracerebroventricular infusion of glucose, insulin, and the adenosine monophosphate-activated kinase activator, 5-aminoimidazole-4-carboxamide-1- β-D-ribofuranoside, controls muscle glycogen synthesis. *Endocrinology*, *145*(9), 4025–4033. https://doi.org/10.1210/en.2004-0270

Pirola, L., Johnston, A. M., & van Obberghen, E. (2004). Modulation of insulin action. *Diabetologia*, *47*(2), 170–184. https://doi.org/10.1007/s00125-003-1313-3

Pivovarova, O., Gögebakan, Ö., & Pfeiffer, A. F. H. (2009). Glucose inhibits the insulin-induced activation of the insulin-degrading enzyme in HepG2 cells. *Diabetologia*, 52(8), 1656–1664. https://doi.org/10.1007/s00125-009-1350-7

Pivovarova, O., Höhn, A., Grune, T., & Pfeiffer, A. F. H. (2016). Insulin-degrading enzyme : new therapeutic target for diabetes and Alzheimer ' s disease ? *Annals of medicine*, 48(8),614-624. *3890*. https://doi.org/10.1080/07853890.2016.1197416

Ploia, C., Sclip, A., Colombo, A., Repici, M., Gardoni, F., di Luca, M., Forloni, G., Antoniou, X., & Borsello, T. (2010). Role of glycogen synthase kinase-3β in APP hyperphosphorylation induced by NMDA stimulation in cortical neurons. *Pharmaceuticals*, *3*(1), 42–58. https://doi.org/10.3390/ph3010042

Pomytkin, I., Costa-Nunes, J. P., Kasatkin, V., Veniaminova, E., Demchenko, A., Lyundup, A., Lesch, K. P., Ponomarev, E. D., & Strekalova, T. (2018). Insulin receptor in the brain: Mechanisms of activation and the role in the CNS pathology and treatment. *CNS Neuroscience and Therapeutics*, *24*(9), 763–774. https://doi.org/10.1111/cns.12866

Pottier, C., Hannequin, D., Coutant, S., Rovelet-Lecrux, A., Wallon, D., Rousseau, S., Legallic, S., Paquet, C., Bombois, S., Pariente, J., Thomas-Anterion, C., Michon, A., Croisile, B., Etcharry-Bouyx, F., Berr, C., Dartigues, J. F., Amouyel, P., Dauchel, H., Boutoleau-Bretonnière, C., … Campion, D. (2012). High frequency of potentially pathogenic SORL1 mutations in autosomal dominant early-onset Alzheimer disease. *Molecular Psychiatry*, *17*(9), 875–879. https://doi.org/10.1038/mp.2012.15

Puente, E. C., Fisher, S. J., Reno, C. M., Kahn, B. B., Bree, A. J., Sheng, Z., Routh, V. H., & Daphna-Iken, D. (2016a). Brain GLUT4 Knockout Mice Have Impaired Glucose Tolerance, Decreased Insulin Sensitivity, and Impaired Hypoglycemic Counterregulation. *Diabetes*, *66*(3), 587–597. https://doi.org/10.2337/db16-0917

Puente, E. C., Fisher, S. J., Reno, C. M., Kahn, B. B., Bree, A. J., Sheng, Z., Routh, V. H., & Daphna-Iken, D. (2016b). Brain GLUT4 Knockout Mice Have Impaired Glucose Tolerance, Decreased Insulin Sensitivity, and Impaired Hypoglycemic Counterregulation. *Diabetes*, *66*(3), 587–597. https://doi.org/10.2337/db16-0917

Pugazhenthi, S., Qin, L., & Reddy, P. H. (2017). Common neurodegenerative pathways in obesity, diabetes, and Alzheimer's disease. *Biochimica et Biophysica Acta - Molecular Basis of Disease*, *1863*(5), 1037–1045. https://doi.org/10.1016/j.bbadis.2016.04.017

Qiu, W. Q., & Folstein, M. F. (2006). Insulin, insulin-degrading enzyme and amyloid-β peptide in Alzheimer's disease: Review and hypothesis. *Neurobiology of Aging*, *27*(2), 190–198. https://doi.org/10.1016/j.neurobiolaging.2005.01.004

Qiu, W. Q., Ye, Z., Kholodenko, D., Seubert, P., & Selkoe, D. J. (1997). Degradation of amyloid β-protein by a metalloprotease secreted by microglia and other neural and non-neural cells. *Journal of Biological Chemistry*, *272*(10), 6641–6646. https://doi.org/10.1074/jbc.272.10.6641

Ramos-Rodriguez, J. J., Jimenez-Palomares, M., Murillo-Carretero, M. I., Infante-Garcia, C., Berrocoso, E., Hernandez-Pacho, F., Lechuga-Sancho, A. M., Cozar-Castellano, I., & Garcia-Alloza, M. (2015). Central vascular disease and exacerbated pathology in a mixed model of type 2 diabetes and Alzheimer's disease. *Psychoneuroendocrinology*, *62*, 69–79. https://doi.org/10.1016/j.psyneuen.2015.07.606

Reitz, C. (2011). Meta-analysis of the Association Between Variants in SORL1 and Alzheimer Disease. *Archives of Neurology*, *68*(1), 99. https://doi.org/10.1001/archneurol.2010.346

Reno, C. M., Puente, E. C., Sheng, Z., Daphna-Iken, D., Bree, A. J., Routh, V. H., Kahn, B. B., & Fisher, S. J. (2017). Brain GLUT4 knockout mice have impaired glucose tolerance, decreased insulin sensitivity, and impaired hypoglycemic counterregulation. *Diabetes*, *66*(3), 587–597. https://doi.org/10.2337/db16-0917

Reusch, J. E. B., & Manson, J. A. E. (2017). Management of type 2 diabetes in 2017 getting to goal. *JAMA - Journal of the American Medical Association*, *317*(10), 1015–1016. https://doi.org/10.1001/jama.2017.0241

Ricciarelli, R., & Fedele, E. (2017). The Amyloid Cascade Hypothesis in Alzheimer's Disease: It's Time to Change Our Mind. *Current Neuropharmacology*, *15*(6), 926–935. https://doi.org/10.2174/1570159x15666170116143743

Rieusset, J., Auwerx, J., & Vidal, H. (1999). Regulation of gene expression by activation of the peroxisome proliferator-activated receptor γ with rosiglitazone (BRL 49653) in human adipocytes. *Biochemical and Biophysical Research Communications*, *265*(1), 265–271. https://doi.org/10.1006/bbrc.1999.1657

Risson, V., Mazelin, L., Roceri, M., Sanchez, H., Moncollin, V., Corneloup, C., Richard-Bulteau, H., Vignaud, A., Baas, D., Defour, A., Freyssenet, D., Tanti, J. F., Le-

Marchand-Brustel, Y., Ferrier, B., Conjard-Duplany, A., Romanino, K., Bauché, S., Hantaï, D., Mueller, M., … Gangloff, Y. G. (2009). Muscle inactivation of mTOR causes metabolic and dystrophin defects leading to severe myopathy. *Journal of Cell Biology*, *187*(6), 859–874. https://doi.org/10.1083/jcb.200903131

Rogaeva, E., Meng, Y., Lee, J. H., Gu, Y., Kawarai, T., Zou, F., Katayama, T., Baldwin, C. T., Cheng, R., Hasegawa, H., Chen, F., Shibata, N., Lunetta, K. L., Pardossi-Piquard, R., Bohm, C., Wakutani, Y., Cupples, L. A., Cuenco, K. T., Green, R. C., … st. George-Hyslop, P. (2007). The neuronal sortilin-related receptor SORL1 is genetically associated with Alzheimer disease. *Nature Genetics*, *39*(2), 168–177. https://doi.org/10.1038/ng1943

Roh, E., Song, D. K., & Kim, M. (2016). Emerging role of the brain in the homeostatic regulation of energy and glucose metabolism. *Experimental and molecular medicine, 48*(3), e216-12. https://doi.org/10.1038/emm.2016.4

Rohe, M., Carlo, A. S., Breyhan, H., Sporbert, A., Militz, D., Schmidt, V., Wozny, C., Harmeier, A., Erdmann, B., Bales, K. R., Wolf, S., Kempermann, G., Paul, S. M., Schmitz, D., Bayer, T. A., Willnow, T. E., & Andersen, O. M. (2008). Sortilin-related receptor with A-type repeats (SORLA) affects the amyloid precursor protein-dependent stimulation of ERK signaling and adult neurogenesis. *Journal of Biological Chemistry*, *283*(21), 14826–14834. https://doi.org/10.1074/jbc.M710574200

Rohe, M., Hartl, D., Fjorback, A. N., Klose, J., & Willnow, T. E. (2013). SORLA-Mediated Trafficking of TrkB Enhances the Response of Neurons to BDNF. *PloS one*, *8*(8), e72164. https://doi.org/10.1371/journal.pone.0072164

Rohe, M., Synowitz, M., Glass, R., Paul, S. M., Nykjaer, A., & Willnow, T. E. (2009). Brain-derived neurotrophic factor reduces amyloidogenic processing through control of SORLA gene expression. *Journal of Neuroscience*, *29*(49), 15472–15478. https://doi.org/10.1523/JNEUROSCI.3960-09.2009

Routh, V. H. (2002). Glucose-sensing neurons: Are they physiologically relevant? *Physiology and Behavior*, *76*(3), 403–413. https://doi.org/10.1016/S0031-9384(02)00761-8

Ruud, J., Steculorum, S. M., & Bruning, J. C. (2017). Neuronal control of peripheral insulin sensitivity and glucose metabolism. *Nature Communications*, *8*(May). https://doi.org/10.1038/ncomms15259

Saltiel, A. R., & Kahn, C. R. (2001). Insulin signalling and the regulation of glucose and lipid metabolism. *Nature*, *414*(6865), 799-806. https://doi.org/10.2174/978160805189211101010001

Sanchez, A. M. J., Candau, R. B., Csibi, A., Pagano, A. F., Raibon, A., & Bernardi, H. (2020). The role of AMP-activated protein kinase in the coordination of skeletal muscle turnover and energy homeostasis. *American journal of physiology. Cell physiology*, *303*(5), C475–C485. https://doi.org/10.1152/ajpcell.00125.2012

Scheltens, P., Blennow, K., Breteler, M. M. B., de Strooper, B., Frisoni, G. B., Salloway, S., & van der Flier, W. M. (2016). Alzheimer's disease. *The Lancet*, *388*(10043), 505–517. https://doi.org/10.1016/S0140-6736(15)01124-1

Scherzer, C., Offe, K., & Lah, J. J. (2004). Loss of Apolipoprotein E Receptor LR11 in Alzheimer Disease. *Archives of Neurology*, *61*, 1200–1205.

Schmidt, V., Baum, K., Lao, A., Rateitschak, K., Schmitz, Y., Teichmann, A., Wiesner, B., Munck, C., Petersen, C. M., Nykjaer, A., Wolf, J., Wolkenhauer, O., & Willnow, T. E. (2012). Quantitative modelling of amyloidogenic processing and its influence by SORLA in Alzheimer's disease. *EMBO Journal*, *31*(1), 187–200. https://doi.org/10.1038/emboj.2011.352

Schmidt, V., Schulz, N., Kern, M., Poy, M. N., Willnow, T. E., Olivecrona, G., Yan, X., Kempa, S., Blüher, M., & Schürmann, A. (2016). SORLA facilitates insulin receptor signaling in adipocytes and exacerbates obesity. *Journal of Clinical Investigation*, *126*(7), 2706–2720. https://doi.org/10.1172/jci84708

Schmidt, V., Subkhangulova, A., & Willnow, T. E. (2017). Sorting receptor SORLA: cellular mechanisms and implications for disease. *Cellular and Molecular Life Sciences*, *74*(8), 1475–1483. https://doi.org/10.1007/s00018-016-2410-z

Schwartz, M. W., Figlewicz, D. F., Kahn, S. E., Baskin, D. G., Greenwood, M. R. C., & Porte, D. (1990). Insulin binding to brain capillaries is reduced in genetically obese, hyperinsulinemic Zucker rats. *Peptides*, *11*(3), 467–472. https://doi.org/10.1016/0196-9781(90)90044-6

Schwartzentruber, J., Cooper, S., Liu, J. Z., Barrio-Hernandez, I., Bello, E., Kumasaka, N., Young, A. M. H., Franklin, R. J. M., Johnson, T., Estrada, K., Gaffney, D. J., Beltrao, P., & Bassett, A. (2021). Genome-wide meta-analysis, fine-mapping and integrative prioritization implicate new Alzheimer's disease risk genes. *Nature Genetics*, *53*(3), 392–402. https://doi.org/10.1038/s41588-020-00776-w

Shen, L., & Jia, J. (2016). An Overview of Genome-Wide Association Studies in Alzheimer's Disease. *Neuroscience Bulletin*, *32*(2), 183–190. https://doi.org/10.1007/s12264-016-0011-3

Shin, A. C., Filatova, N., Lindtner, C., Chi, T., Degann, S., Oberlin, D., & Buettner, C. (2017). Insulin receptor signaling in POMC, but not AgRP, neurons controls adipose tissue insulin action. *Diabetes*, *66*(6), 1560–1571. https://doi.org/10.2337/db16-1238

Smith, E. N., Chen, W., Kähönen, M., Kettunen, J., Lehtimäki, T., Peltonen, L., Raitakari, O. T., Salem, R. M., Schork, N. J., Shaw, M., Srinivasan, S. R., Topol, E. J., Viikari, J. S., Berenson, G. S., & Murray, S. S. (2010). Longitudinal genome-wide association of cardiovascular disease risk factors in the bogalusa heart study. *PLoS Genetics*, *6*(9). https://doi.org/10.1371/journal.pgen.1001094

Solano, D. C., Sironi, M., Bonfini, C., Solerte, S. B., Govoni, S., & Racchi, M. (2000). Insulin regulates soluble amyloid precursor protein release via phosphatidyl inositol 3 kinase-dependent pathway. *The FASEB Journal*, *14*(7), 1015–1022. https://doi.org/10.1096/fasebj.14.7.1015

Son, S. M., Cha, M. Y., Choi, H., Kang, S., Choi, H., Lee, M. S., Park, S. A., & Mook-Jung, I. (2016). Insulin-degrading enzyme secretion from astrocytes is mediated by an autophagy-based unconventional secretory pathway in Alzheimer disease. *Autophagy*, *12*(5), 784–800. https://doi.org/10.1080/15548627.2016.1159375

Song, E. S., Rodgers, D. W., & Hersh, L. B. (2018). Insulin-degrading enzyme is not secreted from cultured cells. *Scientific Reports*, *8*(1), 8–15. https://doi.org/10.1038/s41598-018-20597-6

Southam, K. A., Stennard, F., Pavez, C., & Small, D. H. (2019). Knockout of Amyloid β Protein Precursor (APP) Expression Alters Synaptogenesis, Neurite Branching and Axonal Morphology of Hippocampal Neurons. *Neurochemical Research*, *44*(6), 1346–1355. https://doi.org/10.1007/s11064-018-2512-0

Spencer, B., Rank, L., Metcalf, J., & Desplats, P. (2018). Identification of Insulin Receptor Splice Variant B in Neurons by in situ Detection in Human Brain Samples. *Scientific Reports*, *November 2017*, 1–8. https://doi.org/10.1038/s41598-018-22434-2

Spoelgen, R., von Arnim, C. A. F., Thomas, A. v., Peltan, I. D., Koker, M., Deng, A., Irizarry, M. C., Andersen, O. M., Willnow, T. E., & Hyman, B. T. (2006). Interaction of the cytosolic domains of sorLA/LR11 with the amyloid precursor protein (APP) and β-secretase β-site APP-cleaving enzyme. *Journal of Neuroscience*, *26*(2), 418–428. https://doi.org/10.1523/JNEUROSCI.3882-05.2006

Stöckli, J., Fazakerley, D. J., & James, D. E. (2012). GLUT4 exocytosis. *Journal of Cell Science*, *124*(24), 4147–4159. https://doi.org/10.1242/jcs.097063

Stoothoff, W. H., & Johnson, G. V. W. (2005). Tau phosphorylation : physiological and pathological consequences. *Biochimica et biophysica acta*, *1739*, 280–297. https://doi.org/10.1016/j.bbadis.2004.06.017

Stupack, J., Xiong, X. P., Jiang, L. L., Zhang, T., Zhou, L., Campos, A., Ranscht, B., Mobley, W., Pasquale, E. B., Xu, H., & Huang, T. Y. (2020). Soluble SORLA enhances neurite outgrowth and regeneration through activation of the EGF receptor/ERK signaling axis. *Journal of Neuroscience*, *40*(31), 5908–5921. https://doi.org/10.1523/JNEUROSCI.0723-20.2020

Subkhangulova, A., Malik, A. R., Hermey, G., Popp, O., Dittmar, G., Rathjen, T., Poy, M. N., Stumpf, A., Beed, P. S., Schmitz, D., Breiderhoff, T., & Willnow, T. E. (2018). SORCS 1 and SORCS 3 control energy balance and orexigenic peptide production . *EMBO Reports*, *19*(4), 1–18. https://doi.org/10.15252/embr.201744810

Szablewski, L. (2017). Glucose Transporters in Brain: In Health and in Alzheimer's Disease. *Journal of Alzheimer's Disease*, *55*(4), 1307–1320. https://doi.org/10.3233/JAD-160841

Tan, M. S., Yu, J. T., & Tan, L. (2013). Bridging integrator 1 (BIN1): Form, function, and Alzheimer's disease. *Trends in Molecular Medicine*, *19*(10), 594–603. https://doi.org/10.1016/j.molmed.2013.06.004

Taniguchi, C. M., Emanuelli, B., & Kahn, C. R. (2006). Critical nodes in signalling pathways: Insights into insulin action. *Nature Reviews Molecular Cell Biology*, *7*(2), 85–96. https://doi.org/10.1038/nrm1837

Tanokashira, D., Mamada, N., Yamamoto, F., Taniguchi, K., Tamaoka, A., Lakshmana, M. K., & Araki, W. (2017). The neurotoxicity of amyloid β-protein oligomers is reversible in a primary neuron model. *Molecular Brain*, *10*(1), 1–10. https://doi.org/10.1186/s13041-016-0284-5

Tellechea, P., Pujol, N., Esteve-Belloch, P., Echeveste, B., García-Eulate, M. R., Arbizu, J., & Riverol, M. (2018). Early- and late-onset Alzheimer disease: Are they the same

entity? *Neurología (English Edition)*, *33*(4), 244–253. https://doi.org/10.1016/j.nrleng.2015.08.009

Tokarz, V. L., MacDonald, P. E., & Klip, A. (2018). The cell biology of systemic insulin function. *Journal of Cell Biology*, *217*(7), 1–17. https://doi.org/10.1083/jcb.201802095

Tundo, G. R., Sbardella, D., Ciaccio, C., Bianculli, A., Orlandi, A., Desimio, M. G., Arcuri, G., Coletta, M., & Marini, S. (2013). Insulin-degrading enzyme (IDE): A novel heat shock-like protein. *Journal of Biological Chemistry*, *288*(4), 2281–2289. https://doi.org/10.1074/jbc.M112.393108

Tundo, G. R., Sbardella, D., Ciaccio, C., Grasso, G., Coletta, A., Polticelli, F., Pierro, D. di, Milardi, D., Endert, V., Marini, S., Coletta, M., Tundo, G. R., Sbardella, D., Ciaccio, C., Grasso, G., Gioia, M., Coletta, A., Polticelli, F., Pierro, D. di, … Coletta, M. (2017). Multiple functions of insulin-degrading enzyme : a metabolic crosslight ? *Critical Reviews in Biochemistry and Molecular Biology*, *0*(0), 1–29. https://doi.org/10.1080/10409238.2017.1337707

Vannucci, S. J., Maher, F., & Simpson, I. A. (1997). Glucose transporter proteins in brain: Delivery of glucose to neurons and glia. *Glia*, *21*(1), 2–21. https://doi.org/10.1002/(SICI)1098-1136(199709)21:1<2::AID-GLIA2>3.0.CO;2-C

Vekrellis, K., Ye, Z., Qiu, W. Q., Walsh, D., Hartley, D., Chesneau, V., Rosner, M. R., & Selkoe, D. J. (2000). Neurons regulate extracellular levels of amyloid β-protein via proteolysis by insulin-degrading enzyme. *Journal of Neuroscience*, *20*(5), 1657–1665. https://doi.org/10.1523/jneurosci.20-05-01657.2000

Velazquez, R., Tran, A., Ishimwe, E., Denner, L., & Dave, N. (2017). Central Insulin Dysregulation and Energy Dyshomeostasis in Two Mouse Models of Alzheimer ' s Disease Neurobiology of Aging Central insulin dysregulation and energy dyshomeostasis in two mouse models of Alzheimer ' s disease. *Neurobiology of Aging*, *58*(October), 1–13. https://doi.org/10.1016/j.neurobiolaging.2017.06.003

Villa-Pérez, P., Merino, B., Fernández-Díaz, C. M., Cidad, P., Lobatón, C. D., Moreno, A., Muturi, H. T., Ghadieh, H. E., Najjar, S. M., Leissring, M. A., Cózar-Castellano, I., & Perdomo, G. (2018). Liver-specific ablation of insulin-degrading enzyme causes hepatic insulin resistance and glucose intolerance, without affecting insulin clearance in mice. *Metabolism: Clinical and Experimental*, *88*, 1–11. https://doi.org/10.1016/j.metabol.2018.08.001

Vishwanath, D., Srinivasan, H., Patil, M. S., Seetarama, S., Agrawal, S. K., Dixit, M. N., & Dhar, K. (2013). Novel method to differentiate 3T3 L1 cells in vitro to produce highly sensitive adipocytes for a GLUT4 mediated glucose uptake using fluorescent glucose analog. *Journal of Cell Communication and Signaling*, *7*(2), 129–140. https://doi.org/10.1007/s12079-012-0188-9

Waterson, M. J., & Horvath, T. L. (2015). Review Neuronal Regulation of Energy Homeostasis : Beyond the Hypothalamus and Feeding. *Cell Metabolism*, *22*(6), 962–970. https://doi.org/10.1016/j.cmet.2015.09.026

Whittle, A. J., Jiang, M., Peirce, V., Relat, J., Virtue, S., Ebinuma, H., Fukamachi, I., Yamaguchi, T., Takahashi, M., Murano, T., Tatsuno, I., Takeuchi, M., Nakaseko, C., Jin, W., Jin, Z., Campbell, M., Schneider, W. J., Vidal-Puig, A., & Bujo, H. (2015). Soluble LR11/SorLA represses thermogenesis in adipose tissue and correlates with

BMI in humans. *Nature Communications*, *6*(May), 1–12. https://doi.org/10.1038/ncomms9951

Willnow, T. E., Petersen, C. M., & Nykjaer, A. (2008). VPS10P-domain receptors - Regulators of neuronal viability and function. *Nature Reviews Neuroscience*, *9*(12), 899–909. https://doi.org/10.1038/nrn2516

Winblad, B., Ferrer, I., Parrado-Fernandez, C., Merino-Serrais, P., Sandebring-Matton, A., Cedazo-Minguez, A., Rabano, A., Ávila, J., & Rodriguez-Rodriguez, P. (2017). Tau hyperphosphorylation induces oligomeric insulin accumulation and insulin resistance in neurons. *Brain*, *140*(12), 3269–3285. https://doi.org/10.1093/brain/awx256

Xu, W., Tan, L., Wang, H. F., Jiang, T., Tan, M. S., Tan, L., Zhao, Q. F., Li, J. Q., Wang, J., & Yu, J. T. (2015). Meta-analysis of modifiable risk factors for Alzheimer's disease. *Journal of Neurology, Neurosurgery and Psychiatry*, *86*(12), 1299–1306. https://doi.org/10.1136/jnnp-2015-310548

Yajima, R., Tokutake, T., Koyama, A., Kasuga, K., Tezuka, T., Nishizawa, M., & Ikeuchi, T. (2015). ApoE-isoform-dependent cellular uptake of amyloid-β is mediated by lipoprotein receptor LR11/SorLA. *Biochemical and Biophysical Research Communications*, *456*(1), 482–488. https://doi.org/10.1016/j.bbrc.2014.11.111

Yamamoto, N., Ishikuro, R., Tanida, M., Suzuki, K., Ikeda-Matsuo, Y., & Sobue, K. (2018). Insulin-signaling Pathway Regulates the Degradation of Amyloid β-protein via Astrocytes. *Neuroscience*, *385*, 227–236. https://doi.org/10.1016/j.neuroscience.2018.06.018

Yamamoto, N., Ueda-Wakagi, M., Sato, T., Kawasaki, K., Sawada, K., Kawabata, K., Akagawa, M., & Ashida, H. (2015). Measurement of Glucose Uptake in Cultured Cells. *Current Protocols in Pharmacology*, *71*(1), 12.14.1-12.14.26. https://doi.org/10.1002/0471141755.ph1214s71

Yasojima, K., Akiyama, H., McGeer, E. G., & McGeer, P. L. (2001). Reduced neprilysin in high plaque areas of Alzheimer brain: A possible relationship to deficient degradation of β-amyloid peptide. *Neuroscience Letters*, *297*(2), 97–100. https://doi.org/10.1016/S0304-3940(00)01675-X

Yiannopoulou, K. G., Anastasiou, A. I., Zachariou, V., & Pelidou, S. H. (2019). Reasons for failed trials of disease-modifying treatments for alzheimer disease and their contribution in recent research. *Biomedicines*, *7*(4), 1–16. https://doi.org/10.3390/biomedicines7040097

Yoon, S. S., & Jo, S. A. (2012). Mechanisms of amyloid-β peptide clearance: Potential therapeutic targets for Alzheimer's disease. *Biomolecules and Therapeutics*, *20*(3), 245–255. https://doi.org/10.4062/biomolther.2012.20.3.245

Young, P. N. E., Estarellas, M., Coomans, E., Srikrishna, M., Beaumont, H., Maass, A., Venkataraman, A. v., Lissaman, R., Jiménez, D., Betts, M. J., McGlinchey, E., Berron, D., O'Connor, A., Fox, N. C., Pereira, J. B., Jagust, W., Carter, S. F., Paterson, R. W., & Schöll, M. (2020). Imaging biomarkers in neurodegeneration: Current and future practices. *Alzheimer's Research and Therapy*, *12*(1), 1–17. https://doi.org/10.1186/s13195-020-00612-7

Yu, J. T., Xu, W., Tan, C. C., Andrieu, S., Suckling, J., Evangelou, E., Pan, A., Zhang, C., Jia, J., Feng, L., Kua, E. H., Wang, Y. J., Wang, H. F., Tan, M. S., Li, J. Q., Hou, X. H., Wan, Y., Tan, L., Mok, V., … Vellas, B. (2020). Evidence-based prevention of Alzheimer's disease: Systematic review and meta-analysis of 243 observational prospective studies and 153 randomised controlled trials. *Journal of Neurology, Neurosurgery and Psychiatry*, *91*(11), 1201–1209. https://doi.org/10.1136/jnnp-2019-321913

Zhan, X., Cao, M., Yoo, A. S., Zhang, Z., Chen, L., Crabtree, G. R., & Wu, J. I. (2015). Generation of BAF53b-Cre transgenic mice with pan-neuronal Cre activities. *Genesis*, *53*(7), 440–448. https://doi.org/10.1002/dvg.22866

Zhang, J., Chen, C., Hua, S., Liao, H., Wang, M., Xiong, Y., & Cao, F. (2017). An updated meta-analysis of cohort studies: Diabetes and risk of Alzheimer's disease. *Diabetes Research and Clinical Practice*, *124*, 41–47. https://doi.org/10.1016/j.diabres.2016.10.024

Zhang, Y., Wang, B., Wan, H., Zhou, Q., & Li, T. (2013). Meta-analysis of the insulin degrading enzyme polymorphisms and susceptibility to Alzheimer's disease. *Neuroscience Letters*, *541*, 132–137. https://doi.org/10.1016/j.neulet.2013.01.051

Zhao, L., Teter, B., Morihara, T., Lim, G. P., Ambegaokar, S. S., Ubeda, O. J., Frautschy, S. A., & Cole, G. M. (2004). Insulin-degrading enzyme as a downstream target of insulin receptor signaling cascade: Implications for Alzheimer's disease intervention. *Journal of Neuroscience*, *24*(49), 11120–11126. https://doi.org/10.1523/JNEUROSCI.2860-04.2004

Zhao, W., de Felice, F. G., Fernandez, S., Chen, H., Lambert, M. P., Quon, M. J., Krafft, G. A., & Klein, W. L. (2008). Amyloid beta oligomers induce impairment of neuronal insulin receptors. *The FASEB Journal*, *22*(1), 246–260. https://doi.org/10.1096/fj.06-7703com

Zhou, L., Wei, C., Huang, W., Bennett, D. A., Dickson, D. W., Wang, R., & Wang, D. (2013). Distinct subcellular patterns of neprilysin protein and activity in the brains of Alzheimer's disease patients, transgenic mice and cultured human neuronal cells. *American Journal of Translational Research*, *5*(6), 608–621.

7 Acknowledgements

I would like to thank Prof. Dr. Thomas Willnow and Dr. Vanessa Schmidt for offering me this exciting project, providing useful insights and constantly supporting me through the PhD journey. I am happy that they provided the right environment for me to nurture and improve on my skills as a scientist which will be useful in different facets of life.

I would also like to thank my university supervisor Prof. Dr. Simone Spuler for reviewing my doctoral thesis.

Moving to a new country is never easy and I would like to thank Sylvia Sibilak from the Graduate Office at MDC for the smooth transition and handling of the necessary paperwork. Willnow lab is incomplete without our super awesome secretary Verona Kuhle and she has been amazing support for research as well as non-research related activities in Berlin.

I have been fortunate enough and would like to thank all the technical staff in the Willnow lab for teaching me the necessary techniques essential for my doctoral work. Special thanks to the technicians in the mouse facility for putting up my requests on short notice and taking care of my mice.PhD life can be tough at times and is largely restricted to labs. But, thanks to the wonderful support system in the lab and the community at MDC that it was great fun to work and party during the beer hours. MDC is a home away from home with some of the best people around- Antonino, Anna Mailk, Lena, Maike, Alexis, Sasha, Peter and Kevin. You guys have shaped me as a person and I will always cherish the memories that I had with you. Special thanks to all my seniors in the Willnow lab for their constant support and guidance. My Indian community in Berlin helped me overcome the tough times and I cannot thank them enough.

Finally, none of this would have been possible without the trust and support from my family. My PhD was our collective dream and we overcame some unfortunate events to get here. I dedicate this thesis to my family and especially my brother, I hope I have made you proud.

8 Curriculum Vitae

For reasons of data protection, the curriculum vitae is not published in the electronic version.

For reasons of data protection, the curriculum vitae is not published in the electronic version.